N(RSAR

NORSAR Scientific Report No. 2-1999/2000

Semiannual Technical Summary

1 October 1999 - 31 March 2000

Frode Ringdal (ed.)

Kjeller, May 2000

REPORT DOCUMENTATION PAGE

Form Approved
OMB No. 0704-0188

1a. REPORT SECURITY CLASSIFICATION	1b. RESTRICTIVE MARKINGS
Unclassified	Not applicable

2a. SECURITY CLASSIFICATION AUTHORITY	3. DISTRIBUTION / AVAILABILITY OF REPORT
Not Applicable	
2b. DECLASSIFICATION / DOWNGRADING SCHEDULE	Approved for public release; distribution unlimited

4. PERFORMING ORGANIZATION REPORT NUMBER(S)	5. MONITORING ORGANIZATION REPORT NUMBER(S)
Scientific Rep.2-1999/200	Scientific Rep. 2-1999/2000

6a. NAME OF PERFORMING ORGANIZATION	6b. OFFICE SYMBOL (if applicable)	7a. NAME OF MONITORING ORGANIZATION
NORSAR		HQ/AFTAC/TTS

6c. ADDRESS (City, State, and ZIP Code)	7b. ADDRESS (City, State, and ZIP Code)
Post Box 51 N-2027 Kjeller, Norway	Patrick AFB, FL 32925-6001

8a. NAME OF FUNDING / SPONSORING ORGANIZATION	8b. OFFICE SYMBOL (if applicable)	9. PROCUREMENT INSTRUMENT IDENTIFICATION NUMBER
Advanced Research Projects Agency/NTPO	NMRO/NTPO	Contract No. F08650-96-C-0001

8c. ADDRESS (City, State, and ZIP Code)	10. SOURCE OF FUNDING NUMBERS

8c. ADDRESS	PROGRAM ELEMENT NO.	PROJECT NO.	TASK NO.	WORK UNIT ACCESSION NO.
1515 Wilson Blvd., Suite 720 Arlington, VA 22209	R&D	NORSAR Phase 3	SOW Task 5.0	Sequence No. 004A2

11. TITLE (include Security Classification)

Semiannual Technical Summary, 1 April - 30 September 1999

12. PERSONAL AUTHOR(S)

13a. TYPE OF REPORT	13b. TIME COVERED	14. DATE OF REPORT (Year, Month, Day)	15. PAGE COUNT
Scientific Summary	FROM 1 Oct 99 TO 31 Mar 00	2000 May	129

16. SUPPLEMENTARY NOTATION

17. COSATI CODES			18. SUBJECT TERMS (Continue on reverse if necessary and identify by block number)
FIELD	GROUP	SUB-GROUP	
8	11		NORSAR, Norwegian Seismic Array

19. ABSTRACT (Continue on reverse if necessary and identify by block number)

This Semiannual Technical Summary describes the operation, maintenance and research activities at the Norwegian Seismic Array (NORSAR), the Norwegian Regional Seismic Array (NORES), the Arctic Regional Seismic Array (ARCES) and the Spitsbergen Regional Array for the period 1 October 1999 - 31 March 2000. Statistics are also presented for additional seismic stations, which through cooperative agreements with institutions in the host countries provide continuous data to the NORSAR Data processing Center (NDPC). These stations comprise the Finnish Regional Seismic Array (FINES), the Hagfors array in Sweden and the regional seismic array in Apatity, Russia.

(cont.)

20001207 160

20. DISTRIBUTION / AVAILABILITY OF ABSTRACT	21. ABSTRACT SECURITY CLASSIFICATION
☐ UNCLASSIFIED/UNLIMITED ☐ SAME AS RPT. ☐ DTIC USERS	
22a. NAME OF RESPONSIBLE INDIVIDUAL	22b. TELEPHONE (Include Area Code)	22c. OFFICE SYMBOL
Mr. Michael C. Baker	(407) 494-7985	AFTAC/TTS

DD Form 1473, JUN 86   *Previous editions are obsolete.*   SECURITY CLASSIFICATION OF THIS PAGE

DTIC QUALITY INSPECTED 4

Abstract (cont.)

Beginning 1 January 1999, the responsibility for funding the operational activities of the seismic field systems and the Norwegian National Data Center (NDC) has been taken over by the Norwegian Government, with the understanding that the funding of IMS-related activities will gradually be arranged through the CTBTO/PTS. Research activities described in this report, as well as transmission of selected data to the United States NDC, are continuing to be funded by the United States Department of Defense.

The NOA Detection Processing system has been operated throughout the period with an average uptime of 99.93%. A total of 1723 seismic events have been reported in the NOA monthly seismic bulletin for October 1999 through March 2000. The performance of the continuous alarm system and the data transmission to AFTAC has been satisfactory. Processing of requests for full NOA and regional array data on magnetic tapes has progressed according to established schedules.

This Semiannual Report also presents statistics from operation of the Regional Monitoring System (RMS). The RMS has been operated in a limited capacity, with continuous automatic detection and location and with analyst review of selected events of special interest for regional monitoring of Fennoscandia and adjacent regions. Data sources for the RMS have comprised all the regional arrays processed at NORSAR. The Generalized Beamforming (GBF) program continues to be used as a pre-processor to RMS.

On-line detection processing and data recording at the NORSAR Data Processing Center (NDPC) of NORES, ARCES and FINES data have been conducted throughout the period. Data from two small-aperture arrays at sites in Spitsbergen and Apatity, Kola Peninsula, as well as the Hagfors array in Sweden, have also been recorded and processed. Processing statistics for the arrays as well as results of the RMS analysis for the reporting period are given.

The operation of the regional arrays has proceeded normally in the period. Maintenance activities in the period comprise preventive/corrective maintenance as required in connection with all of the NOA subarrays as well as the refurbished ARCES array. Other activities have involved repair of defective electronic equipment, cable splicing and work in connection with the SPITS array. Work is also continuing in making the modifications required for formal certification of the NOA array.

A summary of the activities related to the GSETT-3 experiment and experience gained at the Norwegian NDC during the reporting period is provided in Section 4. Norway is now contributing primary station data from two seismic arrays: ARCES and NOA and one auxiliary array (SPITS). These data are being provided to the IDC via the global communications infrastructure (GCI). Continuous data from all three arrays are in addition being transmitted to the US NDC, and continuous data from SPITS are transmitted to the PIDC. Our link to the PIDC is also used to transmit data from the NORES array and the NIL station in Pakistan. The transmission speed of the NORSAR-PIDC link was reduced on 8 March 2000 from 256 Kbps to 128 Kbps.

During September 1999, the ARCES array was upgraded with completely new electronics, under a contract with the Provisional Technical Secretariat (PTS). The ARCES data transmission, which includes the conversion of data to the CD1-format used by the IDC, has been carried out successfully during the period, and ARCES processing at the PIDC has been

proceeding normally after the installation was completed. The ARCES array is now in a testing and evaluation phase, and is expected to be considered for certification later this year.

The PrepCom has encouraged states that operate IMS-designated stations to continue to do so on a voluntary basis and in the framework of the GSETT-experiment until such time that the stations have been certified for formal inclusion in IMS. In line with this, we envisage continuing the provision of data from Norwegian IMS-designated stations in accordance with current procedures.

Summaries of seven scientific and technical contributions are presented in Chapter 6 of this report.

Section 6.1 contains a report from the meeting of the IDC Technical Experts Group on Seismic Event Location in Oslo, Norway on 20-24 March 2000. This was the second meeting of the Experts Group in support of Working Group B of the CTBTO Preparatory Commission. At its first meeting in January 1999, the Experts Group developed plans and recommendations for a global calibration program, and presented its report to Working Group B in February 1999. The second meeting had the following objectives:

- To review proposals for detailed station-specific regional corrections to be applied for IMS stations in North America, Europe, North Africa, Asia and Australia

- To recommend a set of such corrections, including appropriate model errors, for incorporation into the Release 3 of the IDC software

- To develop a plan for future extensions and improvements of this regional correction data base, to be incorporated into future IDC software releases

- To review progress in the general recommendations from the January 1999 meeting, and make adjustments and updates to these recommendations as required.

The primary task of the meeting was to assess the status and availability of such calibration information for the regions being considered, and to plan for implementing regional location calibration at the IDC, both for Release 3 of the IDC applications software and for implementation in the longer term. The second meeting was attended by sixty technical experts, coming from fifteen signatory countries and the Provisional Technical Secretariat. Dr. Frode Ringdal of Norway chaired the meeting.

The meeting was organized into four sessions, including Working Group discussions to address the technical issues in detail during the meeting. Topics were:

- Collection of Calibration Information
- Application of Calibration Information
- Validation of Calibration Information
- Specific recommendations for IDC Release 3

Detailed recommendations were developed for each of these subject matters, and will be presented to Working Group B in Vienna during its May 2000 session.

Section 6.2 is entitled "Locating Seismic Events in Northern Eurasia" and is a summary of a paper presented at the Oslo location workshop. The paper discusses the application of the velocity model previously developed for the Barents region (the Barents model) to seismic

events in a larger area, and compares the results to those obtained using the IASPEI-91 model. It concludes that the Barents model, which is known to give accurate locations in the Fennoscandian and NW Russia area, can be successfully applied to the more general northern Eurasia region. The paper also contains analysis of seismic events in specific regions of interest, and provides a table of ground truth locations (1 km accuracy) of a set of nuclear explosions at Novaya Zemlya, inferred from study of satellite imagery.

Section 6.3 is a follow-up study to the initial analysis of data from the Eurobridge experiment presented in the preceding Semiannual Technical Summary. Eurobridge comprised a 1130 km seismic refraction profile crossing the Baltic Shield in the northwest and the Ukrainian Shield in the southeast. There were three series of shots, one in 1995 and two in 1996. Observations of these explosions at the Fennoscandian arrays (ARCES, FINES, Hagfors, and NORES) provide an opportunity to check the accuracy of the travel-time tables in use at NORSAR for Fennoscandia. At the same time, these refraction shots provide a useful extension to the pIDC ground-truth database.

P-phases from most of the Eurobridge shots were observed at the FINES, HAGFORS and NORES arrays, and even at the more distant ARCES array as many as 12 out of the 29 events were seen. We have investigated in detail observed deviations in P-wave travel times from those predictions by the Fennoscandian crustal and upper mantle velocity model. Our study has revealed several instances of documented timing errors at the various arrays. Even when accounting for these timing errors, there remains a considerable scatter in the travel times as compared to the theoretical model. The interpretation of these anomalies in terms of crustal and upper mantle structure is not obvious. An important outcome of this study is the development of a method to identify possible timing anomalies at IMS stations. This method could be useful both in validating calibration data and in providing a tool for continuously checking the timing accuracy and consistency of IMS stations.

Section 6.4 contains an analysis of data recorded at the SPITS array for some recent profiling experiments near Spitsbergen. Data from airgun shots in the water as well as small underwater explosions of 25 to 50 kg conventional explosives could be observed at distances up to 350 km when using the double-beam technique for SNR enhancement. Not unexpectedly, the study has demonstrated that the crust and uppermost mantle around the SPITS station is very heterogeneous. However, with the exact travel times available through this study for different azimuths in the range 0-3 degrees, the location and detection processing of local and near-regional events at SPITS will be considerably improved.

This is particularly important because there are large numbers of local events recorded at SPITS every day, and a correct location and phase identification will help eliminate these phases from interfering in the Generalized Beamforming process for network association and event definition analysis. Furthermore, the ground-truth data base developed during this study will be used to reanalyze in more detail the large observed slowness deviations at SPITS reported in previous Semiannual Technical Summaries.

Section 6.5 addresses the waveform quality of SPITS recordings. The problem of spikes in the data streams for individual sensors (in particular the SPB5_sz sensor) has been a recurring problem at this array. Until the problem can be technically corrected, which will probably require a complete refurbishment of the array electronics, it is important to automatically iden-

tify and (if possible) correct these spikes so that they do not interfere with the array detection analysis.

In this contribution, a new method to detect and correct for one-sample spikes (which is the most typical spike observed at SPITS channels) is developed and tested. A particular challenge has been to develop an algorithm that does not trigger any spike correction on real, impulsive signals, which are quite often seen at this array. The paper concludes that the spike detector and the corresponding data correction procedure provides an efficient method to identify and remove one-sample spikes from the seismic data stream, and that the procedure could be useful for general application to systems that experience similar kinds of technical problems.

Section 6.6 is entitled: "Third Level Seismo-geographical Regionalization of Fennoscandia". This work has been undertaken by the Nordic countries in response to an initiative by IASPEI in 1985. The purpose is to refine the current global regionalization, which has two levels: Level 1 (Gutenberg-Richter) comprising 50 regions, and Level 2 (Flinn-Engdahl) with 728 regions.

The detailed zonation presented in this contribution comprises 74 regions for the Level 3 zonation of Fennoscandia. This is almost an order of magnitude more than the corresponding Flinn-Engdahl subdivision, which has about 10 regions covering this area. The regions along the outer borders of the Nordic countries have been defined in cooperation with those countries for which Level 3 regionalization already exists. The Level 3 zonation described in this paper has been implemented in the current NORSAR regional seismic bulletin production.

Section 6.7 is a study of the crustal structure of the Barents Sea, with a discussion of how the crustal configuration and composition affects regional models for seismic velocities and travel-times. In recent years, deep seismic reflection and refraction data have greatly improved our understanding of the deep basins and the underlying crystalline crust in the Barents Sea and of the crustal transition across the western continental margin. The data base for the present study includes a comprehensive set of such profiles along with gravity and magnetic data as well as general geological information. The crustal and seismic velocity structure of the Barents Sea is found to vary significantly, and the approximate range is as follows:

- Thickness of sedimentary cover varies between 0 – 20 km
- Depth to Moho varies between 20 – 45 km
- Thickness of crystalline crust varies between 10 – 45 km

The crustal heterogeneity of the Barents Sea region implies that very detailed regional travel-time models may be required for accurately locating seismic events in this region.

Frode Ringdal

AFTAC Project Authorization	:	T/6141/NORSAR
ARPA Order No.	:	4138 AMD # 53
Program Code No.	:	0F10
Name of Contractor	:	The Norwegian Research Council (NFR)
Effective Date of Contract	:	1 Oct 1995
Contract Expiration Date	:	30 Sep 2000
Project Manager	:	Frode Ringdal +47 63 80 59 00
Title of Work	:	The Norwegian Seismic Array (NORSAR) Phase 3
Amount of Contract	:	$ 3,083,528
Contract Period Covered by Report	:	1 October 1999 - 31 March 2000

NORSAR Contribution No. 687

Table of Contents

1 Summary

This Semiannual Technical Summary describes the operation, maintenance and research activities at the Norwegian Seismic Array (NOA), the Norwegian Regional Seismic Array (NORES), the Arctic Regional Seismic Array (ARCES) and the Spitsbergen Regional Array (SPITS) for the period 1 October 1999 - 31 March 2000. Statistics are also presented for additional seismic stations, which through cooperative agreements with institutions in the host countries provide continuous data to the NORSAR Data Processing Center (NPDC). These stations comprise the Finnish Regional Seismic Array (FINES), the Hagfors array in Sweden and the regional seismic array in Apatity, Russia.

Beginning 1 January 1999, the responsibility for funding the operational activities of the seismic field systems and the Norwegian National Data Center (NDC) has been taken over by the Norwegian Government, with the understanding that the funding of IMS-related activities will gradually be arranged through the CTBTO/PTS. Research activities described in this report, as well as transmission of selected data to the United States NDC, are continuing to be funded by the United States Department of Defense.

The NOA Detection Processing system has been operated throughout the period with an average uptime of 99.93%. A total of 1723 seismic events have been reported in the NOA monthly seismic bulletin for October 1999 through March 2000. The performance of the continuous alarm system and the data transmission to AFTAC has been satisfactory. Processing of requests for full NOA and regional array data on magnetic tapes has progressed according to established schedules.

This Semiannual Report also presents statistics from operation of the Regional Monitoring System (RMS). The RMS has been operated in a limited capacity, with continuous automatic detection and location and with analyst review of selected events of special interest for regional monitoring of Fennoscandia and adjacent regions. Data sources for the RMS have comprised all the regional arrays processed at NORSAR. The Generalized Beamforming (GBF) program continues to be used as a pre-processor to RMS.

On-line detection processing and data recording at the NORSAR Data Processing Center (NDPC) of NORES, ARCES and FINES data have been conducted throughout the period. Data from two small-aperture arrays at sites in Spitsbergen and Apatity, Kola Peninsula, as well as the Hagfors array in Sweden, have also been recorded and processed. Processing statistics for the arrays as well as results of the RMS analysis for the reporting period are given.

The operation of the regional arrays has proceeded normally in the period. Maintenance activities in the period comprise preventive/corrective maintenance as required in connection with all of the NOA subarrays as well as the refurbished ARCES array. Other activities have involved repair of defective electronic equipment, cable splicing and work in connection with the SPITS array. Work is also continuing in making the modifications required for formal certification of the NOA array.

A summary of the activities related to the GSETT-3 experiment and experience gained at the Norwegian NDC during the reporting period is provided in Section 4. Norway is now contributing primary station data from two seismic arrays: ARCES and NOA and one auxiliary array (SPITS). These data are being provided to the IDC via the global communications infrastructure (GCI). Continuous data from all three arrays are in addition being transmitted to the US NDC,

and continuous data from SPITS are transmitted to the PIDC. Our link to the PIDC is also used to transmit data from the NORES array and the NIL station in Pakistan. The transmission speed of the NORSAR-PIDC link was reduced on 8 March 2000 from 256 Kbps to 128 Kbps.

During September 1999, the ARCES array was upgraded with completely new electronics, under a contract with the Provisional Technical Secretariat (PTS). The ARCES data transmission, which includes the conversion of data to the CD1-format used by the IDC, has been carried out success-fully during the period, and ARCES processing at the PIDC has been proceeding normally after the installation was completed. The ARCES array is now in a testing and evaluation phase, and is expected to be considered for certification later this year.

The PrepCom has encouraged states that operate IMS-designated stations to continue to do so on a voluntary basis and in the framework of the GSETT-experiment until such time that the stations have been certified for formal inclusion in IMS. In line with this, we envisage continuing the pro-vision of data from Norwegian IMS-designated stations in accordance with current procedures.

Summaries of seven scientific and technical contributions are presented in Chapter 6 of this report.

Section 6.1 contains a report from the meeting of the IDC Technical Experts Group on Seismic Event Location in Oslo, Norway on 20-24 March 2000. This was the second meeting of the Experts Group in support of Working Group B of the CTBTO Preparatory Commission. At its first meeting in January 1999, the Experts Group developed plans and recommendations for a glo-bal calibration program, and presented its report to Working Group B in February 1999. The sec-ond meeting had the following objectives:

- To review proposals for detailed station-specific regional corrections to be applied for IMS stations in North America, Europe, North Africa, Asia and Australia
- To recommend a set of such corrections, including appropriate model errors, for incorporation into the Release 3 of the IDC software
- To develop a plan for future extensions and improvements of this regional correction data base, to be incorporated into future IDC software releases
- To review progress in the general recommendations from the January 1999 meeting, and make adjustments and updates to these recommendations as required.

The primary task of the meeting was to assess the status and availability of such calibration infor-mation for the regions being considered, and to plan for implementing regional location calibra-tion at the IDC, both for Release 3 of the IDC applications software and for implementation in the longer term. The second meeting was attended by sixty technical experts, coming from fifteen sig-natory countries and the Provisional Technical Secretariat. Dr. Frode Ringdal of Norway chaired the meeting.

The meeting was organized into four sessions, including Working Group discussions to address the technical issues in detail during the meeting. Topics were:

- Collection of Calibration Information
- Application of Calibration Information
- Validation of Calibration Information
- Specific recommendations for IDC Release 3

Detailed recommendations were developed for each of these subject matters, and will be pre-sented to Working Group B in Vienna during its May 2000 session.

Section 6.2 is entitled "Locating Seismic Events in Northern Eurasia" and is a summary of a paper presented at the Oslo location workshop. The paper discusses the application of the velocity model previously developed for the Barents region (the Barents model) to seismic events in a larger area, and compares the results to those obtained using the IASPEI-91 model. It concludes that the Barents model, which is known to give accurate locations in the Fennoscandian and NW Russia area, can be successfully applied to the more general northern Eurasia region. The paper also contains analysis of seismic events in specific regions of interest, and provides a table of ground truth locations (1 km accuracy) of a set of nuclear explosions at Novaya Zemlya, inferred from study of satellite imagery.

Section 6.3 is a follow-up study to the initial analysis of data from the Eurobridge experiment presented in the preceding Semiannual Technical Summary. Eurobridge comprised a 1130 km seismic refraction profile crossing the Baltic Shield in the northwest and the Ukrainian Shield in the southeast. There were three series of shots, one in 1995 and two in 1996. Observations of these explosions at the Fennoscandian arrays (ARCES, FINES, Hagfors, and NORES) provide an opportunity to check the accuracy of the travel-time tables in use at NORSAR for Fennoscandia. At the same time, these refraction shots provide a useful extension to the pIDC ground-truth database.

P-phases from most of the Eurobridge shots were observed at the FINES, HAGFORS and NORES arrays, and even at the more distant ARCES array as many as 12 out of the 29 events were seen. We have investigated in detail observed deviations in P-wave travel times from those predictions by the Fennoscandian crustal and upper mantle velocity model. Our study has revealed several instances of documented timing errors at the various arrays. Even when accounting for these timing errors, there remains a considerable scatter in the travel times as compared to the theoretical model. The interpretation of these anomalies in terms of crustal and upper mantle structure is not obvious. An important outcome of this study is the development of a method to identify possible timing anomalies at IMS stations. This method could be useful both in validating calibration data and in providing a tool for continuously checking the timing accuracy and consistency of IMS stations.

Section 6.4 contains an analysis of data recorded at the SPITS array for some recent profiling experiments near Spitsbergen. Data from airgun shots in the water as well as small underwater explosions of 25 to 50 kg conventional explosives could be observed at distances up to 350 km when using the double-beam technique for SNR enhancement. Not unexpectedly, the study has demonstrated that the crust and uppermost mantle around the SPITS station is very heterogeneous. However, with the exact travel times available through this study for different azimuths in the range 0-3 degrees, the location and detection processing of local and near-regional events at SPITS will be considerably improved.

This is particularly important because there are large numbers of local events recorded at SPITS every day, and a correct location and phase identification will help eliminate these phases from interfering in the Generalized Beamforming process for network association and event definition analysis. Furthermore, the ground-truth data base developed during this study will be used to reanalyze in more detail the large observed slowness deviations at SPITS reported in previous Semiannual Technical Summaries.

Section 6.5 addresses the waveform quality of SPITS recordings. The problem of spikes in the data streams for individual sensors (in particular the SPB5_sz sensor) has been a recurring problem at this array. Until the problem can be technically corrected, which will probably require a complete refurbishment of the array electronics, it is important to automatically identify and (if possible) correct these spikes so that they do not interfere with the array detection analysis.

In this contribution, a new method to detect and correct for one-sample spikes (which is the most typical spike observed at SPITS channels) is developed and tested. A particular challenge has been to develop an algorithm that does not trigger any spike correction on real, impulsive signals, which are quite often seen at this array. The paper concludes that the spike detector and the corresponding data correction procedure provides an efficient method to identify and remove one-sample spikes from the seismic data stream, and that the procedure could be useful for general application to systems that experience similar kinds of technical problems.

Section 6.6 is entitled: "Third Level Seismo-geographical Regionalization of Fennoscandia". This work has been undertaken by the Nordic countries in response to an initiative by IASPEI in 1985. The purpose is to refine the current global regionalization, which has two levels: Level 1 (Gutenberg-Richter) comprising 50 regions, and Level 2 (Flinn-Engdahl) with 728 regions.

The detailed zonation presented in this contribution comprises 74 regions for the Level 3 zonation of Fennoscandia. This is almost an order of magnitude more than the corresponding Flinn-Engdahl subdivision, which has about 10 regions covering this area. The regions along the outer borders of the Nordic countries have been defined in cooperation with those countries for which Level 3 regionalization already exists. The Level 3 zonation described in this paper has been implemented in the current NORSAR regional seismic bulletin production.

Section 6.7 is a study of the crustal structure of the Barents Sea, with a discussion of how the crustal configuration and composition affects regional models for seismic velocities and travel-times. In recent years, deep seismic reflection and refraction data have greatly improved our understanding of the deep basins and the underlying crystalline crust in the Barents Sea and of the crustal transition across the western continental margin. The data base for the present study includes a comprehensive set of such profiles along with gravity and magnetic data as well as general geological information. The crustal and seismic velocity structure of the Barents Sea is found to vary significantly, and the approximate range is as follows:

- Thickness of sedimentary cover varies between 0 – 20 km
- Depth to Moho varies between 20 – 45 km
- Thickness of crystalline crust varies between 10 – 45 km

The crustal heterogeneity of the Barents Sea region implies that very detailed regional travel-time models may be required for accurately locating seismic events in this region.

Frode Ringdal

2   Operation of International Monitoring System (IMS) Stations in Norway

2.1   PS27 — Primary Seismic Station NOA

The average recording time was 99.93% as compared to 99.77% for the previous reporting period.

Table 2.1.1 lists the reasons for and times of the main outages in the reporting period.

Date	Time	Cause
30 Dec	1604 - 1710	Problems at NDPC
09 Jan	1526 - 1720	Problems at NDPC

Table 2.1.1. *The major downtimes in the period 1 October 1999 - 31 March 2000.*

Monthly uptimes for the NORSAR on-line data recording task, taking into account all factors (field installations, transmissions line, data center operation) affecting this task were as follows:

October 99	:	100.00%
November	:	100.00%
December	:	99.84%
January 00	:	99.74%
February	:	100.00%
March	:	100.00%

J. Torstveit

RD3NB2 uptime for Oct. 1999 (This month: 100.00 percent)

RD3NB2 uptime for Nov. 1999 (This month: 100.00 percent)

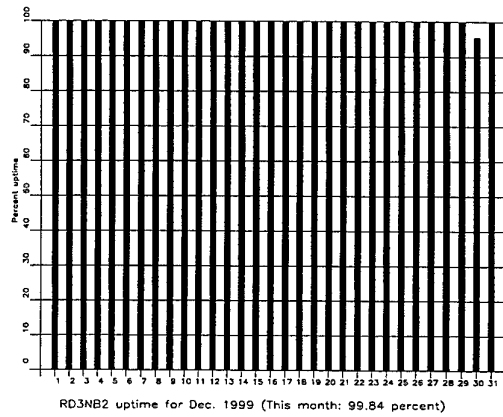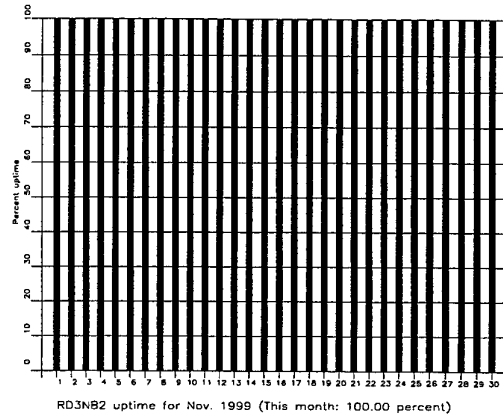RD3NB2 uptime for Dec. 1999 (This month: 99.84 percent)
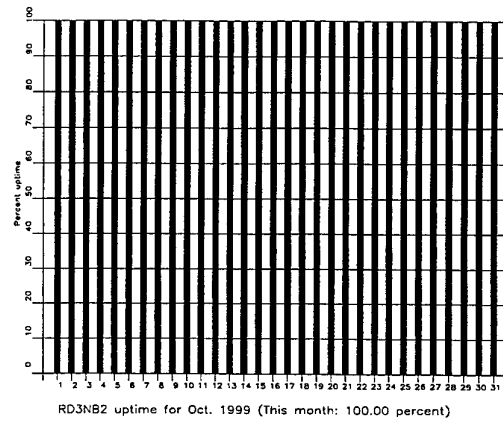
Fig. 2.1.1. *The figure shows the uptime for the data recording task, or equivalently, the availability of NOA data in our tape archive, on a day-by-day basis, for the reporting period. (Page 1 of 2, Oct-Dec 1999).*
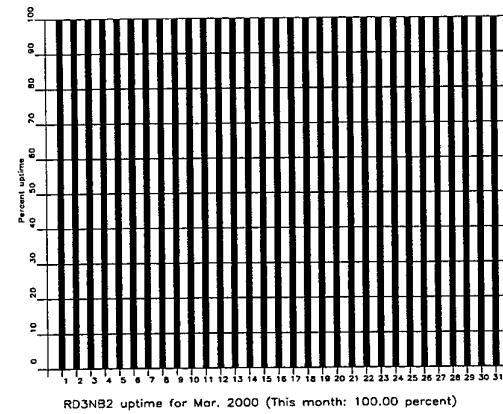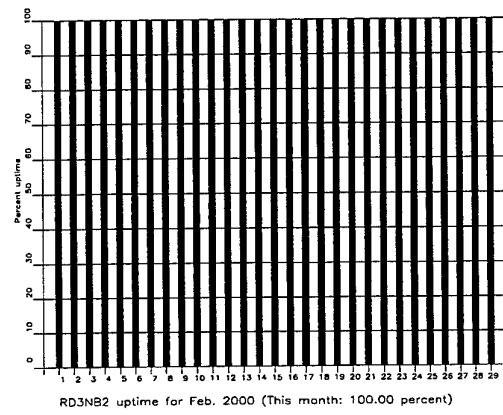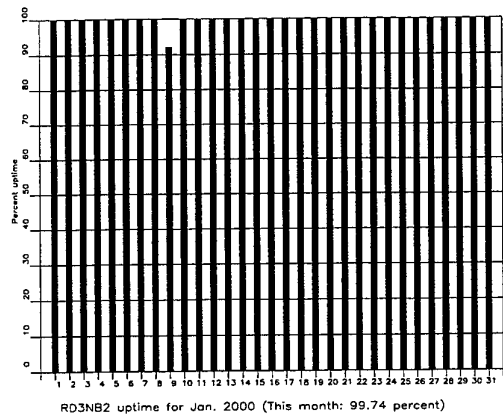
RD3NB2 uptime for Jan. 2000 (This month: 99.74 percent)

RD3NB2 uptime for Feb. 2000 (This month: 100.00 percent)

RD3NB2 uptime for Mar. 2000 (This month: 100.00 percent)

Fig. 2.1.1. *(cont.) (Page 2 of 2, Jan-Mar 2000).*

NOA Event Detection Operation

In Table 2.1.2 some monthly statistics of the Detection and Event Processor operation are given. The table lists the total number of detections (DPX) triggered by the on-line detector, the total number of detections processed by the automatic event processor (EPX) and the total number of events accepted after analyst review (teleseismic phases, core phases and total).

	Total DPX	Total EPX	Accepted Events		Sum	Daily
			P-phases	Core Phases		
Oct 99	10,382	834	242	55	297	9.6
Nov 99	11,561	895	301	49	350	11.7
Dec 99	12,017	879	254	62	316	10.2
Jan 00	11,850	843	187	65	252	8.1
Feb 00	12,066	1036	171	44	215	7.4
Mar 00	11,886	886	225	68	293	9.5
	69,762	5373	1380	343	1723	9.4

Table 2.1.2. *Detection and Event Processor statistics, 1 October 1999 - 31 March 2000.*

NOA detections

The number of detections (phases) reported by the NORSAR detector during day 274, 1999, through day 092 , 2000, was 69,762, giving an average of 381 detections per processed day (183 days processed).

B. Paulsen

U. Baadshaug

2.2   PS28 — Primary Seismic Station ARCES

The average recording time was 98.90% as compared to 99.72% for the previous period.

Table 2.2.1 lists the reasons for and times of the main outages in the reporting period.

Date	Time			Cause
18 Oct	0944	-	1050	System test
19 Oct	0415	-	0545	System test
21 Oct	0819	-	0943	System test
10 Nov	1301	-	1549	System test
15 Nov	1340	-	1410	System test
19 Nov	0000	-	0858	System test
22 Nov	1035	-	1052	System test
24 Nov	0742	-	0808	System test
24 Nov	0914	-	1008	System test
26 Nov	1326	-	1442	System test
29 Nov	1211	-	1231	System test
30 Nov	1447	-	1550	System test
01 Dec	1111	-	1134	System test
20 Jan	1601	-	2222	Hub failure
28 Jan	0904	-	0921	Hub failure

Table 2.2.1. *The main interruptions in recording of ARCES data at NDPC 1 October 1999- 31 March 2000.*

Monthly uptimes for the ARCESS on-line data recording task, taking into account all factors (field installations, transmission lines, data center operation) affecting this task were as follows:

October 99	:	99.35%
November	:	97.47%
December	:	99.83%
January 00	:	98.92%
February	:	99.49%
March	:	98.35%

J. Torstveit

ARCESS uptime for Oct. 1999 (This month: 99.35 percent)

ARCESS uptime for Nov. 1999 (This month: 97.47 percent)

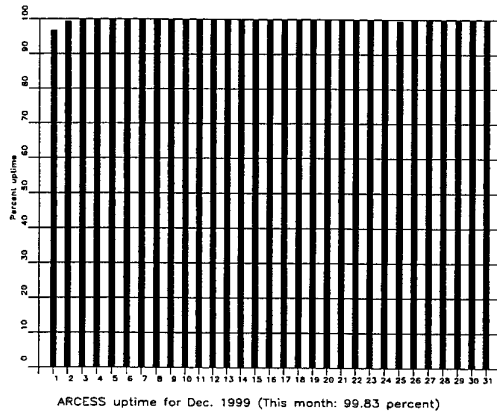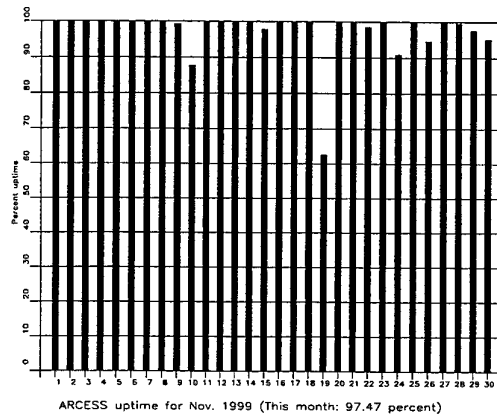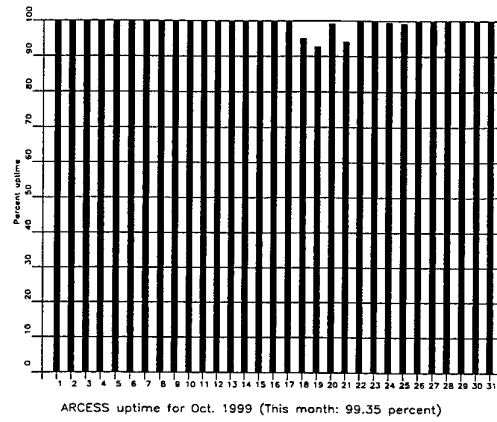ARCESS uptime for Dec. 1999 (This month: 99.83 percent)

Fig. 2.2.1. *The figure shows the uptime for the data recording task, or equivalently, the availability of ARCES data in our tape archive, on a day-by-day basis, for the reporting period. (Page 1 of 2, Oct-Dec 1999)*
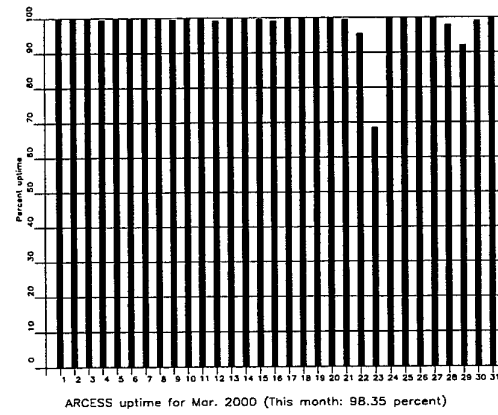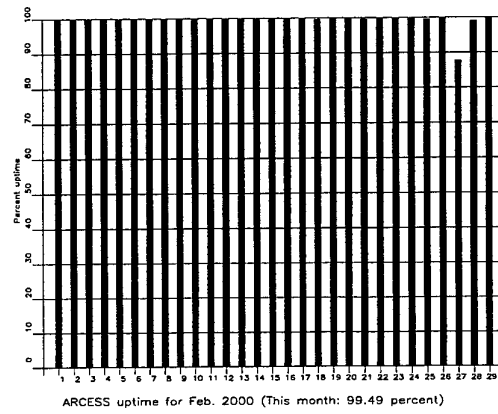
ARCESS uptime for Jan. 2000 (This month: 98.92 percent)

ARCESS uptime for Feb. 2000 (This month: 99.49 percent)

ARCESS uptime for Mar. 2000 (This month: 98.35 percent)
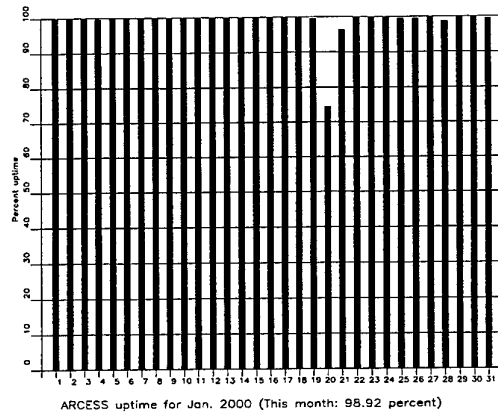
Fig. 2.2.1 *(cont.) (Page 2 of 2, Jan-Mar 2000).*

Event Detection Operation

ARCES detections

The number of detections (phases) reported during day 274, 1999, through day 092, 2000, was 136,824, giving an average of 748 detections per processed day (183 days processed).

Events automatically located by ARCES

During days 274, 1999, through 092, 2000, 7916 local and regional events were located by ARCES, based on automatic association of P- and S-type arrivals. This gives an average of 43.0 events per processed day (184 days processed). 53% of these events are within 300 km, and 81% of these events are within 1000 km.

U. Baadshaug

2.3   AS72 — Auxiliary Seismic Station Spitsbergen

The average recording time was 95.50% as compared to 97.53% for the previous reporting period.

Table 2.3.1 lists the reasons for and time periods of the main downtimes in the reporting period.

Date	Time	Cause
04 OCT	2200-2254	Communication failure
04 OCT	2318-2349	Communication failure
11 OCT	1404-1420	Communication failure
15 OCT	1042-1508	Communication failure, most data lost
25 OCT	1041-1140	Communication failure
25 OCT	1230-1243	Communication failure
25 OCT	1323-1340	Communication failure
25 OCT	1503-1521	Communication failure
25 OCT	1618-1634	Communication failure
25 OCT	1728-1745	Communication failure
25 OCT	1823-1839	Communication failure
25 OCT	1928-1946	Communication failure
25 OCT	2107-2120	Communication failure
25 OCT	2306-2320	Communication failure
26 OCT	0112-0124	Communication failure
26 OCT	0207-0221	Communication failure
26 OCT	0323-0338	Communication failure
26 OCT	0442-0455	Communication failure
26 OCT	0545-0558	Communication failure
03 NOV	0955-1010	Communication failure
03 NOV	1045-1100	Communication failure
03 NOV	1151-1203	Communication failure
03 NOV	1218-1234	Communication failure
03 NOV	1251-1304	Communication failure
03 NOV	1326-1338	Communication failure
03 NOV	1428-1445	Communication failure
03 NOV	1555-1608	Communication failure
03 NOV	1724-1739	Communication failure
03 NOV	1918-1933	Communication failure
03 NOV	1958-2013	Communication failure

Date	Time	Cause
03 NOV	2032-2043	Communication failure
03 NOV	2132-2144	Communication failure
03 NOV	2227-2240	Communication failure
03 NOV	2350-0004	Communication failure
04 NOV	0033-0048	Communication failure
04 NOV	0206-0218	Communication failure
04 NOV	0345-0358	Communication failure
04 NOV	0444-0506	Communication failure
04 NOV	2213-2229	Communication failure
04 NOV	2317-2330	Communication failure
05 NOV	0013-0030	Communication failure
05 NOV	0348-0404	Communication failure
05 NOV	0623-0638	Communication failure
05 NOV	0724-0738	Communication failure
05 NOV	1010-1025	Communication failure
05 NOV	1213-1229	Communication failure
05 NOV	1339-1352	Communication failure
05 NOV	1554-1610	Communication failure
05 NOV	1714-1730	Communication failure
05 NOV	1843-1901	Communication failure
05 NOV	2009-2025	Communication failure
05 NOV	2253-2308	Communication failure
06 NOV	0003-0019	Communication failure
06 NOV	0157-0209	Communication failure
06 NOV	0306-0319	Communication failure
06 NOV	0419-0433	Communication failure
06 NOV	0458-0513	Communication failure
06 NOV	0521-0541	Communication failure
06 NOV	0553-0608	Communication failure
06 NOV	0633-0648	Communication failure
06 NOV	0729-0745	Communication failure
06 NOV	0835-0849	Communication failure
06 NOV	0920-0933	Communication failure
06 NOV	1022-1040	Communication failure
06 NOV	1148-1204	Communication failure

Date	Time	Cause
06 NOV	1447-1501	Communication failure
08 NOV	1203-1244	Communication failure
08 NOV	1303-1318	Communication failure
12 NOV	1326-1608	Communication failure
14 NOV	1709-	Communication failure
15 NOV	-0215	Communication failure
15 NOV	0734-0749	Communication failure
16 NOV	0917-0950	Communication failure
16 NOV	1008-1023	Communication failure
17 NOV	1224-1310	Communication failure
18 NOV	1243-	Communication failure
19 NOV	-1128	Communication failure
20 NOV	1507-1816	Communication failure
21 NOV	1729-2052	Communication failure
04 DEC	0501-0853	Communication failure
16 DEC	0237-0700	Communication failure
23 DEC	0802-0825	Communication failure
23 DEC	1001-1019	Communication failure
24 DEC	1512-2341	Communication failure
28 DEC	1024-1048	Communication failure
19 JAN	1118-	Y2k problem with NORAC
22 JAN	-1119	--
07 FEB	0346-	Power failure array, windmill broken
08 FEB	-1549	--

Table 2.3.1. *The main interruptions in recording of Spitsbergen data at NDPC, 1 October 1999 - 31 March 2000.*

Monthly uptimes for the Spitsbergen on-line data recording task, taking into account all factors (field installations, transmissions line, data center operation) affecting this task were as follows:

October 99	:	98.67%
November	:	92.01%
December	:	97.56%
January 00	:	90.12%
February	:	94.82%
March	:	99.82%

J. Torstveit

RD3SVA uptime for Oct. 1999 (This month: 98.67 percent)

RD3SVA uptime for Nov. 1999 (This month: 92.01 percent)

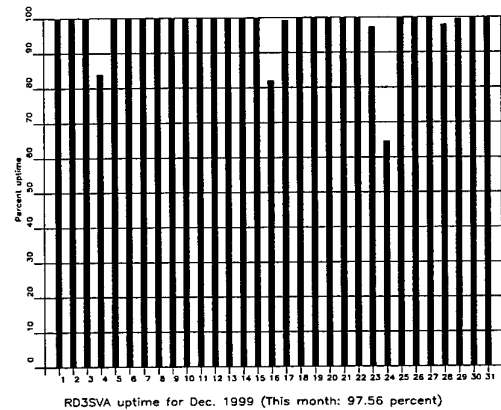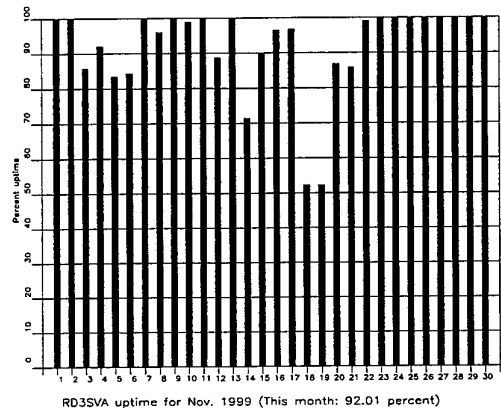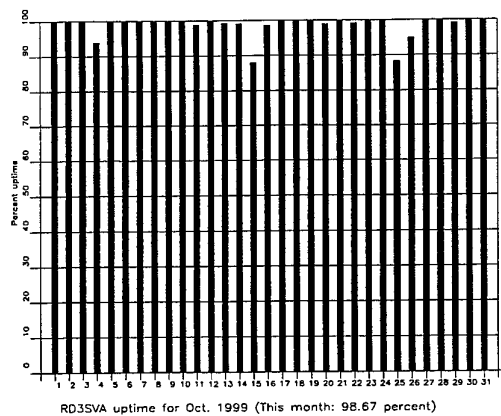RD3SVA uptime for Dec. 1999 (This month: 97.56 percent)

Fig. 2.3.1. *The figure shows the uptime for the data recording task, or equivalently, the availability of Spitsbergen data in our tape archive, on a day-by-day basis, for the reporting period. (Page 1 of 2, Oct-Dec 1999).*
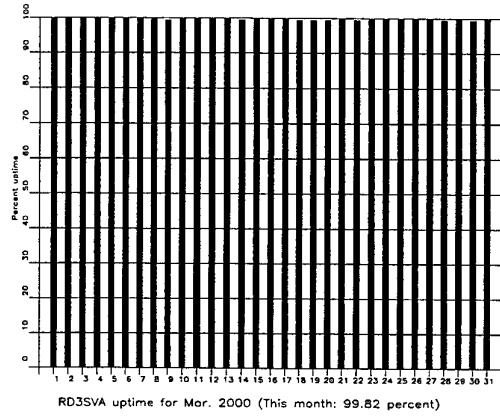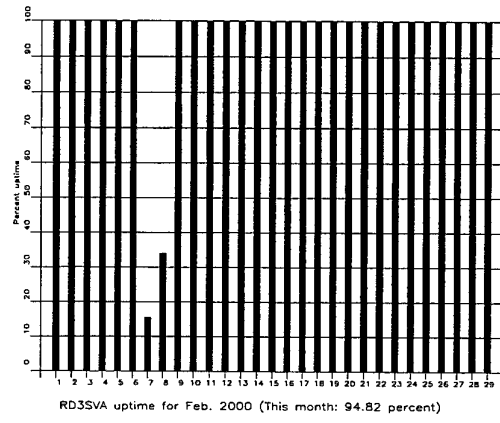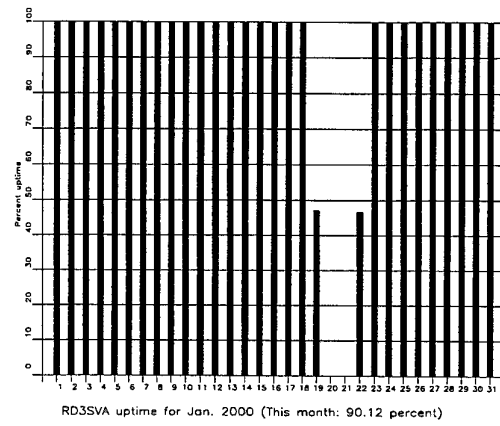
RD3SVA uptime for Jan. 2000 (This month: 90.12 percent)

RD3SVA uptime for Feb. 2000 (This month: 94.82 percent)

RD3SVA uptime for Mar. 2000 (This month: 99.82 percent)

Fig. 2.3.1 *(cont.) (Page 2 of 2, Jan-Mar 2000).*

Event Detection Operation

Spitsbergen array detections

The number of detections (phases) reported from day 274, 1999, through day 092, 2000, was 172,051, giving an average of 951 detections per processed day (181 days processed).

Events automatically located by the Spitsbergen array

During days 274, 1999, through 092, 2000, 17,538 local and regional events were located by the Spitsbergen array, based on automatic association of P- and S-type arrivals. This gives an average of 96.4 events per processed day (182 days processed). 72% of these events are within 300 km, and 87% of these events are within 1000 km.

U. Baadshaug

2.4 AS73 — Auxiliary Seismic Station Jan Mayen

The IMS auxiliary seismic network will include a three-component station at the Norwegian island of Jan Mayen. The station location given in the protocol to the Comprehensive Nuclear Test-Ban Treaty is 70.9°N, 8.7°W.

The University of Bergen has operated a seismic station at this location since 1970. An investment in the new station at Jan Mayen will be made in due course and in accordance with Prep-Com budget decisions. In the meanwhile, NORSAR has, in cooperation with the University of Bergen, been looking into technical possibilities of transmitting data from the existing station at Jan Mayen. A VSAT link for this purpose was installed in April 2000, and data from the existing seismic station at Jan Mayen are now transmitted to the NDC at Kjeller and to the University of Bergen.

S. Mykkeltveit

2.5 IS37 — Infrasound Station at Karasjok

The IMS infrasound network will include a station at Karasjok in northern Norway. The coordinates given for this station are 69.5°N, 25.5°E. These coordinates coincide with those of the primary seismic station PS28.

A site survey for this station was carried out during June/July 1998 as a cooperative effort between the Provisional Technical Secretariat of the CTBTO and NORSAR. Analysis of the data collected at several potential locations for this station in and around Karasjok has been completed. The results of this analysis have lead to a recommendation on the exact location of the infrasound station. Planning work for installation at this site has commenced, and will result in an application to the relevant local authorities to obtain the permissions required in this regard. We expect station installation to take place in the year 2001.

S. Mykkeltveit

2.6 RN49 — Radionuclide Station on Spitsbergen

The IMS radionuclide network will include a station at Longyearbyen on the island of Spitsbergen, at location 78.2°N, 16.4°E. These coordinates coincide with those of the auxiliary seismic station AS72. According to PrepCom decision, this station will also be among those IMS radionuclide stations that will have a capability of monitoring for the presence of relevant noble gases upon entry into force of the CTBT.

A site survey for this station was carried out in August of 1999 by NORSAR, in cooperation with the Norwegian Radiation Protection Authority. The site survey report to the PTS contains a recommendation to establish this station at Platåberget, some 20 km away from the Treaty location. The PrepCom approved the corresponding coordinate change in its meeting in May 2000. The station installation is part of PrepCom's work program for the year 2000.

S. Mykkeltveit

3   Operation of Regional Seismic Arrays

3.1   NORES

Average recording time was 98.67 as compared to 99.33 for the previous period.

Table 3.1.1 lists the reasons for and times of the main outages in the reporting period.

Date	Time			Cause
14 Oct	1439	-	1640	Power break NDPC
16 Feb	1114	-		Upgrading field installations
17 Feb		-	1503	
24 Feb	0635	-		Upgrading field installations
25 Feb		-	1120	

Table 3.1.1. *The main interruptions in recording of NORES data at the NDC 1 October 1999 - 31 March 2000.*

Monthly uptimes for the NORES on-line data recording task, taking into account all factors (field installations, transmissions line, data center operation) affecting this task were as follows

October 99	:	99.68%
November	:	99.99%
December	:	99.99%
January 00	:	99.91%
February	:	91.85%
March	:	100.00%

J. Torstveit

NNORES uptime for Oct. 1999 (This month: 99.68 percent)

NNORES uptime for Nov. 1999 (This month: 99.99 percent)

NNORES uptime for Dec. 1999 (This month: 99.99 percent)
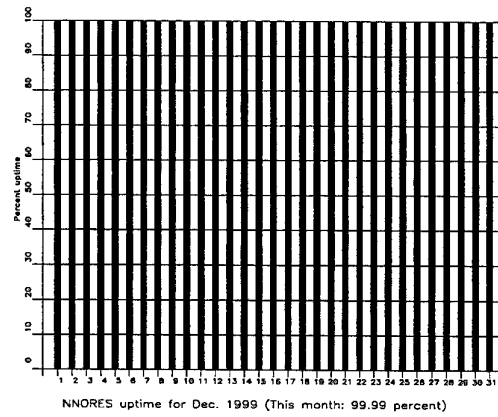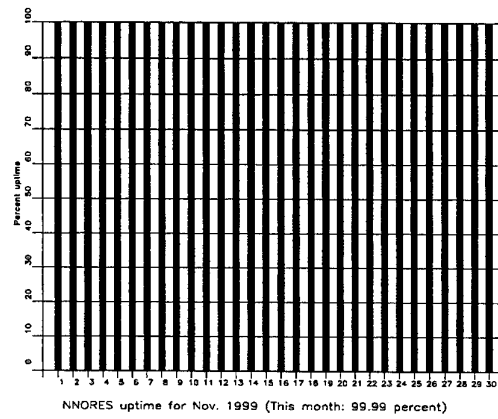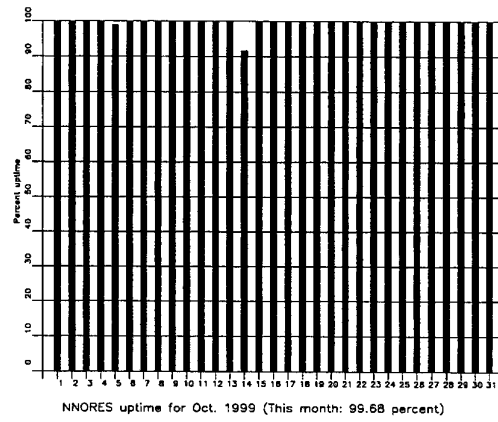
Fig. 3.1.1. *The figure shows the uptime for the data recording task, or equivalently, the availability of NORES data in our tape archive, on a day-by-day basis, for the reporting period (Page 1 of 2, Oct-Dec 1999).*
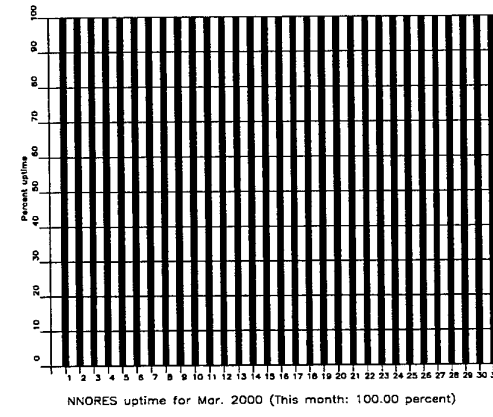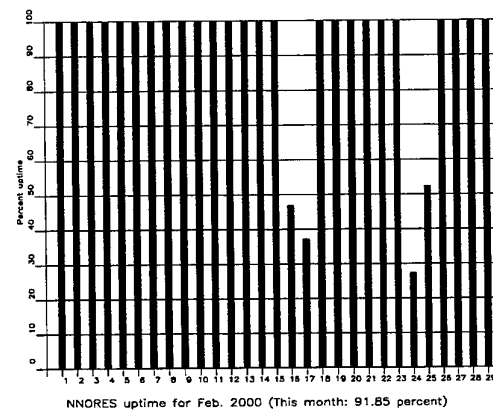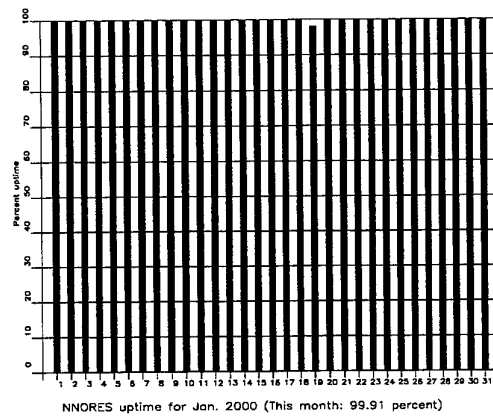
NNORES uptime for Jan. 2000 (This month: 99.91 percent)

NNORES uptime for Feb. 2000 (This month: 91.85 percent)

NNORES uptime for Mar. 2000 (This month: 100.00 percent)

Fig. 3.1.1 *(cont.) (Page 2 of 2, Jan-Mar 2000).*

NORES Event Detection Operation

NORES detections

The number of detections (phases) reported from day 274, 1999, through day 092, 2000, was 79,645, giving an average of 435 detections per processed day (183 days processed).

Events automatically located by NORES

During days 274, 1999, through 092, 2000, 2591 local and regional events were located by NORES, based on automatic association of P- and S-type arrivals. This gives an average of 14.1 events per processed day (184 days processed). 59% of these events are within 300 km, and 84% of these events are within 1000 km.

U. Baadshaug

3.2   Hagfors (IMS Station AS101)

The average recording time was 97.02% as compared to 99.99% for the previous reporting period.

Table 3.2.1 lists the reasons for and times of the main outages in the reporting period.

Date	Time			Cause
28 Oct	0900	-	0930	Hardware maintenance NDPC
17 Nov	2036	-		Upgrading hard- and software at
19 Nov		-	0944	NDPC and field
16 Dec	2105	-		Problems at field installations
21 Dec		-	1059	
22 Dec	1923	-		Problems at field installations
23 Dec		-	0833	
27 Dec	0953	-	1114	Problems at field installations

Table 3.2.1. *The main interruptions in Hagfors recordings at the NDC, 1 October 1999 - 31 March 2000.*

Monthly uptimes for the Hagfors on-line data recording task, taking into account all factors (field installations, transmissions line, data center operation) affecting this task were as follows:

October 99	:	99.93%
November	:	94.84%
December	:	87.36%
January 00	:	100.00%
August	:	100.00%
September	:	100.00%

J. Torstveit

RD3HFS uptime for Oct. 1999 (This month: 99.93 percent)

RD3HFS uptime for Nov. 1999 (This month: 94.84 percent)

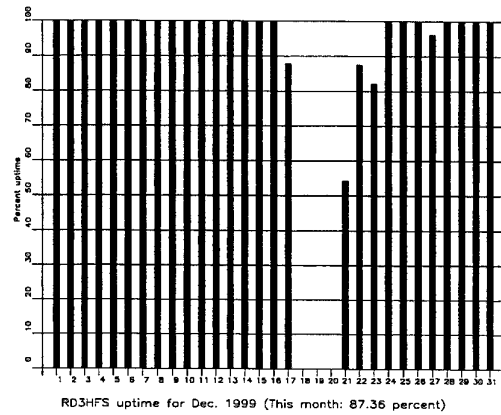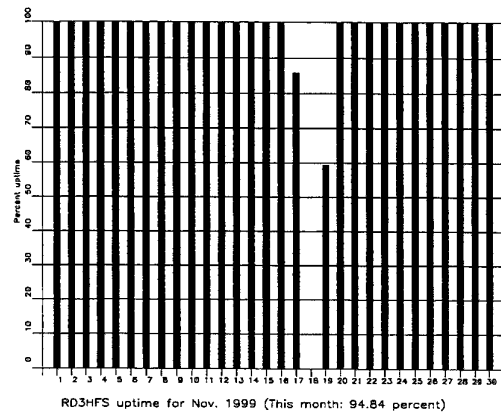RD3HFS uptime for Dec. 1999 (This month: 87.36 percent)
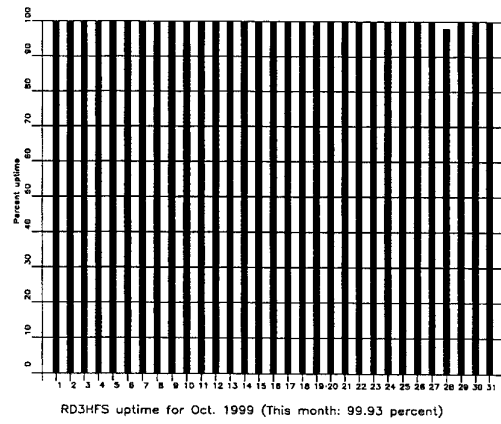
Fig. 3.2.1. *The figure shows the uptime for the data recording task, or equivalently, the availability of Hagfors data in our tape archive, on a day-by-day basis, for the reporting period (Page 1 of 2, Oct-Dec 1999).*
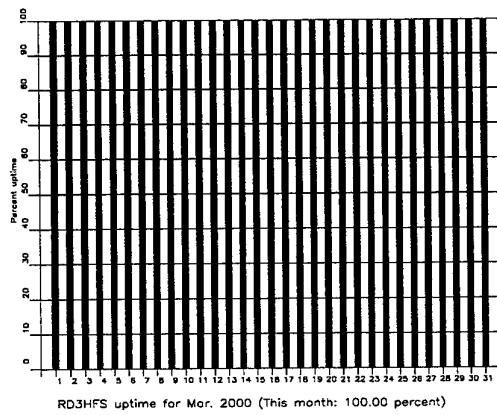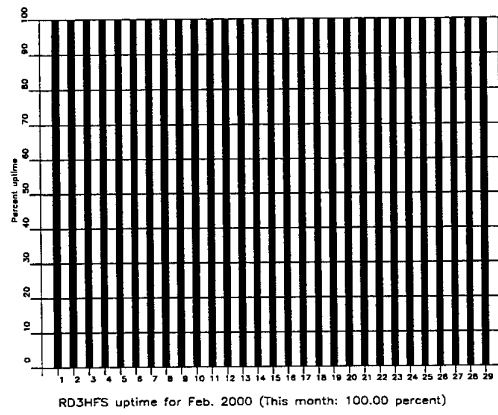
RD3HFS uptime for Jan. 2000 (This month: 100.00 percent)

RD3HFS uptime for Feb. 2000 (This month: 100.00 percent)

RD3HFS uptime for Mar. 2000 (This month: 100.00 percent)
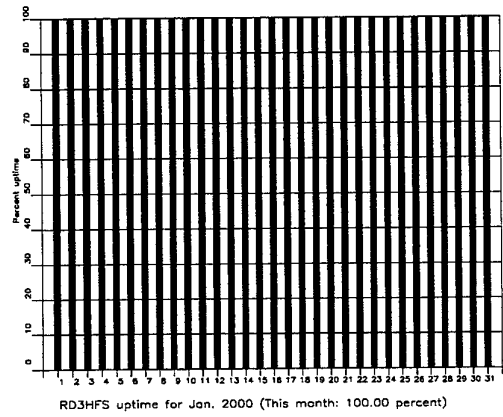
Fig. 3.2.1 *(cont.) (Page 2 of 2, Jan-Mar 2000).*

Hagfors Event Detection Operation

Hagfors array detections

The number of detections (phases) reported from day 274, 1999, through day 092, 2000, was 109,532, giving an average of 605 detections per processed day (181 days processed).

Events automatically located by the Hagfors array

During days 274, 1999, through 092, 2000, 2511 local and regional events were located by the Hagfors array, based on automatic association of P- and S-type arrivals. This gives an average of 14.3 events per processed day (175 days processed). 57% of these events are within 300 km, and 83% of these events are within 1000 km.

U. Baadshaug

3.3   FINES

The average recording time was 93.67% as compared to 73.78% for the previous reporting period.

Table 3.3.1 lists the reasons for and times of the main outages during the reporting period.

Date	Time	Cause
07 Oct	2355-	Problems in Helsinki
08 Oct	-0053	
30 Oct	0940-2017	Problems in Helsinki
31 Oct	0706-0743	Problems in Helsinki
31 Oct	0845-1015	Problems in Helsinki
31 Oct	1135-1248	Problems in Helsinki
08 Dec	0901-1538	Upgrading UPS in Helsinki
06 Jan	1152-1416	Problems with SIM in Helsinki
07 Jan	1017-	Problems with UPS in Helsinki
12 Jan	-1115	
13 Jan	1624-1641	Problems in Helsinki
13 Jan	1828-	Problems in Helsinki
14 Jan	-0857	
14 Jan	1057-1218	Problems in Helsinki
29 Jan	2010-	Problems in Helsinki
30 Jan	-0939	
05 Feb	0130-0847	Problems with SIM in Helsinki
07 Feb	0304-0606	Problems with SIM in Helsinki
07 Feb	1028-1158	Problems with SIM in Helsinki
08 Feb	0510-0530	Problems in Helsinki
10 Feb	1014-1107	Problems in Helsinki
11 Feb	1805-1848	Problems in Helsinki
14 Feb	0737-0758	Problems in Helsinki
14 Feb	1410-1442	Problems in Helsinki
17 Feb	2219-2245	Problems in Helsinki
18 Feb	0026-0611	Problems in Helsinki
21 Feb	0053-0749	Problems in Helsinki
24 Feb	0906-1023	Software upgrade in Helsinki
24 Feb	1119-1349	Software upgrade in Helsinki
26 Feb	2208-2339	Problems in Helsinki

Date	Time	Cause
23 Mar	0721-	Firewall problems in Helsinki
26 Mar	-0705	Firewall problems in Helsinki

Table 3.3.1. *The main interruptions in FINES recordings at the NDC, 1 October 1999 - 31 March 2000.*

Monthly uptimes for the FINES on-line data recording task, taking into account all factors (field installations, transmissions line, data center operation) affecting this task were as follows:

October 99	:	97.99%
November	:	100.00%
December	:	99.11%
January 00	:	79.42%
February	:	95.14%
March	:	90.33%

J. Torstveit
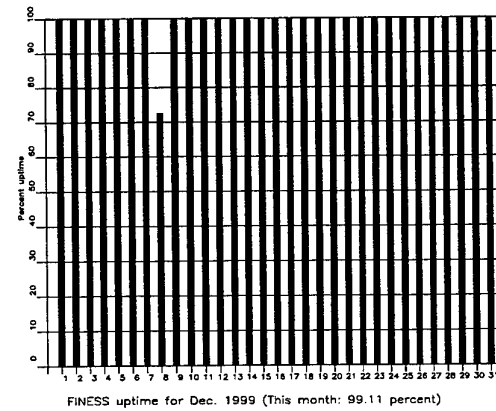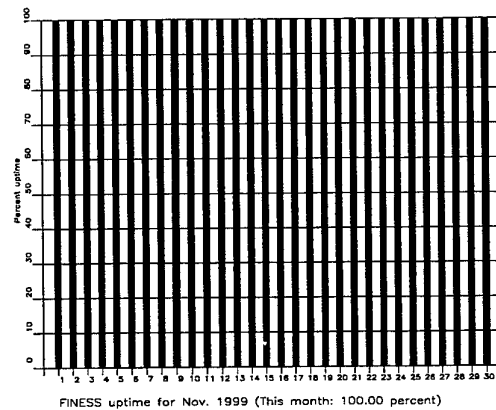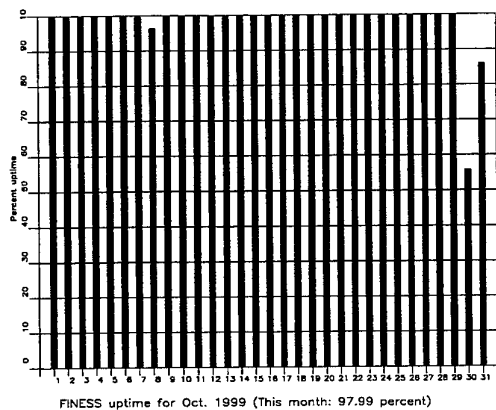
Fig. 3.3.1. *The figure shows the uptime for the data recording task, or equivalently, the availability of FINES data in our tape archive, on a day-by-day basis, for the reporting period (Page 1 of 2, Oct-Dec 1999).*

FINESS uptime for Jan. 2000 (This month: 79.42 percent)

FINESS uptime for Feb. 2000 (This month: 95.14 percent)

FINESS uptime for Mar. 2000 (This month: 90.33 percent)
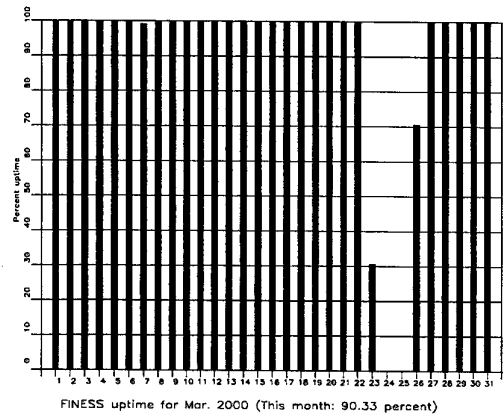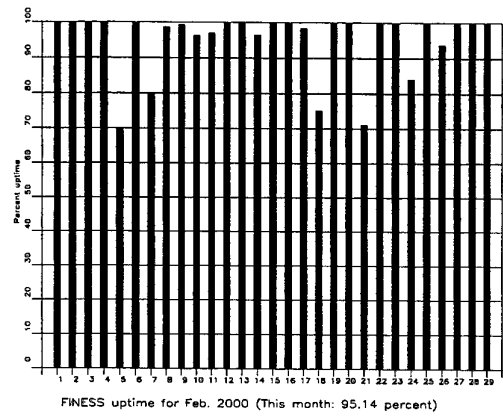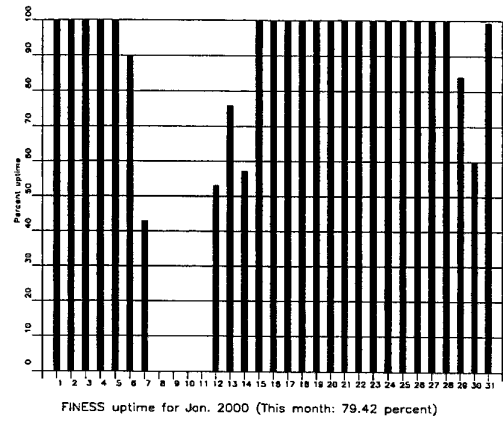
Fig. 3.3.1 *(cont.) (Page 2 of 2, Jan-Mar 2000)*

FINES Event Detection Operation

FINES detections

The number of detections (phases) reported during day 2874, 1999, through day 092, 2000, was 42,002, giving an average of 237 detections per processed day (177 days processed).

Events automatically located by FINES

During days 274, 1999, through 092, 2000, 3603 local and regional events were located by FINESS, based on automatic association of P- and S-type arrivals. This gives an average of 20.4 events per processed day (177 days processed). 77% of these events are within 300 km, and 89% of these events are within 1000 km.

U. Baadshaug

3.4   Apatity

The average recording time was 96.14% in the reporting period compared to 99.01% during the previous period.

Table 3.4.1 lists the reasons for and times of the main outages during the reporting period.

Date	Time	Cause
08 Oct	1127-1149	Stop in Apatity
29 Oct	1507-1539	Stop in Apatity
01 Nov	0636-0658	Stop in Apatity
01 Nov	1041-1258	Stop in Apatity
10 Nov	0723-0853	Stop in Apatity
10 Nov	1141-1231	Stop in Apatity
12 Nov	0704-0909	Stop in Apatity
11 Dec	0602-0919	Stop in Apatity
13 Dec	0919-1111	Upgrading hardware in Apatity
13 Dec	1257-1449	Upgrading hardware in Apatity
13 Dec	1547-1557	Upgrading hardware in Apatity
03 Jan	0404-0432	Hardware problems in Apatity
03 Jan 04 Jan	0841- -0655	Hardware problems in Apatity
17 Jan	1005-1151	Hardware problems in Apatity
19 Jan	1249-1654	Hardware problems in Apatity
24 Jan 25 Jan	1304- -0721	Hardware problems in Apatity
25 Jan 26 Jan	0820- -0649	Hardware problems in Apatity
26 Jan	1000-1045	Hardware problems in Apatity
26 Jan	1125-1152	Hardware problems in Apatity
26 Jan	1224-1308	Hardware problems in Apatity
26 Jan 27 Jan	1613- -0907	Hardware problems in Apatity
27 Jan	1021-1059	Hardware problems in Apatity
27 Jan	1349-1405	Hardware problems in Apatity
28 Jan	1936-1956	Hardware problems in Apatity
28 Jan 30 Jan	2016- -1256	Hardware problems in Apatity
31 Jan	1312-	Hardware problems in Apatity

Date	Time	Cause
01 Feb	-1345	Hardware problems in Apatity
13 Feb	1405-1420	Stop in Apatity
21 Mar	1001-1026	Stop in Apatity
23 Mar	1000-1030	Stop in Apatity

Table 3.4.1. *The main interruptions in Apatity recordings at the NDC, 1 October 1999 - 31 March 2000.*

Monthly uptimes for the Apatity on-line data recording task, taking into account all factors (field installations, transmissions line, data center operation) affecting this task were as follows:

October 99	:	99.86%
November	:	99.02%
December	:	98.99%
January 00	:	81.09%
February	:	97.99%
March	:	99.88%

J. Torstveit

RD3APA uptime for Oct. 1999 (This month: 99.86 percent)

RD3APA uptime for Nov. 1999 (This month: 99.02 percent)

RD3APA uptime for Dec. 1999 (This month: 98.99 percent)
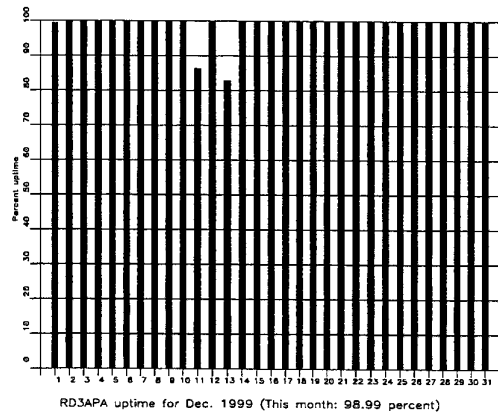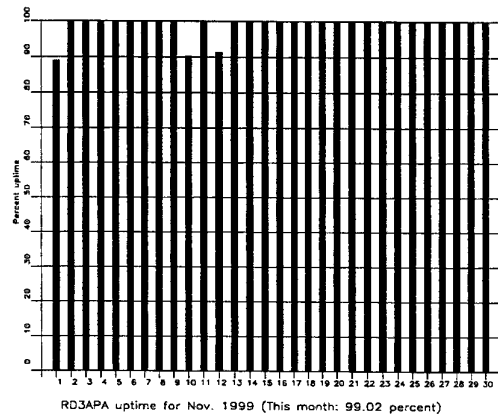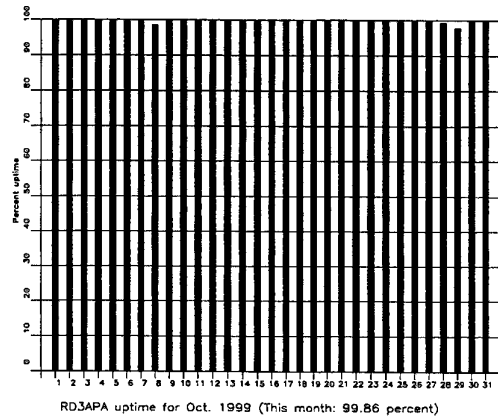
Fig. 3.4.1. *The figure shows the uptime for the data recording task, or equivalently, the availability of Apatity data in our tape archive, on a day-by-day basis, for the reporting period (Page 1 of 2, Oct-Dec 1999).*
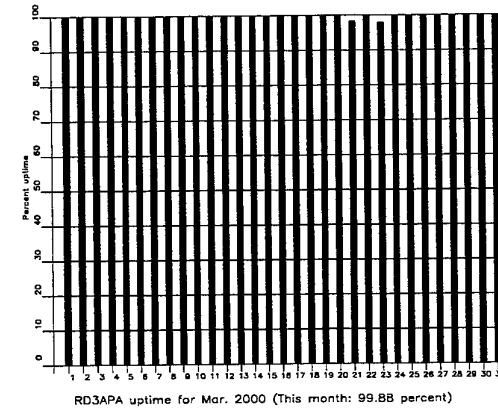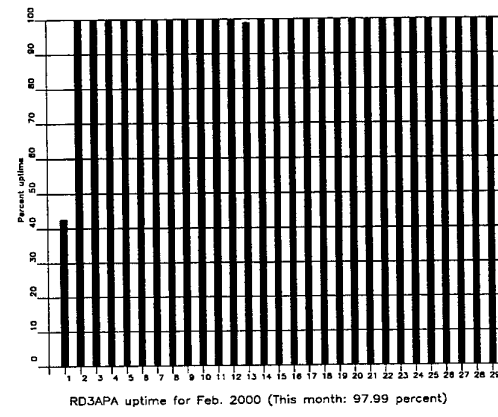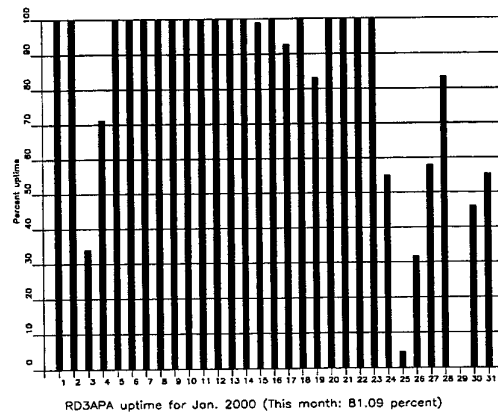
RD3APA uptime for Jan. 2000 (This month: 81.09 percent)

RD3APA uptime for Feb. 2000 (This month: 97.99 percent)

RD3APA uptime for Mar. 2000 (This month: 99.88 percent)

Fig. 3.4.1 *(cont.) (Page 2 of 2, Jan-Mar 2000)*

Apatity Event Detection Operation

Apatity array detections

The number of detections (phases) reported from day 274, 1999, through day 092, 2000, was 134,352, giving an average of 738 detections per processed day (182 days processed).

As described in earlier reports, the data from the Apatity array are transferred by one-way (simplex) radio links to Apatity city. The transmission suffers from radio disturbances that occasionally result in a large number of small data gaps and spikes in the data. In order for the communication protocol to correct such errors by requesting retransmission of data, a two-way radio link would be needed (duplex radio). However, it should be noted that noise from cultural activities and from the nearby lakes cause most of the unwanted detections. These unwanted detections are "filtered" in the signal processing, as they give seismic velocities that are outside accepted limits for regional and teleseismic phase velocities.

Events automatically located by the Apatity array

During days 274, 1999, through 092, 2000, 1793 local and regional events were located by the Apatity array, based on automatic association of P- and S-type arrivals. This gives an average of 9.8 events per processed day (183 days processed). 45% of these events are within 300 km, and 78% of these events are within 1000 km.

U. Baadshaug

3.5   Regional Monitoring System Operation and Analysis

The Regional Monitoring System (RMS) was installed at NORSAR in December 1989 and was operated at NORSAR from 1 January 1990 for automatic processing of data from ARCES and NORES. A second version of RMS that accepts data from an arbitrary number of arrays and single 3-component stations was installed at NORSAR in October 1991, and regular operation of the system comprising analysis of data from the 4 arrays ARCES, NORES, FINES and GERES started on 15 October 1991. As opposed to the first version of RMS, the one in current operation also has the capability of locating events at teleseismic distance.

Data from the Apatity array were included on 14 December 1992, and from the Spitsbergen array on 12 January 1994. Detections from the Hagfors array were available to the analysts and could be added manually during analysis from 6 December 1994. After 2 February 1995, Hagfors detections were also used in the automatic phase association.

Since 24 April 1999, RMS has processed data from all the seven regional arrays ARCES, NORES, FINES, GERES (until January 2000), Apatity, Spitsbergen, and Hagfors. Starting 19 September 1999, waveforms and detections from the NORSAR array have also been available to the analyst.

Phase and event statistics

Table 3.5.1 gives a summary of phase detections and events declared by RMS. From top to bottom the table gives the total number of detections by the RMS, the number of detections that are associated with events automatically declared by the RMS, the number of detections that are not associated with any events, the number of events automatically declared by the RMS, the total number of events defined by the analyst, and finally the number of events accepted by the analyst without any changes (i.e., from the set of events automatically declared by the RMS).

New criteria for interactive event analysis were introduced from 1 January 1994. Since that date, only regional events in areas of special interest (e.g, Spitsbergen, since it is necessary to acquire new knowledge in this region) or other significant events (e.g, felt earthquakes and large industrial explosions) were thoroughly analyzed. Teleseismic events of special interest are also analyzed.

To further reduce the workload on the analysts and to focus on regional events in preparation for Gamma-data submission during GSETT-3, a new processing scheme was introduced on 2 February 1995. The GBF (Generalized Beamforming) program is used as a pre-processor to RMS, and only phases associated to selected events in northern Europe are considered in the automatic RMS phase association. All detections, however, are still available to the analysts and can be added manually during analysis.

	Oct 99	Nov 99	Dec 99	Jan 00	Feb 00	Mar 00	Total
Phase detections	137033	106796	144545	98243	96545	113002	696164
- Associated phases	4009	5315	5805	3068	3700	4126	26023
- Unassociated phases	133024	101481	138740	95175	92845	108876	670141
Events automatically declared by RMS	736	953	1222	574	616	698	4799
No. of events defined by the analyst	88	124	76	65	72	81	506

Table 3.5.1. *RMS phase detections and event summary.*

U. Baadshaug
B. Paulsen

4   NDC and Field Activities

4.1   NDC Activitities

NORSAR will function as the Norwegian National Data Center (NDC) for treaty verification. Six monitoring stations, comprising altogether 119 field instruments, will be located on Norwegian territory as part of the future IMS as described elsewhere in this report. The four seismic IMS stations are all in operation today, with three of them contributing data to GSETT-3. The infrasound station in northern Norway and the radionuclide station at Spitsbergen will need to be established within the next few years. Data recorded by the Norwegian stations will be transmitted in real time to the Norwegian NDC, and provided to the IDC through the Global Communications Infrastructure (GCI). Norway is now connected to the GCI with a frame relay link to Vienna.

Operating the Norwegian IMS stations will require increased resources and additional personnel both at the NDC and in the field. It will require establishing new and strictly defined procedures as well as increased emphasis on regularity of data recording and timely data transmission to the IDC in Vienna. Anticipating these requirements, a new organizational unit has been established at NORSAR to form a core group for the future Norwegian NDC for treaty monitoring. The NDC will carry out all the technical tasks required in support of Norway's treaty obligations. NORSAR will also carry out assessments of events of special interest, and advise the Norwegian authorities in technical matters relating to treaty compliance.

Verification functions

After the CTBT enters into force, the IDC will provide data for a large number of events each day, but will not assess whether any of them are likely to be nuclear explosions. Such assessments will be the task of the States Parties, and it is important to develop the necessary national expertise in the participating countries.

Monitoring the Arctic region

Norway will have monitoring stations of key importance for covering the Arctic, including Novaya Zemlya, and Norwegian experts have a unique competence in assessing events in this region. On several occasions in the past, seismic events near Novaya Zemlya have caused political concern, and NORSAR specialists have contributed to clarifying these issues.

Information received from IDC

The IDC will provide regular bulletins of detected events as well as numerous other products, but will not assess the nature of each individual event. An important task for the Norwegian NDC will be to make independent assessments of events of particular interest to Norway, and to communicate the results of these analyses to the Norwegian Ministry of Foreign Affairs.

International cooperation

After entry into force of the treaty, a number of countries are expected to establish national expertise to contribute to the treaty verification on a global basis. Norwegian experts have been in contact with experts from several countries with the aim to establish bilateral or multilateral

cooperation in this field. One interesting possibility for the future is to establish NORSAR as a regional center for European cooperation in the CTBT verification activities.

NORSAR event processing

The automatic routine processing of NORSAR events as described in NORSAR Sci. Rep. No. 2-93/94, has been running satisfactorily. The analyst tools for reviewing and updating the solutions have been continuously modified to simplify operations and improve results. NORSAR is currently applying teleseismic detection and event processing using the large-aperture NORSAR array as well as regional monitoring using the network of small-aperture arrays in Fennoscandia and adjacent areas.

Y2K

NORSAR made extensive preparations to ensure that all systems at the NDC and in the field were Y2K compliant, and all systems passed the millenium changeover without major problems.

Technical Training Program

The Norwegian NDC organized the second international training program for seismic station operators at NORSAR in the fall of 1999, with participation from 13 countries in all areas of the world. The course contents included functions at the NDC as well as field maintenance procedures, with emphasis on hands-on demonstrations. The program was carried out very successfully, and may be followed by additional such training courses in the future.

Certification of PS27

IMS station PS27-NOA is currently being considered by the PTS for formal certification. PTS personnel visited the station in June 1998, and carried out a detailed technical evaluation. As a result of this inspection and subsequent discussions between NORSAR and the PTS, and following further discussions of the certification requirements during Working Group B meetings, it is now concluded that PS27 needs the following enhancements:

- A tamper detector to be emplaced at every seismometer and at the subarray central vaults
- A centralized authentication process in each subarray as well as at the central array recording facility
- Establishment of a GCI connection at the central array facility
- Addition of a 3-component seismometer in order to satisfy the technical requirements for short-period 3-component recording.

These enhancements are now being implemented.

Establishing an independent subnetwork

Norway has elected to use the option for an independent subnetwork, which will connect with all the IMS stations operated by NORSAR with an interface to the GCI. A contract has been concluded and VSAT antennas have been installed at each station in the network.

The Norwegian NDC has been cooperating with several institutions in other countries for transmission of IMS data to the Prototype IDC during GSETT-3. During the reporting period, several changes were made to these arrangements. Details on this can be found in Section 4.2.

Upgrade of PS28

IMS station PS28-ARCES was selected by the PrepCom for hardware upgrade in 1999, and this effort has been concluded. All the digitizers and data acquisition equipment have been replaced. Data from the upgraded array are now being transmitted from the NDC to PIDC, IDC and US_NDC. Its is expected that PS28 will now undergo a testing and evaluation phase, leading up to certification of this station, perhaps by the end of 2000.

Jan Fyen

4.2   Status Report: Norway's Participation in GSETT-3

Introduction

This contribution is a report for the period October 1999 - March 2000 on activities associated with Norway's participation in the GSETT-3 experiment, which is now being coordinated by PrepCom's Working Group B. This report represents an update of contributions that can be found in previous editions of NORSAR's Semiannual Technical Summary.

Norwegian GSETT-3 stations and communications arrangements

During the reporting interval 1 October 1999 - 31 March 2000, Norway has provided data to the GSETT-3 experiment from the three seismic stations shown in Fig. 4.2.1. The NORSAR array (station code NOA) is a 60 km aperture teleseismic array, comprised of 7 subarrays, each containing six vertical short period sensors and a three-component broadband instrument. ARCES is a 25-element regional array with an aperture of 3 km, whereas the Spitsbergen array (station code SPITS) has 9 elements within a 1-km aperture. ARCES and SPITS both have a broadband three-component seismometer at the array center.

Data from these three stations are transmitted continuously and in real time to NOR_NDC. During the reporting period, some components of the new so-called independent subnetwork for transmission of data from Norwegian IMS stations to NOR_NDC were installed and put into operation. Transmission from these stations to the NOR_NDC has thus been achieved by a mixture of these new lines and previously existing ones, in the following way:

- The NOA data have been transmitted using dedicated land lines as before, but new VSAT satellite links, based on TDMA technology, have been installed and used in a test mode in parallel with the land lines. When transmission via the new VSAT links from the various subarrays of NOA has been verified with respect to the appropriate technical requirements, the land lines will be discontinued.

- The ARCES data have been transmitted since late September 1999 from the ARCES site to NOR_NDC using a new 64 kbits/s satellite link, based on BOD technology.

- The SPITS data are still transmitted to NOR_NDC using the same arrangements that have existed for several years (terrestrial line to Isfjord Radio at the west coast of Spitsbergen,

and a VSAT satellite link from there to NOR_NDC). A modification to this system is
expected during the summer of 2000.

The NOA and ARCES arrays are primary stations in the GSETT-3 network, which implies that
data from these stations are transmitted continuously to the receiving international data center.
Since October 1999, these data have been transmitted (from NOR_NDC) via the Global Com-
munications Infrastructure (GCI) to the IDC in Vienna, whereas transmission of the same data
to the PIDC was discontinued on 7 February 2000. The SPITS array is an auxiliary station in
GSETT-3, and the SPITS data have been available to both the IDC and the PIDC throughout
the reporting period on a request basis via use of the AutoDRM protocol (Kradolfer, 1993; Kra-
dolfer, 1996). The Norwegian stations are thus participating in GSETT-3 with the same status
(primary/auxiliary seismic stations) they have in the International Monitoring System (IMS)
defined in the protocol to the Comprehensive Nuclear-Test-Ban Treaty. In addition, continuous
data from all three arrays are being transmitted to the US NDC.

Uptimes and data availability

Figs. 4.2.2 - 4.2.3 show the monthly uptimes for the Norwegian GSETT-3 primary stations
ARCES and NOA, respectively, for the period 1 October 1999 - 31 March 2000, given as the
hatched (taller) bars in these figures. These barplots reflect the percentage of the waveform data
that are available in the NOR_NDC tape archives for these two arrays. The downtimes inferred
from these figures thus represent the cumulative effect of field equipment outages, station site
to NOR_NDC communication outage, and NOR_NDC data acquisition outages.

Figs. 4.2.2-4.2.3 also give the data availability for these two stations as reported by the PIDC in
the PIDC Station Status reports. The main reason for the discrepancies between the
NOR_NDC and PIDC data availabilities as observed from these figures is the difference in the
ways the two data centers report data availability for arrays: Whereas NOR_NDC reports an
array station to be up and available if at least one channel produces useful data, the PIDC uses
weights where the reported availability (capability) is based on the number of actually operat-
ing channels. On 7 February 2000, NOR_NDC stopped sending ARCES and NOA data
directly to the PIDC.

Experience with the AutoDRM protocol

NOR_NDC's AutoDRM has been operational since November 1995 (Mykkeltveit & Baads-
haug, 1996).

The PIDC started actively and routinely using NOR_NDC's AutoDRM service after SPITS
changed its station status from primary to auxiliary on 1 October 1996. For the month of Octo-
ber 1996, the NOR_NDC AutoDRM responded to 12338 requests for SPITS waveforms from
two different accounts at the PIDC: 9555 response messages were sent to the "pipeline"
account and 2783 to "testbed". Following this initial burst of activity, the number of "pipeline"
requests stabilized at a level between 5000 and 7000 per month. Requests from the "testbed"
account show large variations. More recently, the number of requests has decreased further.
"Pipeline" requests for the reporting period range between 700 and 1200 per month.

The monthly number of requests by PIDC for SPITS data for the period October 1999 - March
2000 is shown in Fig. 4.2.4.

NDC automatic processing and data analysis

These tasks have proceeded in accordance with the descriptions given in Mykkeltveit and Baadshaug (1996). For the period October 1999 - March 2000, NOR_NDC derived information on 489 supplementary events in northern Europe and submitted this information to the Finnish NDC as the NOR_NDC contribution to the joint Nordic Supplementary (Gamma) Bulletin, which in turn is forwarded to the PIDC. These events are plotted in Fig. 4.2.5.

Data forwarding for GSETT-3 stations in other countries

NOR_NDC continued to forward data to the PIDC from GSETT-3 primary stations in several countries until 31 December 1999. These included FINESS (Finland), GERESS (Germany) and Sonseca (Spain). From 1 January 2000 data from these stations are sent directly to the IDC in Vienna via new links of the GCI. We are continuing to provide communications for the GSETT-3 auxiliary station at Nilore, Pakistan, through a VSAT satellite link between NOR_NDC and Pakistan's NDC in Nilore. The PIDC as well as the IDC obtain data from the Hagfors array (HFS) in Sweden through requests to the AutoDRM server at NOR_NDC (in the same way requests for Spitsbergen array data are handled, see above). Fig. 4.2.6 shows the monthly number of requests for HFS data from the two PIDC accounts "pipeline" and "testbed".

Current developments and future plans

NOR_NDC is continuing the efforts towards improvements and hardening of all critical data acquisition and data forwarding hardware and software components, so as to meet future requirements related to operation of IMS stations to the maximum extent possible.

The PrepCom has tasked its Working Group B with overseeing, coordinating, and evaluating the GSETT-3 experiment. The PrepCom has also encouraged states that operate IMS-designated stations to continue to do so on a voluntary basis and in the framework of the GSETT-experiment until such time that the stations have been certified for formal inclusion in IMS. In line with this, and provided that adequate funding is obtained, we envisage continuing the provision of data from Norwegian IMS-designated stations without interruption to the IDC in Vienna.

U. Baadshaug
S. Mykkeltveit
J. Fyen

References

Kradolfer, U. (1993): Automating the exchange of earthquake information. *EOS, Trans., AGU*, 74, 442.

Kradolfer, U. (1996): AutoDRM — The first five years, *Seism. Res. Lett.*, 67, 4, 30-33.

Mykkeltveit, S. & U. Baadshaug (1996): Norway's NDC: Experience from the first eighteen months of the full-scale phase of GSETT-3. *Semiann. Tech. Summ., 1 October 1995 - 31 March 1996*, NORSAR Sci. Rep. No. 2-95/96, Kjeller, Norway.
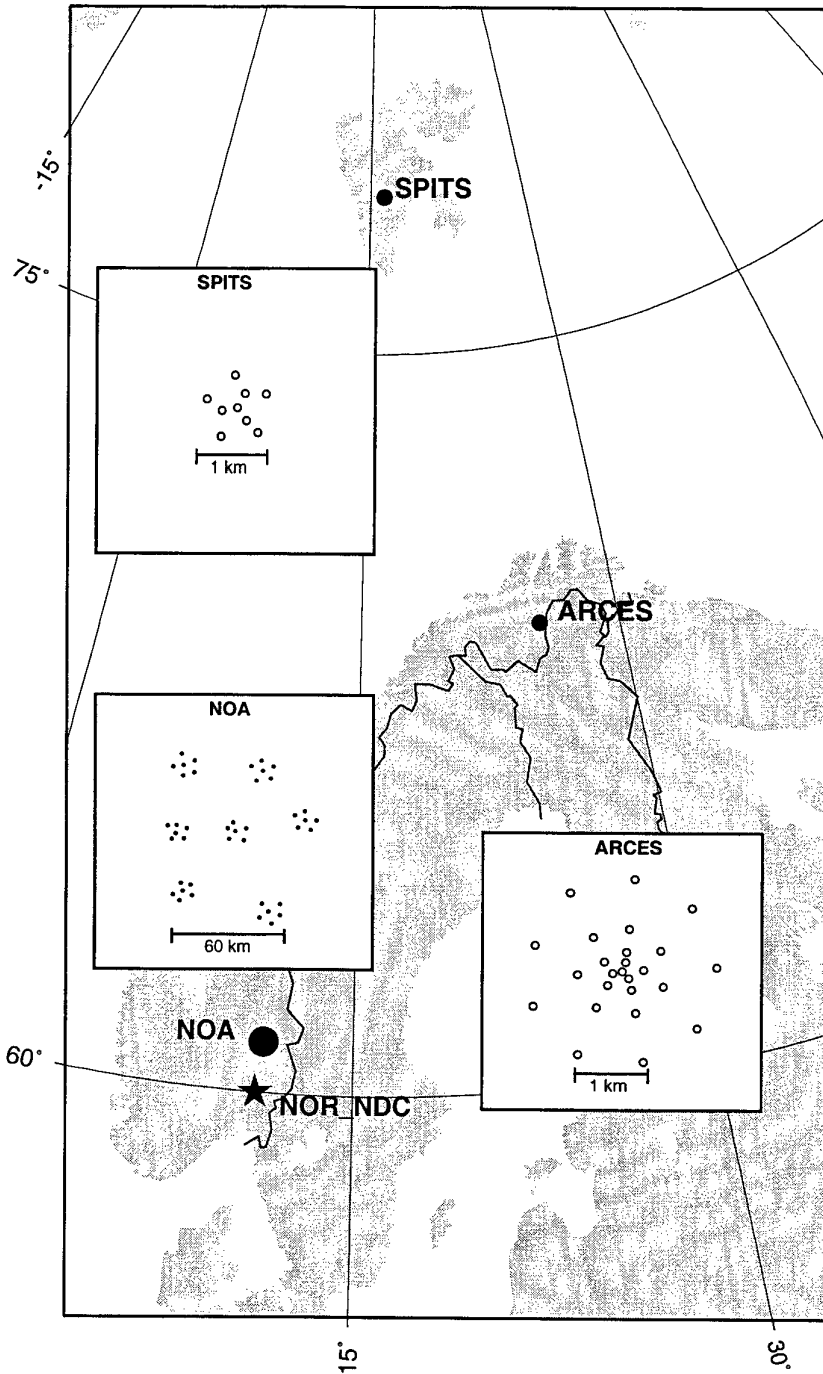
Fig. 4.2.1. The figure shows the locations and configurations of the three Norwegian seismic array
stations that have provided data to the GSETT-3 experiment during the period 1 October 1999
- 31 March 2000. The data from these stations are transmitted continuously and in real time to
the Norwegian NDC (NOR_NDC). The stations NOA and ARCES have participated in
GSETT-3 as primary stations, whereas SPITS has contributed as an auxiliary station.
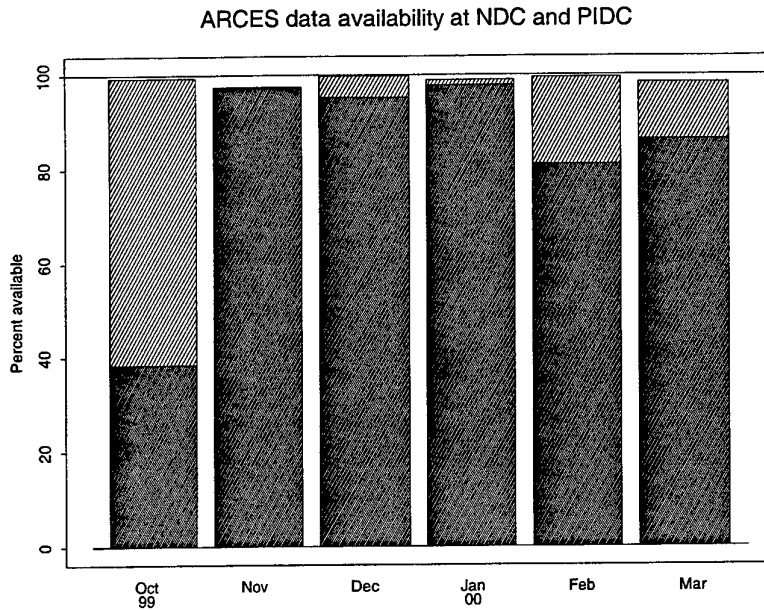
ARCES data availability at NDC and PIDC

Fig. 4.2.2. The figure shows the monthly availability of ARCES array data for the period October 1999 - March 2000 at NOR_NDC and the PIDC. See the text for explanation of differences in definition of the term "data availability" between the two centers. The higher values (hatched bars) represent the NOR_NDC data availability.

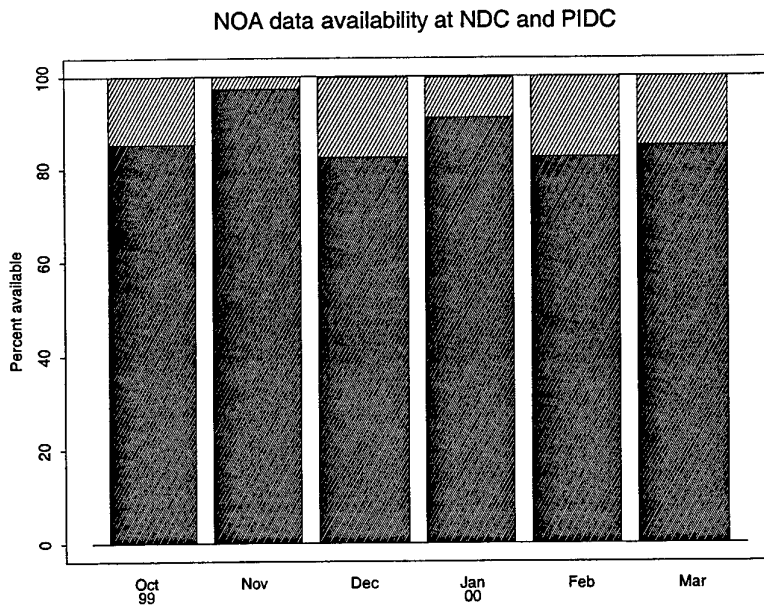## NOA data availability at NDC and PIDC

Fig. 4.2.3. The figure shows the monthly availability of NORSAR array data for the period October 1999 - March 2000 at NOR_NDC and the PIDC. See the text for explanation of differences in definition of the term "data availability" between the two centers. The higher values (hatched bars) represent the NOR_NDC data availability.
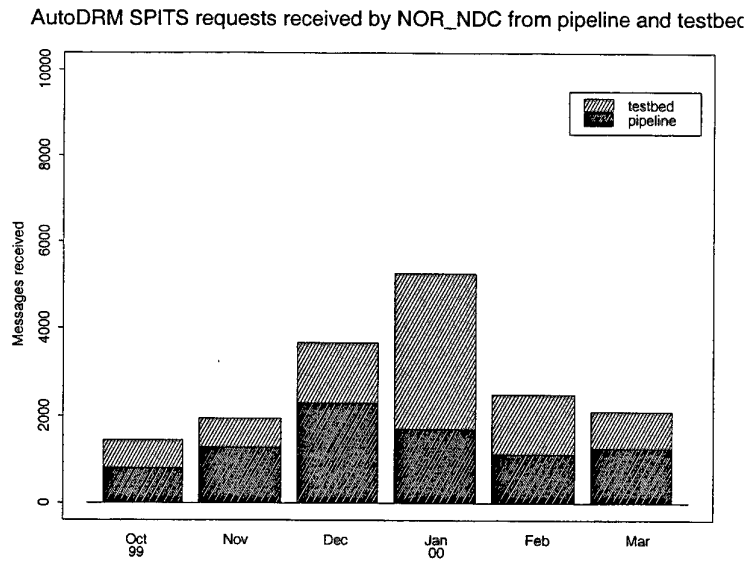
AutoDRM SPITS requests received by NOR_NDC from pipeline and testbec

Fig. 4.2.4. The figure shows the monthly number of requests received by NOR_NDC from the PIDC for SPITS waveform segments during October 1999 - March 2000.
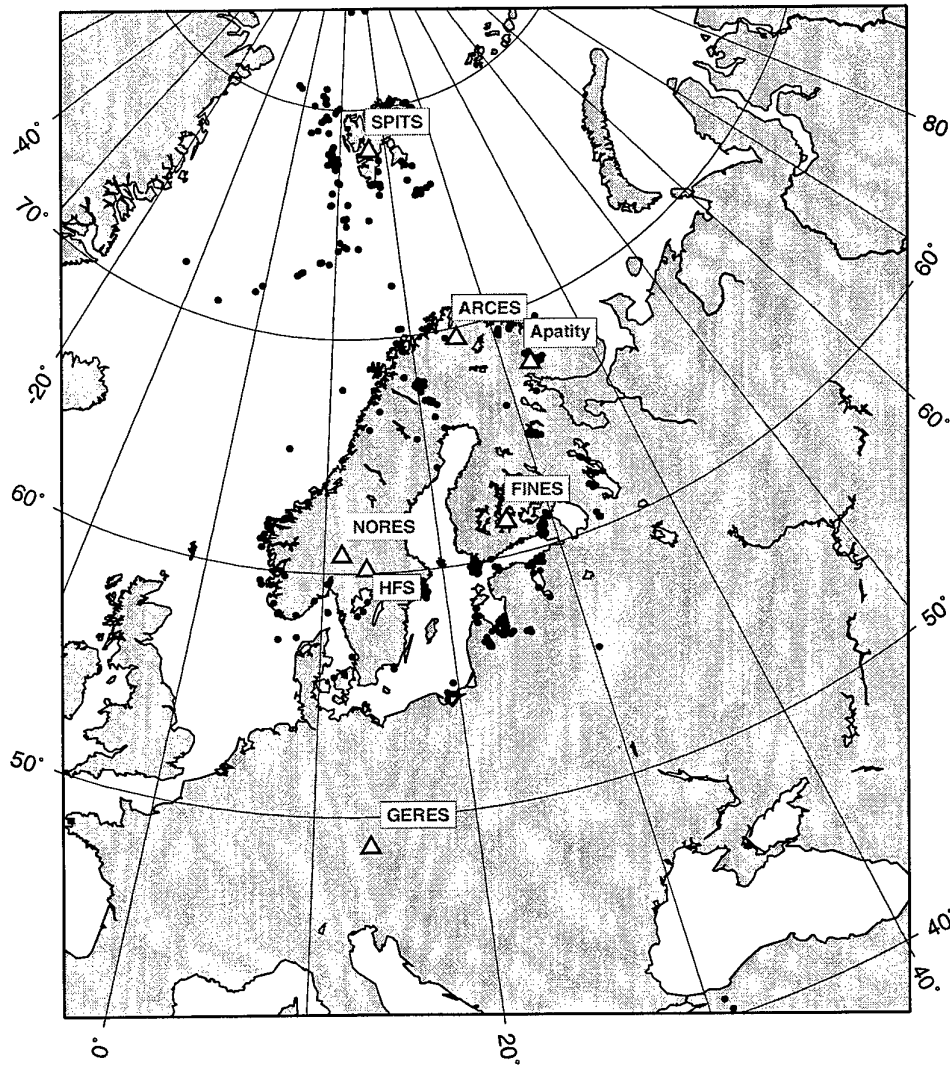
Reviewed Supplementary events

Fig. 4.2.5. The map shows the 489 events in and around Norway contributed by NOR_NDC during October 1999 - March 2000 as supplementary (Gamma) events to the PIDC, as part of the Nordic supplementary data compiled by the Finnish NDC. The map also shows the seismic stations used in the data analysis to define these events.

AutoDRM HFS requests received by NOR_NDC from pipeline and testbed
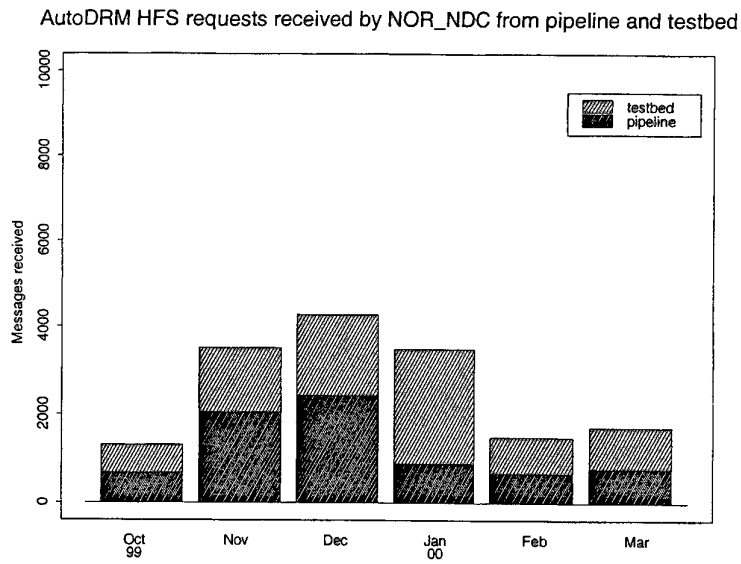

Fig. 4.2.6. The figure shows the monthly number of requests received by NOR_NDC from the PIDC for HFS waveform segments during October 1999 - March 2000.

4.3   Field Activities

Activities in the field and at the Maintenance Center

This section summarizes the activities at the Maintenance Center (NMC) Hamar, and includes activities related to monitoring and control of the NORSAR teleseismic array, as well as the NORES, ARCES, FINES, Apatity, Spitsbergen, and Hagfors small-aperture arrays.

Activities also involve preventive and corrective maintenance, planning and activities related to the refurbishment of the NORSAR teleseismic array.

Details for the reporting period are provided in Table 4.3.1 below.

P.W. Larsen
K.A. Løken

Subarray/ area	Task	Date
October 1999		
NORSAR		October
02C	Installation of VSAT antenna system	11/10
01B	Installation of VSAT antenna system	12/10
02B-03C	Installation of VSAT antenna system	13/10
03C-04C	Installation of VSAT antenna system	14/10
01A	Installation of VSAT antenna system	15/10
01A-01B-02C	Adjustment of elevation and azimuth of the VSAT antenna	19/10
02B-03C-04C	Adjustment of elevation and azimuth of the VSAT antenna	20/10
02B-05	Preventive maintenance of vault, including installation of new lid	22/10
04C-01-00	Replacement of GPS receiver	26/10
ARCES	Testing of new GPS cards received from Nanometrics. The new cards did not work, so the old cards had to be put back in operation.	6-8/10
NMC	Repair of defective electronic equipment	October

Subarray/ area	Task	Date
November 1999		
NORSAR		November
02C-02	Installation of new software for the AIM-24	1/11
02C-05	Installation of new software for the AIM-24	2/11
04C-03	Installation of new software for the AIM-24	22/11
ARCES	Installation of SUN workstation	25-26/11
NORES	Repair of digitizer equipment at B3, C4 and C7	29/11
NMC	Repair of defective electronic equipment.	November
December 1999		
NORSAR		December
01A	Installation of SUN workstation	2/12
NORES	Preventive maintenance of vaults at B3, C2, C3, D1, D2 and D7	2/12
NMC	Repair of defective electronic equipment. Planning new equipment for ARCES	December
January 2000		
NORSAR		January
03C	Installation of SUN workstation	6/1
04C	Installation of SUN workstation	6/1
01B	Installation of SUN workstation	17/1
02B	Installation of SUN workstation	17/1
02C	Installation of SUN workstation	18/1
NMC	Repair of defective electronic equipment. Planning new equipment for ARCES.	January

Subarray/ area	Task	Date
February 2000		
NORSAR		February
01A-01B-04C	Adjustment of router for the VSAT system	17/2
06C	Installation of SUN workstation	17/2
SVAES	Maintenance of the windmill	8-10/2
NMC	Planning, acquisition and system integration of equipment for the upgrade of ARCES	February
March 2000		
ARCES	Installation of new GPS cards	21-24/3
NORES	Repair of digitizer equipment at B3, C2, C3 and D9	13/3

Table 4.3.1. *Activities in the field and the NORSAR Maintenance Center during 1 October 1999 - 31 March 2000.*

5 Documentation Developed

Byrkjeland, U., H. Bungum & O. Eldholm (2000): Seismotectonics of the Mid-Norwegian continental margin. *J. Geophys. Res.*, in press.

Faleide, J.I. (2000): Crustal structure of the Barents Sea — important constraints for regional seismic velocity and travel-time models, **In:** Semiannual Tech. Summ., 1 October 1999 - 31 March 2000, NORSAR Sci. Rep. 2-1999/2000, Kjeller, Norway.

Hicks, E., H. Bungum & C. Lindholm (2000): Seismic activity, inferred crustal stresses and seismotectonics in the Rana region, Northern Norway. *Quat. Sci. Reviews*, in press.

Kremenetskaya, E.O., V.E. Asming & F. Ringdal (2000): Locating seismic events in northern Eurasia, **In:** *Semiannual Tech. Summ., 1 October 1999 - 31 March 2000*, NORSAR Sci. Rep. 2-1999/2000, Kjeller, Norway.

Kværna, T. (2000): The Eurobridge Profile — Ground Truth observations at the Fennoscandian arrays, **In:** Conf. Proc., Workshop on IMS Location Calibration, Oslo, 21-23 March 2000.

Kværna, T. (2000): Waveform quality analysis and data conditioning for the SPITS array, **In:** *Semiannual Tech. Summ., 1 October 1999 - 31 March 2000*, NORSAR Sci. Rep. 2-1999/2000, Kjeller, Norway.

Kværna, T., J. Schweitzer & L. Taylor (2000): The Eurobridge Profile: Analysis of time residuals at the Fennoscandian arrays, **In:** *Semiannual Tech. Summ., 1 October 1999 - 31 March 2000*, NORSAR Sci. Rep. 2-1999/2000, Kjeller, Norway.

Lindholm, C., H. Bungum, E. Hicks & M. Villagran (2000): Crustal stress and tectonics in Norwegian regions determined from earthquake focal mechanisms. *J. Geol. Soc. London*, in press.

Lindholm, C., J. Schweitzer, E. Wolf, H. Bungum, K. Atakan, S. Gregersen, K. Arhe & J. Malaska (2000): Third level seismo-geographical regionalization of Fennoscandia, **In:** *Semiannual Tech. Summ., 1 October 1999 - 31 March 2000*, NORSAR Sci. Rep. 2-1999/2000, Kjeller, Norway.

NORSAR (1999): Semiannual Tech. Summ., 1 April - 30 September 1999, NORSAR Sci. Rep. 1-1999/2000, Kjeller, Norway.

Ringdal, F. (2000): Overview— Technical Issues for the Workshop, **In:** Conf. Proc., Workshop on IMS Location Calibration, Oslo, 21-23 March 2000.

Ringdal, F. (2000): Seismic Event Location Calibration, **In:** *Semiannual Tech. Summ., 1 October 1999 - 31 March 2000*, NORSAR Sci. Rep. 2-1999/2000, Kjeller, Norway.

Schweitzer, J. (2000): Recent Profiling Experiments in the Spitsbergen Area — Calibration Data for the SPITS Array, **In:** Conf. Proc., Workshop on IMS Location Calibration, Oslo, 21-23 March 2000.

Schweitzer, J. (1999): Influence on source radiation patterns on globally observed short-period magnitude estimates (m_b). *Bull. Seism. Soc. Am.*, 89, 342-347.

Schweitzer, J. (2000): Recent profiling experiments in the Spitsbergen area — calibration data for the SPITS array, **In**: *Semiannual Tech. Summ., 1 October 1999 - 31 March 2000*, NORSAR Sci. Rep. 2-1999/2000, Kjeller, Norway.

6   Summary of Technical Reports / Papers Published

6.1   Seismic Event Location Calibration

Report from the IDC Technical Experts Meeting in Oslo, Norway 20-24 March 2000

6.1.1 Introduction

During the 1998 meetings of Working Group B of the CTBTO Preparatory Commission, the International Data Centre (IDC) Expert Group identified the need for highly-focused work to provide regionalized travel times to improve seismic location methods used in the IDC. The Expert Group suggested that initial focus should be given to the following geographical regions: North America, Eurasia, Northern Africa and Australia.

To assist with the developments of the IDC applications software relating to the location calibration problem, an informal meeting of the IDC Technical Experts Group on Seismic Event Location was held in Oslo, Norway on 20-24 March 2000. Sixty technical experts, coming from fifteen signatory countries and the Provisional Technical Secretariat, participated in the meeting. Dr. Frode Ringdal of Norway chaired the meeting.

6.1.2 Background and technical objectives

Working Group B has repeatedly encouraged States Signatories to support the location improvement efforts by supplying relevant location calibration information for their own territories as well as for other regions where they have such information available. The following types of calibration information were proposed in the document CTBT/WGB-6/CRP.26:

- Precise information on location, depth, and origin time of previous nuclear explosions or large chemical explosions
- Similar information on other seismic events that have been located by regional networks with sufficient precision.
- Data as appropriate on seismic travel-time models
- Any other information (e.g., geologic or tectonic maps) that would be useful
- Ground truth data from chemical explosions.

The IDC Technical Experts Group on Seismic Event Location has carried out considerable work in supporting the overall calibration effort, including the compilation of data of the types listed above. At its first meeting in January 1999, the Experts Group developed plans and recommendations for a global calibration program, and presented its report to Working Group B in February 1999 (CTBT/WGB/TL-2/18).

The second meeting of the Experts Group (20-24 March 2000) had the following objectives:

- To review proposals for detailed station-specific regional corrections to be applied for IMS stations in North America, Europe, North Africa, Asia and Australia
- To recommend a set of such corrections, including appropriate model errors, for incorporation into the Release 3 of the IDC software
- To develop a plan for future extensions and improvements of this regional correction data base, to be incorporated into future IDC software releases
- To review progress in the general recommendations from the January 1999 meeting, and make adjustments and updates to these recommendations as required.

The primary task of the meeting was to assess the status and availability of such calibration information for the regions being considered, and to plan for implementing regional location calibration at the IDC, both for Release 3 of the IDC applications software and for implementation in the longer term.

6.1.3 Technical issues

Presentations during the meeting

A number of papers relating to the collection, application and validation of calibration information were presented by participants. Models for regionalization on a global basis were presented and discussed. Specific presentations were made by several experts describing regional velocity models and calibration data for the general geographic regions being considered initially for calibration in Release 3.

It was noted that for some regions, information was incomplete or lacking, and the use of default "generic" velocity models for various tectonic regions was discussed in some detail. Valuable new data on ground truth information for seismic events was presented, and will be communicated to the IDC and the prototype IDC. Countries were encouraged to continue to provide relevant calibration data for the purpose of developing accurate seismic travel-time curves for various geographical regions.

Reports were presented on a number of modelling studies, some of which showed significant improvement in location precision when applied to test sets of seismic events. For example, one-dimensional regional Pn, Pg, Sn, and Lg travel time curves were shown to provide improvements for the Baltic shield and the Barents region. Three-dimensional models were introduced for North America and Western Russia and were found to provide considerable improvements in location accuracy compared to standard (IASPEI-91) models.

Techniques for improved regional processing using sparse seismic networks as well as improved azimuth determination for regional arrays were presented and discussed. The application of special location techniques was also addressed.

Working Group Discussions

Three Working Groups, each focusing on specific regions of the world, were established to discuss technical issues in detail during the workshop:

> Working Group 1: Northern Eurasia and East Asia
> Working Group 2: Southwestern Asia and the African/Mediterranean area
> Working Group 3: North and South America, Australia

The Working Groups were given a mandate with a list of specific questions addressing the following topics:

> Topic 1: Implementing regional corrections for IDC Release 3
> Topic 2: Collection of Regional Calibration Information
> Topic 3: Application of Regional Calibration Information
> Topic 4: Validation of Regional Calibration Information

The results of the Working Groups were presented and discussed in a plenary session. These discussions have provided the basis for the recommendations presented below.

6.1.4 Recommendations

General

The Experts Group considers it essential for the success of the calibration program that States Signatories contribute actively toward this purpose, by supplying relevant location calibration information for their own territories as well as for other regions where they have such information available. The relevant location information is defined in CTBT/WGB-6/CRP.26.

The Experts Group recommends that the IDC make openly available to the scientists involved in the location calibration effort all of the waveform data and associated IDC products that are needed in order to successfully carry out the calibration program.

A continued full utilization of the resources of the prototype IDC will be essential for future IDC development. The Experts Group recommends that the prototype IDC should act as a resource facility for the international location calibration effort, thus compiling, organizing and making openly available to the scientific community all relevant information on calibration events, travel-time curves, geological/ geophysical information and other ground truth data. The responsibility for these calibration data and the associated processing software will over the next several years be transferred from the prototype IDC to the IDC on a stage-by-stage basis.

The Experts Group commends the IDC for preparations taken to begin an external calibration program. The Group recommends that this program give high priority to facilitating collection and validation of ground truth and waveform data.

The Experts Group considers that Confidence-Building Measures, especially chemical calibration explosions, are important to regional calibration, and encourage States Signatories to carry out additional such explosions or to take advantage of such explosions conducted for other purposes. The Group recognizes the valuable experience obtained from the recent chemical calibration explosions in Kazakhstan and Israel. The Experts Group recommends that the PTS solicit from States Signatories waveform data recorded on national seismic stations of such calibration explosions.

Site survey data collected by the PTS should be made openly available to States Signatories. Consideration should be given by the PTS to using GPS to check the location of relevant surrogate stations, such as nearby station during certification of IMS installations. The IDC and prototype IDC should provide a mechanism for archival and distribution of historical non-IMS data to promote calibration. The PTS should place a priority on connecting auxiliary seismic stations to the GCI for purposes of collecting calibration data as soon as possible.

Topic 1: Implementing regional corrections for IDC Release 3

For Region 1 (Northern Eurasia and East Asia) there will not be additional source-specific station corrections (SSSCs) beyond the Fennoscandian SSSCs already implemented in Release 2.

There is a reasonable chance that SSSCs will be available, possibly for most of Eastern Asia, by Release 4. Complete validation of corrections by this time will be more problematic.

For Region 2 (Southwestern Asia and the African/Mediterranean area) no travel time calibrations will be available for the Release 3 delivery in 2000. Delivery of a preliminary set of limited regional travel time corrections (surface source only with conservative modeling errors) may be available late in 2001 suitable for incorporation into Release 4 delivery, Refined and extended calibrations will be available in 2003.

For Region 3 (North and South America, Australia) there have been some recent developments. SSSCs for all IMS stations in Canada and the USA were implemented at the prototype IDC in February 2000, and will thus be available for IDC Release 3 delivery. The work on SSSCs derived from a 3-D model for this region is now considered to be sufficiently advanced that it should be possible to document the methods and data used to generate the corrections, and validate them, by November 2000.

Topic 2: Collection of Regional Calibration Information

Regional review

Region 1 (Northern Eurasia and East Asia): A large amount of Ground Truth data exists for this region, e.g., Soviet PNEs, but most of the IMS stations were not installed at that time. This means that the use of surrogate stations will be required. Many regional travel-time curves, models, and geological/geophysical surveys also exist, but are not always easily available. It would be desirable to make an effort to obtain this type of data. The recent calibration explosions in Kazakhstan are excellent examples of the type of calibration events that will be the most useful for future developments.

Region 2 (Southwestern Asia and the African/Mediterranean area): Most of the information available for this region is from geological/geophysical surveys and regional travel-time models. Local travel time tables (and curves) as well as crustal and upper mantle velocity models are readily available for Egypt, Turkey, Israel, Romania, East Africa, and several other countries in the region. As with Region 1, much additional information exists, but is difficult to access. The amount of Ground Truth information is limited, but a notable recent development is the Dead Sea calibration explosion of November 1999.

Region 3 (North and South America, Australia): Considerable calibration information is available, but geographical coverage is poor, particularly for the eastern U.S., Canada, Alaska, Mexico, Central and South America. Additional events, preferably of GT5 or better and magnitude >3.5, should be identified. The current Ground Truth Database for this and other regions should be reviewed and revised where necessary.

General comments:

Every effort should be made to support "target of opportunity" experiments, particularly in areas such as South America which currently lacks detailed regional travel time curves. Special consideration should be given to large well-designed mine blast experiments, such as contained single blasts, that would provide unique source phenomenology information.

Existing facilities (stations and arrays) with enhanced capabilities (such as long-period arrays) should be maintained as part of the IMS seismic system.

The term "Calibration Event Bulletin" is misleading, and should be changed to Reference Event Database (REDB). The number of events available for the Reference Event Database since 1994 is small, and it should be possible to analyze most of them comprehensively, given participation by the States concerned. Efforts should be made to expand both the Reference Event Database and the Ground Truth Database. This information, including associated waveform data, should be made available from the IDC and the prototype IDC in an unrestricted manner, through Web pages, AutoDRM, ftp, and direct electronic access to the relational databases.

Possibilities for improving the Ground Truth database include good (internal to the network) local network solutions, calibration shots, mining and construction explosions. The most useful data would be Ground Truth information for events in REB. It may be desirable to consider some form of funding for collecting Ground Truth information on seismic events and delivering it to the IDC.

Topic 3: Application of Regional Calibration Information

Use of historic data

Historic data may be used to derive models, including travel time curves. It may be possible to perform Joint Hypocentral Determination analysis on old data and stations and apply derived corrections to new IMS stations. Care is needed in questions of timing, station location, and instrument changes for old stations; the network operators should be contacted if possible. Instrument response changes can affect phase arrival time picks; if repeated events are available they can be used to check consistency. Careful checking for outlier data should be made.

The historic database should be exploited to identify and validate GT5 events and GT5 clusters. In cases where IMS stations are not available, the event-specific corrections to surrogate IMS stations and to stations with unique locations and validated operational characteristics should be used.

Processing techniques

The Experts Group draws attention to the availability of the LocSAT program on the prototype IDC ftp site. This program has the full location capability of the IDC location programs, including SSSCs, but does not require the ORACLE database; instead it uses standard files for input and output.

The prototype IDC and the IDC should be prepared at any time to examine new techniques in location estimation.Examples for relatively short term consideration include full use of the Joint Hypocentral Determination method with events in the reference data base, cluster analysis, and local-only locations. In the longer term, grid search techniques and correlation methods for location, 3-D ray tracing by Gaussian beams or finite difference, and 3-D tomography should be considered. Depth estimation is a continuing concern, elevation corrections may be helpful, and depth phases for refracted arrivals might be useful.

The Experts Group recommends that error estimation of phase arrival time picks should be re-examined. The general feeling of the experts is that errors are currently underestimated. It was suggested that a single Gaussian pdf should not be used, but some pdf with "tails" to handle large errors. Better analyst tools could include use of array analysis to find coherent information, and multistation methods such as generalized beamforming to check arrivals.

Suggestions were made that analysts could be presented the ranges of predicted arrival times based on modeling error and/or analysts could specify a range of arrival times for low SNR picks. It is desirable that filter parameters used in interactive processing should be recorded.

Cepstral techniques for the identification of depth phases should be further investigated. The long term goal for depth dependent regional corrections is reiterated. Depth-dependent SSSCs should be accommodated in the IDC software. Wavelet decomposition and other automated methods for the more consistent identification of phase onsets, particularly Lg, should be further developed and tested.

Baseline errors are expected to result when combining calibrated and non-calibrated station sets. These baseline incompatibilities are expected to result in origin time and/or depth shifts until all phases and stations are calibrated. However, uncalibrated data should not be excluded. At this time inverse variance weighting is a reasonable approach to combining calibrated and uncalibrated data. Nevertheless, calibrated and uncalibrated data should be combined only when the variances used for each accurately reflect the relative uncertainties. It was also suggested to calibrate whole regions so that we do not mix uncalibrated and calibrated stations; as an example, it may be feasible to add to the calibrated Fennoscandian region incrementally.

Topic 4: Validation of Regional Calibration Information

Assessment of current efforts

The Fennoscandian SSSCs have been implemented, and improvements in location has been documented for Fennoscandian and Kola events. It appears that a single regional model may be useful for all of NW Russia. However, this is not fully validated. On validation, a period of testing is needed before a CCB proposal.

The SSSCs for North America that were approved for implementation at the prototype IDC in February 2000 are based upon a division of Canada and the USA into three distinct regions, the assignment of a travel-time curve to each region, and a simple linear combination of travel times in each region. The data and the methods used are quite well-documented. The location improvements demonstrated in the validation of these SSSCs were very modest, and illustrate the need for more sophisticated corrections based on additional data and more complex models. Some of the data used for validation was of questionable quality.

The basic divisions for North America are reflected in the corrections described above. The main boundaries are quite well-defined but there is scope for refinement of the travel-time curves and subdivision into additional regions. Well-calibrated events should be directly used in the derivation of the correction surfaces. For North America, enough information should be available to do this for station PDAR as a test case.

Validation data bases

Validation databases should be chosen carefully, and the phase arrivals should be repicked. Repeated events should be exploited to check data quality. The importance of the seismic data (i.e., picks) equals the importance of the GT data. It is important that the phase data used for validation be obtained through careful analysis of waveform data, ideally from IMS stations.

Historic data using past nuclear and chemical explosions has been used extensively in the work for the refinement of 3-D models and the travel curves used for each region, respectively. The accuracy of such information, particularly for chemical explosions, should be carefully assessed and adequate documentation and references must be provided. Newly available commercial satellite imagery will be useful in this regard.

Web and Ftp sites should be established at the IDC and the prototype IDC to receive contributed models, ground truth, and metadata (velocity models, travel time curves, phase/group velocity curves, crustal thickness, origins, arrivals, and waveforms). This would serve to encourage contributions and broaden access.

Configuration Control Board and Location Calibration Board

The Experts Group reiterates the recommendation for establishment of a Location Calibration Board (LCB). Currently, the Configuration Control Board (CCB) addresses the effects on the overall system (e.g. integration) of new corrections, to a greater extent than their scientific validity. For proposals involving location calibration corrections, additional expertise should be drawn upon. The LCB would comprise a designated panel of experts to review CCB proposals relating to location calibration and make recommendations to the CCB of the IDC concerning their acceptability.

A period of testing will be required before a CCB proposal relating to location calibration can be considered. The R&D testbed at the prototype IDC will be helpful for this purpose. It would be desirable for the CCB proposal requirements to be documented, with examples, and made easier if possible. CCB proposals should continue to be placed on the prototype IDC Web Page. The main responsibility for validating calibration information should remain on the proposer.

Validation metrics

Methods of calculating error ellipses from data rather than *a priori* should be explored, and the two methods compared. Possibilities are repeated events, bootstrapping, and Joint Hypocenter Determination using groups of events.

An important question is how to validate partial SSSCs. One desirable task is to determine the crossover between Pn, Sn, and P, S, which is region-dependent. There is a question as to whether we should be correcting IASPEI or finding new absolute tables at regional/local distances; the IASPEI phases are not in general the ones present. It was pointed out that none of the national networks uses IASPEI to locate events. It would be desirable to have the national travel-time curves for all regions. States Signatories are again requested to provide all available regional travel-time curves. However, there is a problem in matching such local/regional

tables with IASPEI for teleseismic distances, and with other regions, as seen in a study in Fennoscandia.

The validation metrics should be revised to include a measure of how well the proposed correction surfaces fit observations at the station for events of known location. The unit test metrics given in WGB/TL2-18 still appear to be appropriate, but may need to be revised. Concern was expressed that situations may arise where the introduction of new corrections may cause a small numbers of events to be significantly worse located than before. The evaluation metrics listed in WGB/TL2-18 should be augmented with tools that enable such situations to be detected.

Frode Ringdal

6.2 Locating Seismic Events in Northern Eurasia

Introduction

As part of a project aimed at improving seismic monitoring capabilities under a CTBT, Kola Regional Seismological Centre (KRSC) and NORSAR are conducting a comprehensive study of seismicity, seismic wave propagation and seismic event location in the European Arctic. For Fennoscandia, excellent velocity models have previously been developed, and one such model is currently used at the prototype IDC (Bondar and Ryaboy, 1997). The velocity model in use at KRSC for the past several years (the Barents Model) is very similar to the model used at the prototype IDC, and is given in Table 6.2.1.

In this paper, we study the improvements that can be achieved when applying the Barents model to seismic events in the general northern Eurasia region, when compared to the IASPEI-91 model (Kennett, 1991).While the IASPEI-91 is an excellent average model for the entire globe, it is well known that regional velocity models can provide improvements in many cases. In particular, we will investigate whether the Barents model, which is known to give accurate locations in the Fennoscandian and NW Russia area, can be successfully applied to the more general northern Eurasia region.

Novaya Zemlya events

We have analyzed several seismic events at Novaya Zemlya, most of them nuclear explosions with quite accurate ground truth location. We have in fact, with the assistance of satellite imagery (Skorve and Skogan, 1992) determined very accurate reference locations for a set of these nuclear explosions. Our ground truth locations for these events, estimated to be within 1 km accuracy, are shown in Table 6.2.2. In the terminology used for the Calibration Database at the PIDC (Bondar and North, 1999) our location estimates would therefore qualify for the GT1 category.

Results from our relocation of five nuclear explosions recorded by the Barents regional network (Kremenetskaya and Asming, 1999) are shown in Figure 6.2.1. Only the four seismic stations in the Barents network (Amderma,Apatity, Barentsburg and Pyramiden) were used for this relocation. From this figure, it is seen that the errors when relocating these Novaya Zemlya nuclear explosions using the data from a regional seismic network with the Barents travel time model are all within about 10 km.

In addition, we have located the small m_b=3.8 nuclear explosion on 26 August 1984, using the Barents network (Fig. 6.2.2). This explosion was listed by Mikhailov et. al. (1996) and given an approximate location, based on NORSAR array observation only, by Ringdal (1997). The explosion was not reported by the ISC, and is not listed in Table 6.2.2. Our location is within the nuclear testing grounds, and is clearly better than the location given by Ringdal (1997). However, no ground truth is known to us for this event, and it is therefore difficult to verify the accuracy of our location. It appears nevertheless that the regional network in the Barents area will be capable of precise location of seismic events much smaller than the nuclear explosions listed in Table 6.2.2.

Events in northern Eurasia

Our next attempt was to study travel times in a much larger region, including the European and some of the Asian parts of the Former Soviet Union. We selected 12 seismic events which occured in FSU during 1984-1990 with known ground truth (See Table 6.2.3). The onset measurements have been taken form the ISC bulletins for all the stations situated closer than 30 degrees to the events (310 stations in FSU and surrounding countries). The travel paths for the station-event combinations are shown in Figure 6.2.3.

Results from comparing the observed P and S travel time to those predicted by the IASPEI-91 tables and the Barents model are shown in Figure 6.2.4. The P-wave travel times calculated using the events and stations mentioned above show considerable scattering, which is probably mainly due to some errors in timekeeping for analog stations in combination with occasional errors in the geographic coordinates of some stations (for former socialist countries). Nevertheless, some conclusions can be drawn :

1. In average, P-wave travel times are different both from the IASPEI-91 curve (about -2.0 sec) and from the Barents curve (about +0.5 sec);

2. Weighted average of IASPEI-91 and Barents curves (the 'COMBINED' travel time model) enables us to improve the event locations and avoid systematic bias in origin time estimation;

3. No systematic separation of travel times along different paths(indicating medium inhomogeneties) can be clearly noticed. This leads us to a preliminary conclusion that the same travel time curve can be used for the whole territory being considered ;

4. It is possible to use origin times estimates obtained by P-waves for calibrating travel times for other seismic phases;

Analysis of the S-wave travel times show even more scattering than for P-waves, and the observed times are situated in general between the IASPEI-91 and Barents curves. This might indicate that the S-arrival readings given in the ISC bulletins are not very accurate. In any case, it is clear that S-wave travel times require more careful calibration, probably using strong seismic events, with coordinates and origin times being estimated by the COMBINED model for P waves.

Events in north Karelia and the Kola Peninsula

The Kola Peninsula and North Karelia are regions of great mining activity and we systematically collect ground truth about mining explosions and mining rockbursts in these areas. Analyzing PIDC results for seismic events in the Kola Peninsula (Figure 6.2.5) we found out that location accuracy of PIDC has improved significantly in 1999 (errors about 15-20 km in comparison with 50-70 km in 1995-1998, with systematic bias almost absent). This is encouraging, and shows that the PIDC regional location calibration of this area has been successful.

A slightly different picture emerges for location of Kostomuksha (North Karelia) mining explosions. The average error is about 50 km with an almost absent systematic bias. This scatter is likely due to errors in onset time measurements (about 1.5-2 sec by our estimation).

PIDC detection capability in 1998-1999 is illustrated in Figure 6.2.6. This capability has deteriorated in comparison with previous years, probably due to changes in the GSETT-3 network configuration. Thus, in 1998 191 seismic events with magnitudes greater than 2.6 took place in the Kola Peninsula and only 16 of them have been located by PIDC. The numbers are about the same in 1999 : 213 events occurred and 15 located by PIDC.

Conclusions

All the observations mentioned above cause us to draw the general conclusion : to solve the problem of events location in our region (and, probably, in all of North-Western Russia) the main focus of study should be shifted from travel time table adjustments (which could already be considered to be done in a first approximation) to other important aspects such as improvements in onset time measurements and more reliable backazimuth computations, including perhaps additional parameters from acoustic systems.

KRSC has begun working on this problem. Thus, an acoustic system containing 3 digital barometers which have been installed in the Apatity Array in 1999 enabled us to calculate very accurate backazimuths to several seismic events of unknown nature occurring in areas where seismic activity has been observed. The existence of acoustic signals helped us to discriminate the events as open-pit explosions.

Additionally, we have started to develop a location algorithm based on the generalized beamforming (GBF) method (Ringdal and Kværna, 1989). Currently the algorithm has been checked for re-locating the 12 calibration events mentioned above by ISC data. Its results appeared to be about the same as when location is done by traditional method. But the GBF algorithm has several advantages: it enables easy automatic removal of wrong onsets and permits including any kinds of additional parameters in the form of weights of grid cells.

One of our main tasks remains the collecting of ground truth data in northern Eurasia. With the help of Valery Nikulin, Geological Survey of Latvia we have obtained ground truth data on explosions in the Baltic countries. These data are promising for improving location in our area.

Elena O. Kremenetskaya, KRSC
Vladimir E. Asming, KRSC
Frode Ringdal, NORSAR

References

Bondar, I. and R.G. North (1999): Development of calibration techniques for the Comprehensive Nuclear-Test-Ban Treaty (CTBT) international monitoring system, *Phys. Earth Plan. Int., 113, 11-24.*

Bondar, I. and V. Ryaboy (1997): Regional travel-time tables for the Baltic Shield region, *Technical Report CMR-97/24,* Center for Monitoring Research, Arlington, Virginia, USA.

Kennett, B.L.N. (1991, Ed.): IASPEI 1991 Seismological Tables, Res School of Earth Sci. Austr. Natl. Univ., Canberra, Australia.

Kremenetskaya, E.O. and V.E. Asming (1999): Seismology on Kola: Monitoring earthquakes and explosions in the Barents Region, *IRIS Newsletter*, Vol XVI No. 2., 11-13.

Mikhailov, V.N. et.al. (1996): USSR Nuclear Weapons Tests and Peaceful Nuclear Explosions, 1949 through 1990, RFNC - VNIIEF, Sarov, 1996, 63 pp.

Ringdal, F. (1997): Study of Low-Magnitude Seismic Events near the Novaya Zemlya Test Site, *Bull. Seism. Soc. Am. 87 No. 6,* 1563-1575.

Ringdal, F. and T. Kværna (1989). A multi-channel processing approach to real time network detection, phase association and threshold monitoring, *Bull. Seism. Soc. Am.* 79, 1927-1940.

Skorve, J. and J.K. Skogan (1992): The NUPI satellite study of the northern underground nuclear test area on Novaya Zemlya, NUPI Report No. 164, Oslo, Norway.

Sultanov, D.D., J.R. Murphy and Kh.D. Rubinstein (1999): A Seismic Source Summary for Soviet Peaceful Nuclear Explosions, *Bull. Seism. Soc. Am. 89 No. 3,* 640-647.

Table 6.2.1. Barents Regional Velocity Model

Depth (km)	V_P (km/s)	V_S (km/s)	Comment
0-16	6.20	3.58	
16-40	6.70	3.87	
40-55	8.10	4.60	
55-210	8.23	4.68	
>210			Same as IASPEI-91

Table 6.2.2. Ground truth data (GT1) for Novaya Zemlya nuclear explosions

No.	Date	Lat (Deg)	Lat(Min)	Lon(Deg)	Lon(Min)
1	18 Sep 64				
2	25 Oct 64	73	22.6	55	9.9
3	27 Oct 66	73	23.0	54	50.5
4	21 Oct 67	73	23.3	54	49.6
5	7 Nov 68	73	23.4	55	52.0
6	14 Oct 69	73	23.4	54	48.2
7	14 Oct 70	73	18.0	55	1.6
8	27 Sep 71	73	23.3	55	54.2
9	28 Aug 72	73	23.1	54	52.0
10	12 Sep 73	73	18.9	55	2.8
11	29 Aug 74	73	23.6	54	56.0
12	23 Aug 75	73	19.9	54	42.3
13	21 Oct 75	73	18.4	55	0.2
14	29 Sep 76	73	21.6	54	51.9
15	20 Oct 76	73	23.9	54	51.0
16	1 Sep 77	73	19.6	54	37.7
17	9 Oct 77	73	23.4	54	50.0
18	10 Aug 78	73	17.9	54	49.4
19	27 Sep 78	73	20.2	54	42.0
20	24 Sep 79	73	19.9	54	40.1
21	18 Oct 79	73	19.1	54	46.3
22A	11 Oct 80	73	18.3	54	48.9
23	1 Oct 81	73	18.3	54	47.1
24	11 Oct 82	73	19.9	54	36.2
25	18 Aug 83	73	21.5	54	56.7
26	25 Sep 83	73	19.2	54	34.6
27	25 Oct 84	73	21.6	54	58.7
28	2 Aug 87	73	19.4	54	36.4
29	7 May 88	73	18.9	54	33.6
30	4 Dec 88	73	22.1	55	0.2
31	24 Oct 90	73	19.0	54	48.3

Table 6.2.3. Calibration events used in this study

No.	Date	Origin time	Latitude (N)	Longitude (E)
1	28.05.1990	02.41.27	55.17	58.72
2	22.08.1988	16.20.00.07	66.28	78.491
3	06.09.1988	16.19.59.94	61.361	48.092
4	03.10.1987	15.15.00.03	47.60	56.20
5	12.08.1987	01.30.00.5	61.45	112.80
6	24.07.1987	02.00.00.0	61.45	112.80
7	19.04.1987	04.00.00.1	60.60	57.20
8	19.04.1987	04.04.59.98	60.80	57.50
9	18.07.1985	21.15:00.29	65.994	41.038
10	27.10.1984	06.00.00.10	46.90	48.15
11	27.10.1984	06.05.00.0	46.95	48.10
12	24.10.1990	14.58.00.0	73.317	54.805
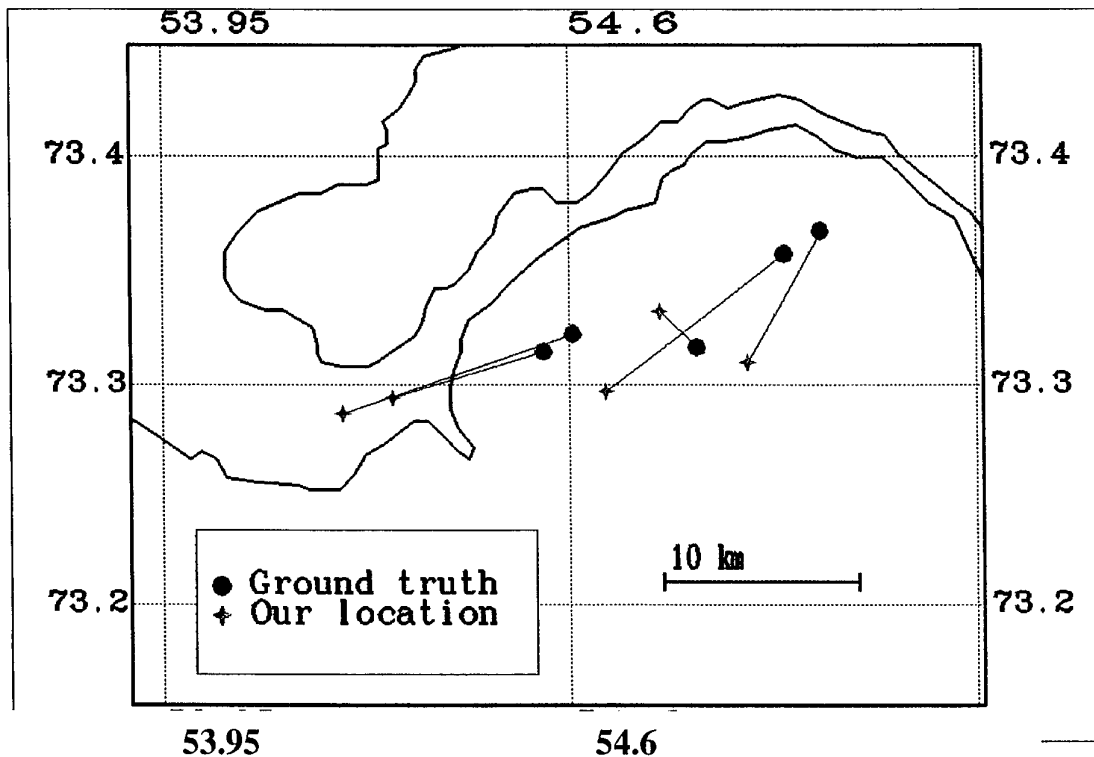
NZ nuclear explosions located by regional stations and BARENTS travel time
model.

Fig. 6.2.1. *Results from locating five nuclear explosions at Novaya Zemlya using the Barents
regional seismic network. The ground truth locations (from Table 6.2.2) are shown for com-
parison. Note that all our locations are accurate to within approximately 10 km.*

Locating the 26 Aug 1984 (mb=3.8) NZ nuclear explosion

Novaya Zemlya 26.08.84 03.30.00 mb 3.8 Stations AMD APA PYR BRB
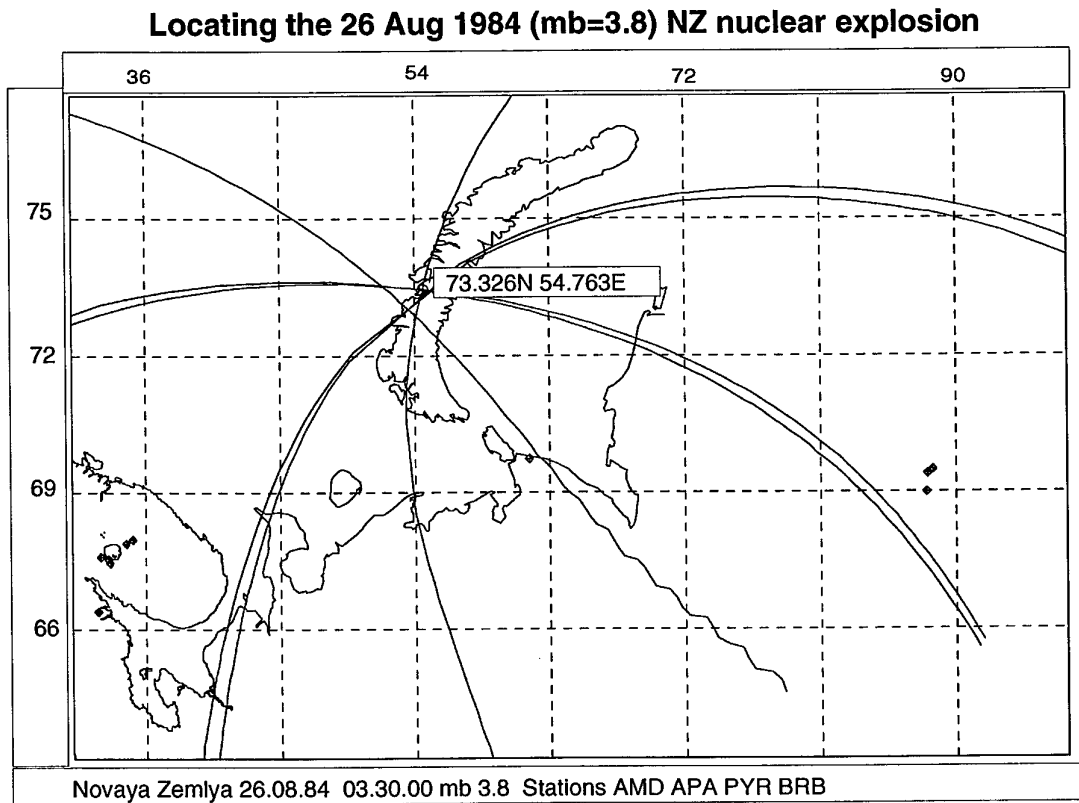
Fig. 6.2.2. *Results from locating the small Novaya Zemlya nuclear explosion (m_b=3.8) on 26 August 1984, using the stations of the Barents network.*

Explosions used for calibration (red) and seismic stations (green).
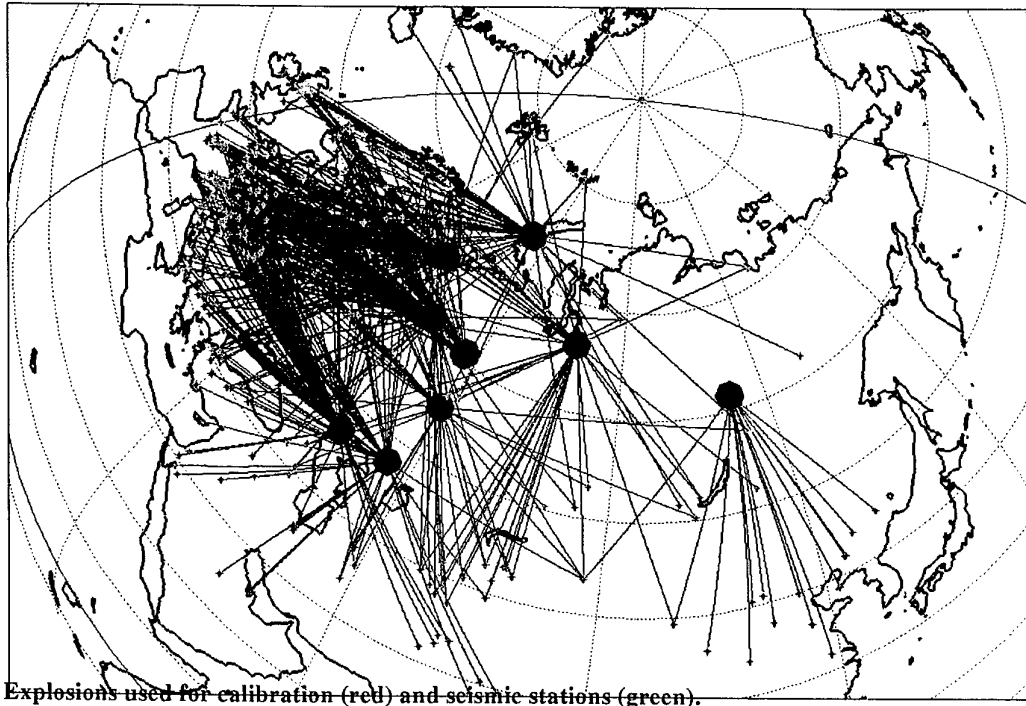
Fig. 6.2.3. *Station-event coverage paths for the 12 calibration events listed in Table 6.2.3.*
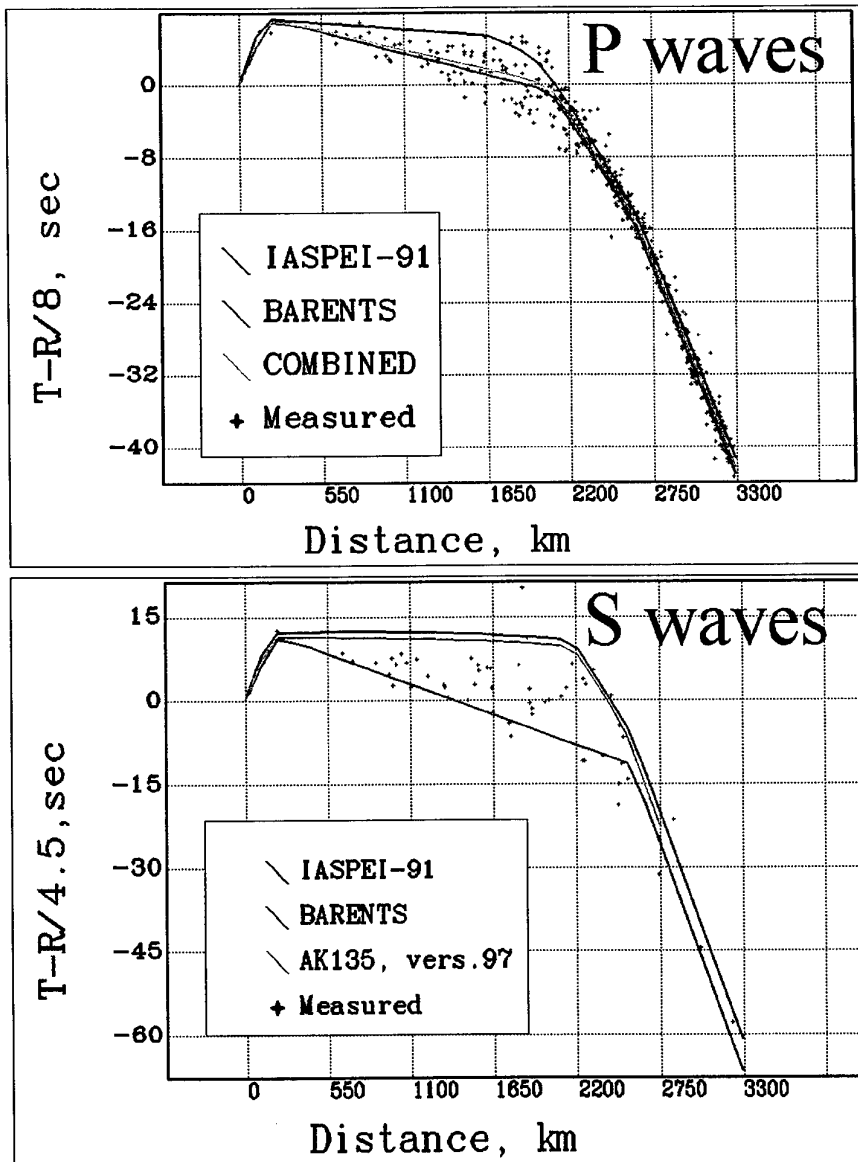
Fig. 6.2.4. *Observed travel times for P and S phases for the calibration event data set. The predicted travel-time curves for the IASPEI-91 model and the Barents model are shown for comparison. We also show the AK135 model (97 version) for the S-phases, and our calculated Combined model, which turns out to be very close to the Barents model for P-phases.*

IDC location of explosions in Khibiny Massif and earthquakes in Lovozero Massif
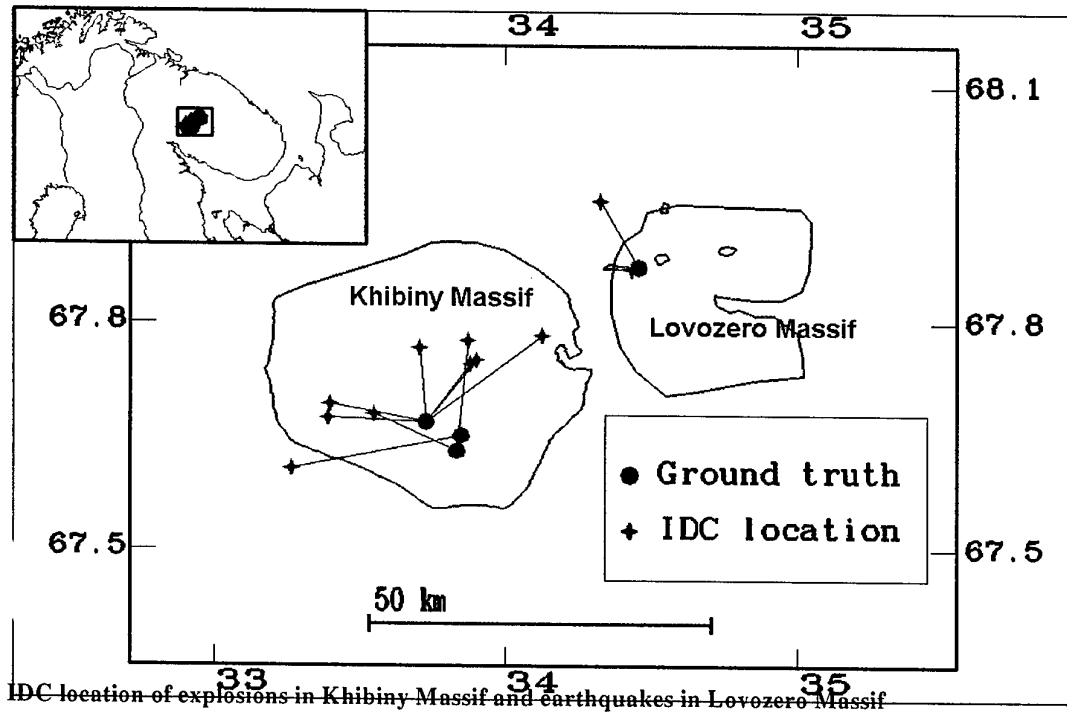
Fig. 6.2.5. *PIDC location errors for Khibiny events during 1999. Ground truth locations for these eventshave been provided by KRSC. The location errors are about 15-20 km, which is much better than for previous years.*

Numbers of events : detected by IDC (blue columns)
true numbers (red columns)
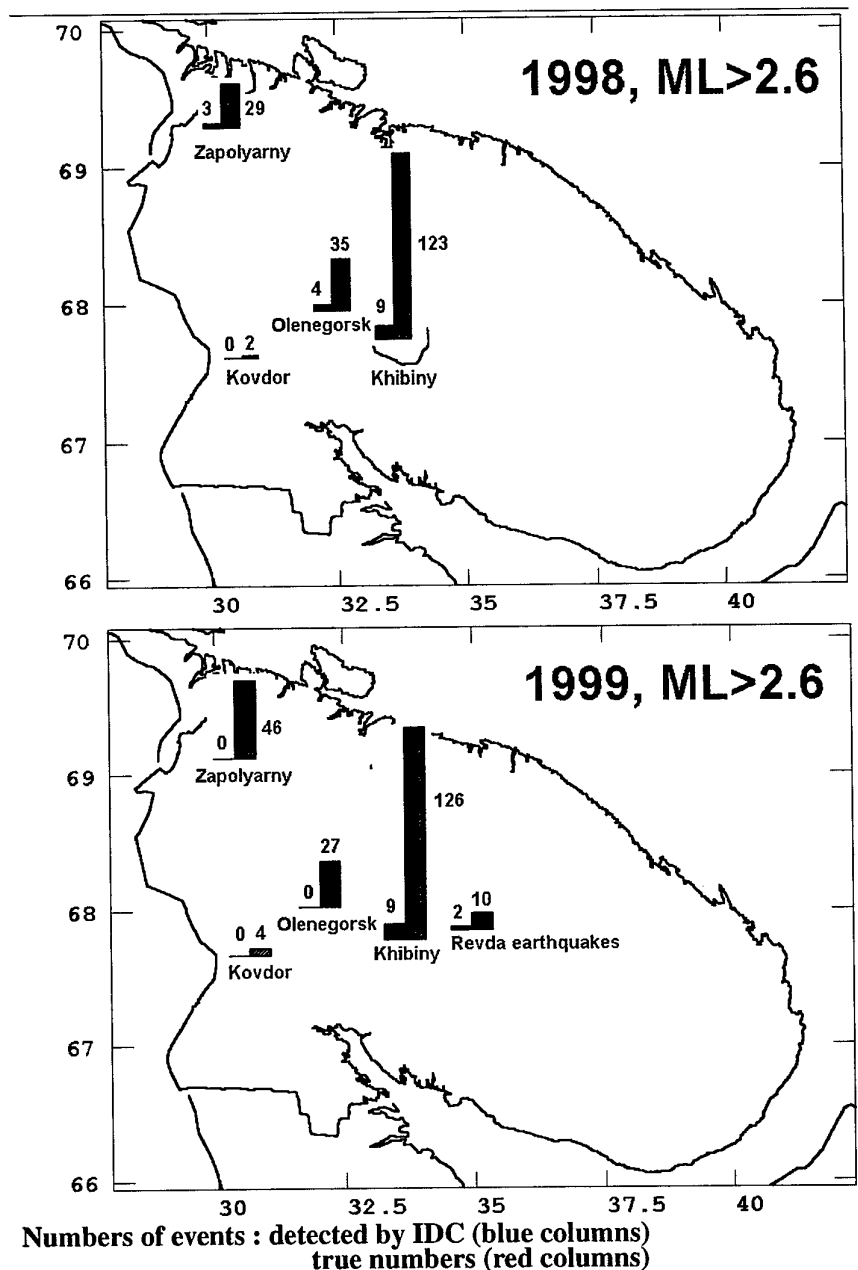
Fig. 6.2.6. *Illustration of event detectability for the Kola Peninsula of the PIDC Reviewed Event Bulletin (REB) for the years 1998-99. The histograms show the number of events exceeding magnitude (m_b) 2.6, as reported in the NORSAR and KRSC regional bulletins, and the number of events located by the PIDC at each of five main sites. The percentage of such events in the REB is much lower than for previous years.*

6.3   The Eurobridge Profile: Analysis of time residuals at the Fennoscandian arrays

Introduction

In the previous NORSAR Semiannual Report (Taylor et. al, 1999), we introduced the recordings of the Eurobridge shots at the Fennoscandian arrays ARCES, FINES, Hagfors (HFS), and NORES. Tables with time residuals relative to the travel-time predictions calculated from the Fennoscandian crustal and upper mantle velocity model (Mykkeltveit and Ringdal, 1981) were presented, and relatively large anomalies were observed at the different arrays. In this contribution we will analyze these observations in more detail.

Time residuals at HFS, NORES and FINES

The shot points of the Eurobridge profile are shown in Fig. 6.3.1, together with the locations of the four arrays investigated in this study. HFS and NORES are located 135 km apart, close to the extension of the profile line, and we therefore expect that the rays from the Eurobridge shots would sample much of the same upper mantle and near source crustal structures. However, when comparing the P-phase travel-time residuals at these two stations (Figs. 6.3.2 and 6.3.3) there are large differences. The arrival times at HFS are consistently late by 1 second or more as compared to NORES, and it requires quite strong structural lateral heterogeneities to provide such large differences.

In order to rule out possible timing errors at any of the arrays, we have analyzed the time residuals reported in the Reviewed Event Bulletins (REBs) of the Prototype International Data Center (pIDC). The REB residuals are relative to the travel-times of the IASP91 model, and _not_ to those of the Fennoscandian model used in Figs. 6.3.2 and 6.3.3. Semiannual median values of the pIDC time residuals for HFS, NORES, and FINES are shown in Fig. 6.3.4. The FINES array has had a stable operation as a GSETT-3 primary station during the entire time period, and we consequently see small temporary variations in the median values of the time residuals.

NORES was used as a GSETT-3 primary station until the end of 1997, and we see from Fig. 6.3.4 that there are small temporal variations in the median time residuals of the pIDC REBs. The closest (and largest) of the Eurobridge shots (A0), having a distance to NORES of about 5 degrees, has a Pn arrival time that fits very well with the predictions of the Fennoscandian model (see Fig. 6.3.3). The timing of this event can be checked with the observations of the co-located large-aperture NORSAR array (NOA). The NOA recordings of Eurobridge shot A0 are shown in Fig. 6.3.5, and we find again a very good fit with the model predictions. The small temporal variations in the median time residuals of the pIDC REBs, together with the consistency of the NORES and NOA recordings, confirm the correct timing of NORES.

For 1995 and the first half of 1996 we see from Fig. 6.3.4 that HFS had positive median residuals, whereas they are negative for the rest of the investigated period. The HFS data are recorded by a Nanometric data acquisition system having a FIR filter that delays the data by 0.493 seconds. The correction for this filter delay was missing at the pIDC until 1 October 1996, which explains the positive residuals. Before 1 October 1996 HFS was used as a primary station in the GSETT-3 network, but was after that date used as an auxiliary station, thus providing data for selected events only. This means that the statistics on HFS time residuals are based on less data as compared to FINES, and can therefore explain the larger temporary variability of the median

HFS time residuals after 1 October 1996. However, the Eurobridge profile was carried out in the summers of 1995 and 1996, for which the median NORES time residuals and the HFS residuals (now corrected for the FIR filter delay) had comparable values. This is to be expected as NORES and HFS are located only 135 km apart, well away from any major tectonic boundaries.

The FIR filter delay is accounted for in the HFS section of the Eurobridge shots shown in Fig. 6.3.2, and based on the arguments above we therefore conclude that the HFS data have correct timing as displayed in Fig. 6.3.2.

In order to investigate the large differences in travel-time residuals between the Eurobridge sections at HFS and NORES (see Figs. 6.3.2 and 6.3.3), we have in Figs 6.3.6 and 6.3.7 plotted the main geological structures and a contoured Moho depth map for Fennoscandia. When comparing the Eurobridge profile line and the locations of HFS and NORES of Fig. 6.3.1 with the geological structures given in Fig. 6.3.6, we find that the ray paths to these stations are crossing provinces with different geology (Svecofennian -> Sveconorwegian). In particular, the ray paths to NORES are approaching the north-eastern part of the Oslo Graben area. The crustal and upper mantle structure of the Oslo Graben and adjacent areas has been investigated by several authors (e.g. Gundem, 1984; Tryti and Sellevoll, 1977; Cassell et al., 1983; Berteussen, 1977). These studies have indicated that the lower crust in the north-eastern border zone of the Oslo Graben (around NORES) area has a stronger velocity gradient than in the adjacent Sveconorwegian province to the east. In addition, the Moho is believed to be slightly uplifted in this area, to a depth of 33-35 km.

The large-scale Moho depth map of Fig. 6.3.7 suggests a gradual increase in the Moho depths eastwards from NORES to HFS, but as seen from the actual data points, these are mainly based on interpolation. However, the EUGENO-S Profile 3 (EUGENO-S Working Group, 1988; Green et al., 1988) supports this trend. But, in order to explain the large differences in travel-time residuals seen from the Eurobridge shots, more detailed information on the crustal structure of southern Sweden would be needed. The Moho depth points of the profile lines, shown in Fig. 6.3.7, show that there are several regions in Fennoscandia with anomalously deep crust. E.g., the region with 50+ km thick crust in southwestern Sweden is located close to the ray paths from the Eurobridge shots to HFS and NORES.

We also can deduce that the inhomogeneities can not be located directly below the receiving stations, because the average time residuals of the pIDC REBs (Fig. 6.3.4), for HFS (after FIR filter correction) and NORES are approximately equal. The REB residuals are entirely based on teleseismic data, and thus only sample the crust and upper mantle at small incidence angles, in the vicinity of the receiving stations.

The Eurobridge record section for FINES is shown in Fig. 6.3.8, with the manually picked P-onsets and the predicted travel-time curve superimposed. Again, the P-arrivals exhibit significant deviations from the predictions of the Fennoscandian model. At the closest distances of about 6 degrees, the onsets are 1-1.5 seconds later than the predictions, whereas between 8.5 and 9.5 degrees distance the onsets are about 1 second early. By comparing locations of FINES, the Eurobridge shot points, the Fennoscandian surface geology, and the Moho depths (Figs 6.3.1, 6.3.6, 6.3.7), we find that the FINES record section is composed of signals sampling regions with different geological and geophysical properties. This can, in general, explain the observed travel time anomalies, although we cannot resolve the individual structures caus-

ing the observed patterns. A composite section containing the P arrival time picks at HFS, NORES and FINES is shown in Fig. 6.3.9. The scatter in the observations clearly demonstrate the need for a regionalized travel-time model if precise event locations are to be provided.

Time residuals at ARCES

At the ARCES array, located between 1400 and 2000 km from the profile line, we were able to pick the P-arrivals for nine events. As seen from Fig. 6.3.10, significant time residuals are observed. In particular, the P-onset from the largest shot A0 has a negative time residual of almost 3 seconds.

Along with the investigation of the timing at HFS, NORES, and FINES, we also retrieved the time residuals of ARCES and some other stations from the pIDC REBs for the 5-year period 1995-2000. Events located with phases at more than 20 stations, having an SNR > 10 at the investigated station were considered. Fig. 6.3.11 summarizes the pIDC time residuals as a function of time, where each data point represents the median of 5 subsequent events. For FINES we see that the time residuals fluctuate within ±1 second around the average, and there are no outliers. The time residuals for GERES exhibit a short time period with negative values in early 1995. These are associated with a reported 3 second timing error associated with a malfunction of the GERES clock.

However, several periods with large negative outliers are seen for ARCES, indicating problems with timing of the system. These time periods are detailed in Table 6.3.1, and typically reflect intervals where three or more subsequent events have negative residuals exceeding 2-3 seconds. One of these intervals (1995, day150) coincides with the largest Eurobridge shot (A0), thus explaining the large negative time residual seen on Fig. 6.3.10 for event A0. For the other Eurobridge shots observed at ARCES we have no indication of such large timing problems. The precise onsets of these P-phases are somewhat uncertain due to the low SNRs. However, except for one event, all arrivals are early relative to the predictions of the Fennoscandian model.

The mechanisms that lead to the timing errors at ARCES are still unknown, but as seen from Table 6.3.1 three of these intervals start at day 180. Until the fall of 1999 ARCES was using a radio controlled timing system, where the long wave signals were received from a transmitter in Germany (DCF 77). A hypothesis is that the problems were associated with the reception of the radio signals during the summer, when we often have poor propagation of long wave signals. In the fall of 1999 the ARCES array was upgraded with new electronics using a GPS based timing system. Since then we have had no indications of such timing errors.

Using the same procedure for analysis of time residuals in the REBs, we also investigated a few other IMS stations. YKA (see Fig. 6.3.12) showed no sign of timing problems, but we found occasional errors at the WRA array during the years 1995, 1996, and early 1997. For ASAR we observe a trend towards more negative residuals during the five-year period. This is very difficult to explain with clock problems, but changes in the network configuration and/or the analysis procedures could have lead to such effects. Interestingly, the other Australian array (WRA) shows a similar tendency.

We believe that the method developed in this study to identify timing anomalies will be useful both in validating location calibration data and in providing a tool for continuously checking the timing accuracy and consistency of the IMS stations.

T. Kværna
J. Schweitzer
L. Taylor

References

Berteussen. K.-A. (1977): Moho depth determination based on spectral-ratio analysis of NORSAR long-period P waves, Phys. Earth Planet. Int., 15, 13-27.

Boyd, R., G. Nilsson, H. Papunen, A. Vorma, V. Zagorodny and V. Robonen (Compilers) (1985): General geological map of the Baltic Shield. In: Papunen, H. and G. I. Garbunov (eds.), Nickel-copper deposits of the Baltic Shield and the Scandinavian Caledonides. Geol. Surv. Finland, Bull., 333, appendix.

Cassell, B. R., S. Mykkeltveit, R. Kanstrøm and E. S. Husebye (1983): A North Sea - southern Norway seismic crustal profile, Geophys. J. R. astr. Soc., 72, 733-753.

EUGENO-S Working Group (1988): Crustal structure and tectonic evolution of the transition between the Baltic Shield and the North German Caledonides (the EUGENO-S Project), Tectonophysics, 150, 253-348.

Green, C.M., Stuart, G.W., Lund, C.-E. and R.G.Roberts (1988): P-wave crustal structure of the Lake Vänern area, Sweden: EUGENO-S Profile 6, Tectonophysics, 150, 349-361.

Gorbatschev, R. (ed.), (1993): The Baltic Shield. Special volume Precambrian Research, 64, 430 pp.

Gundem, M. B. (1984): 2-D Seismic Synthesis of the Oslo Graben. Cand. Scient Thesis, University of Oslo.

Luosto, U. (1991): Moho depth map of the Fennoscandian Shield based on seismic refraction data. In: H. Korhonen and A. Lipponen (eds.), Structure and Dynamics of the Fennoscandian Lithosphere. Proceedings of the Second Workshop on Investigation of the Lithosphere in the Fennoscandian Shield by Seismological Methods, Helsinki, May 14-18, 1990. Inst. Seismology, Univ. Helsinki, Report S-25, 43-49.

Mykkeltveit, S. and F. Ringdal (1981): Phase identification and event location at regional distance using small-aperture array data. In: Husebye, E.S. and S. Mykkeltveit (eds.), 1981: *Identification of seismic sources - earthquake or underground explosion*. D. Reidel Publishing Company, 467-481.

Taylor, L., J. Schweitzer, and T. Kværna. (1999): Eurobridge - ground truth observations at the Fennoscandian arrays. In: NORSAR Semiannual Tech. Summ. 1 April - 30 September 1999, *NORSAR Sci. Rep. 1-99-00*, Kjeller, Norway, 108-121.

Tryti, J. and M. A. Sellevoll (1977): Seismic crustal study of the Oslo Rift, Pure and Appl. Geophys., 115, 1061-1085.

Table 6.3.1 Days with large timing errors at ARCES

1995-137
1995-150
1996-161 to 1996-162
1996-180 to 1996-181
1998-146 to 1998-149
1998-180 to 1998-185
1999-180 to 1999-185
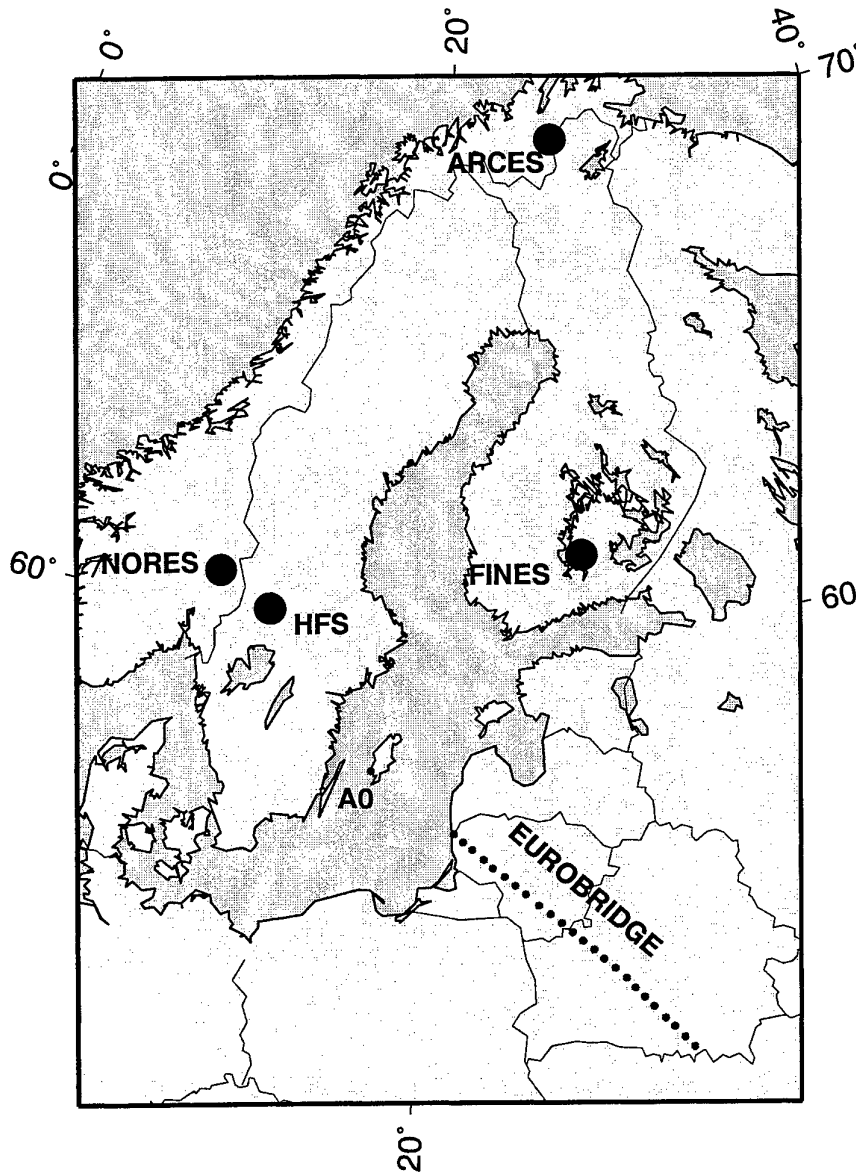
Fig. 6.3.1. *Map showing the locations of the Eurobridge shots and the four arrays included in this study (ARCES, FINES, HFS, and NORES). A0, located off the southern coast of Gotland, was part of the Eurobridge experiment.*
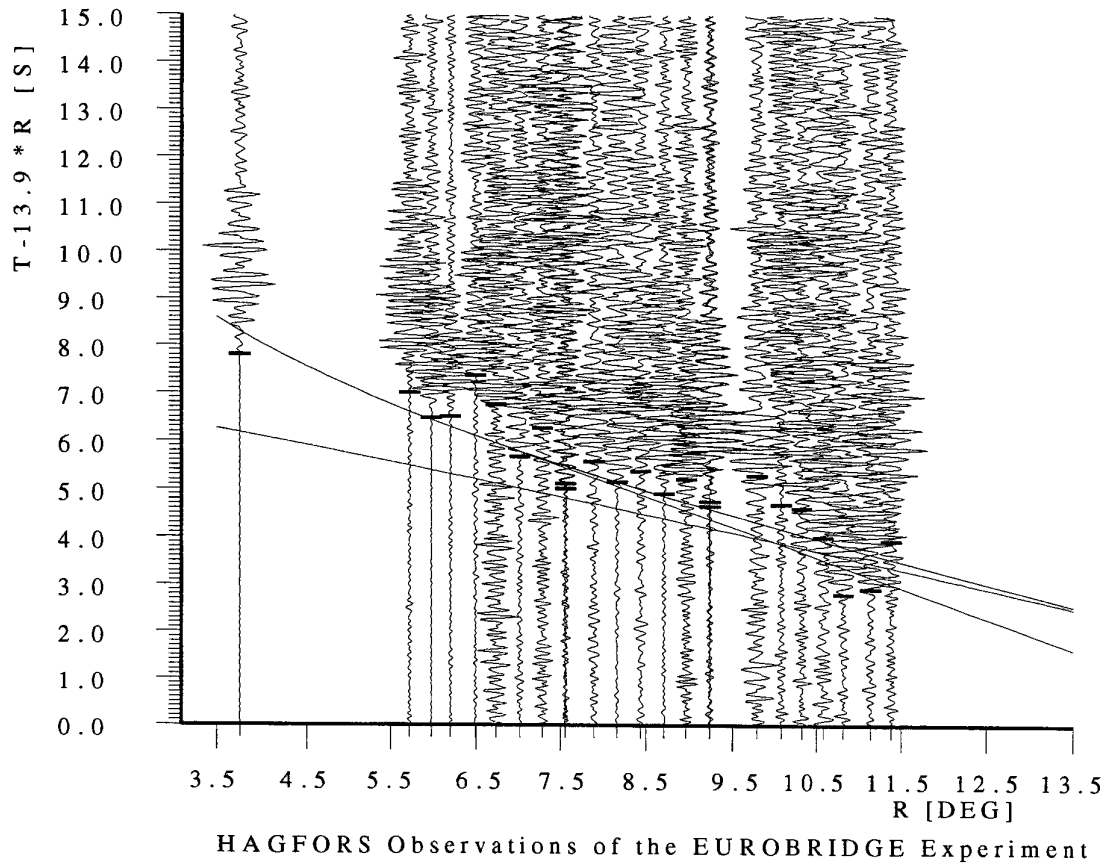
Fig. 6.3.2. *Section of Eurobridge shots recorded at Hagfors (HFS) with travel-time curves of the Fennoscandian model superimposed. The manually picked arrival times are shown by bold bars. Each trace shows a coherent beam steered with the azimuth and apparent velocity of the arriving P-phase. The bandpass filter providing the best SNR was applied to each trace.*
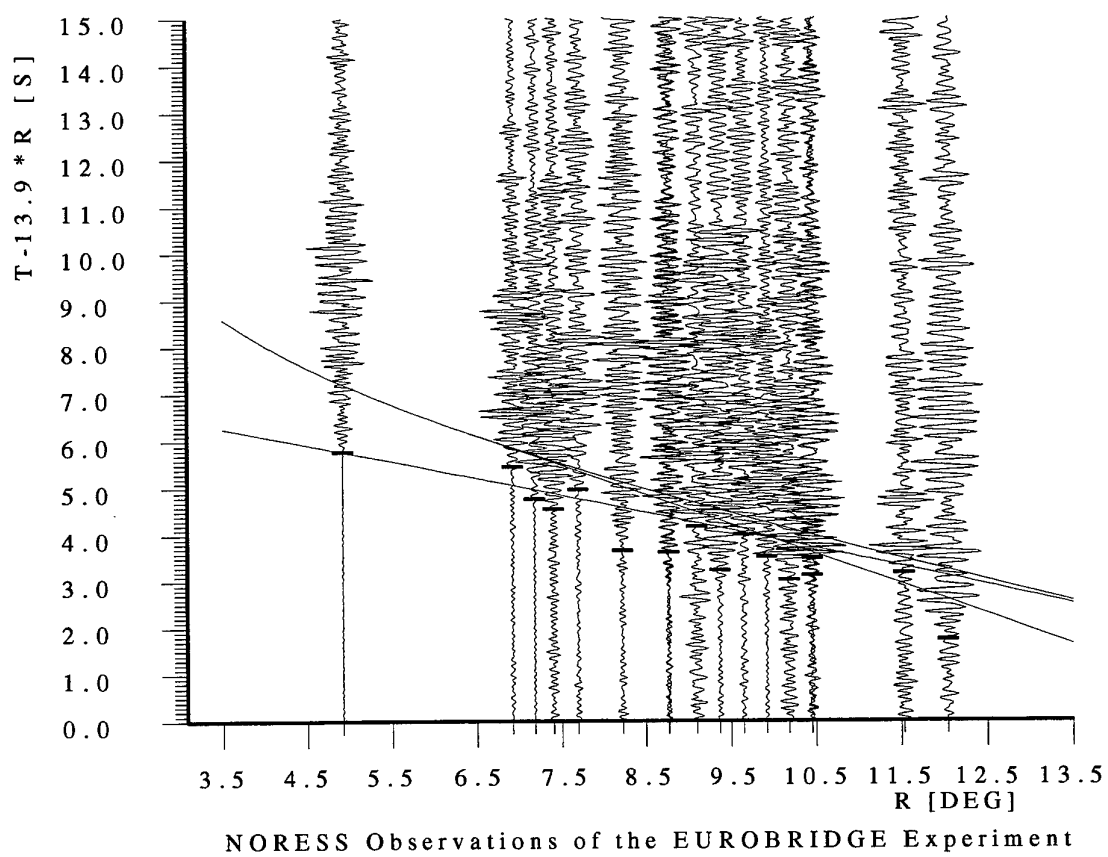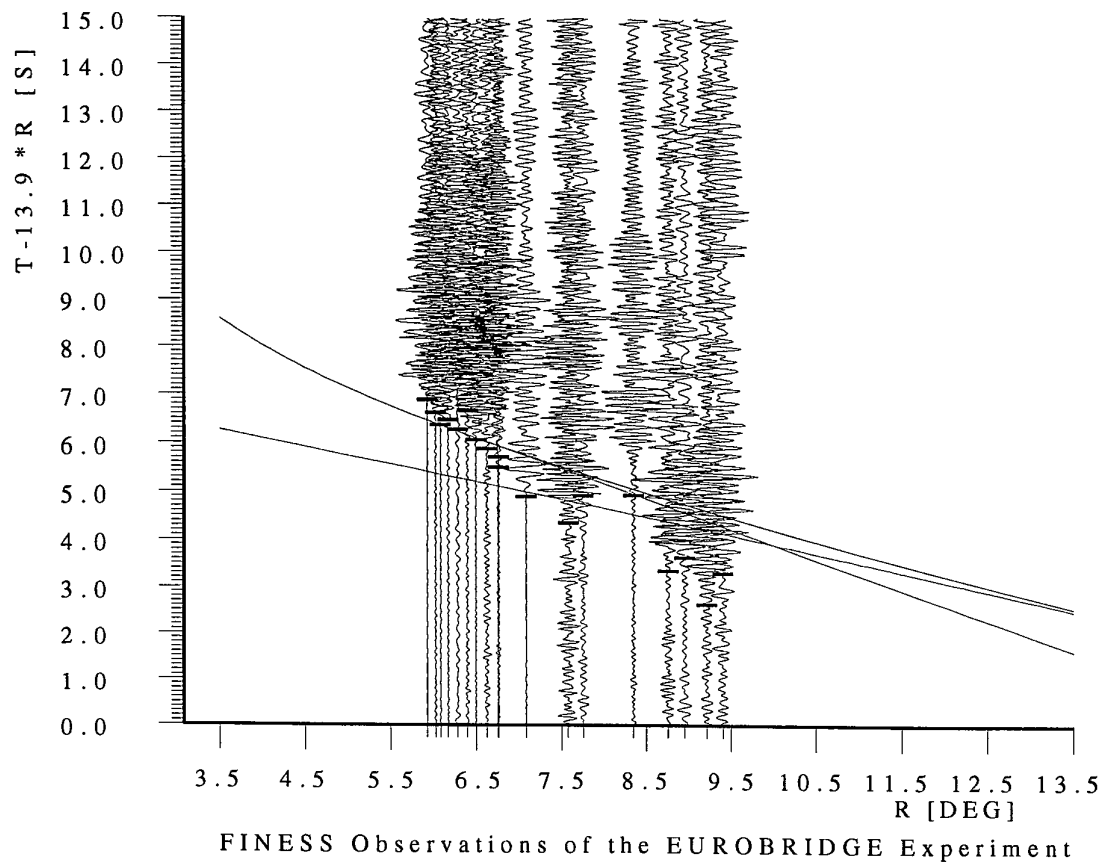
Fig. 6.3.3. *Section of Eurobridge shots recorded at NORES with travel-time curves of the Fennos-candian model superimposed. The manually picked arrival times are shown by bold bars.*
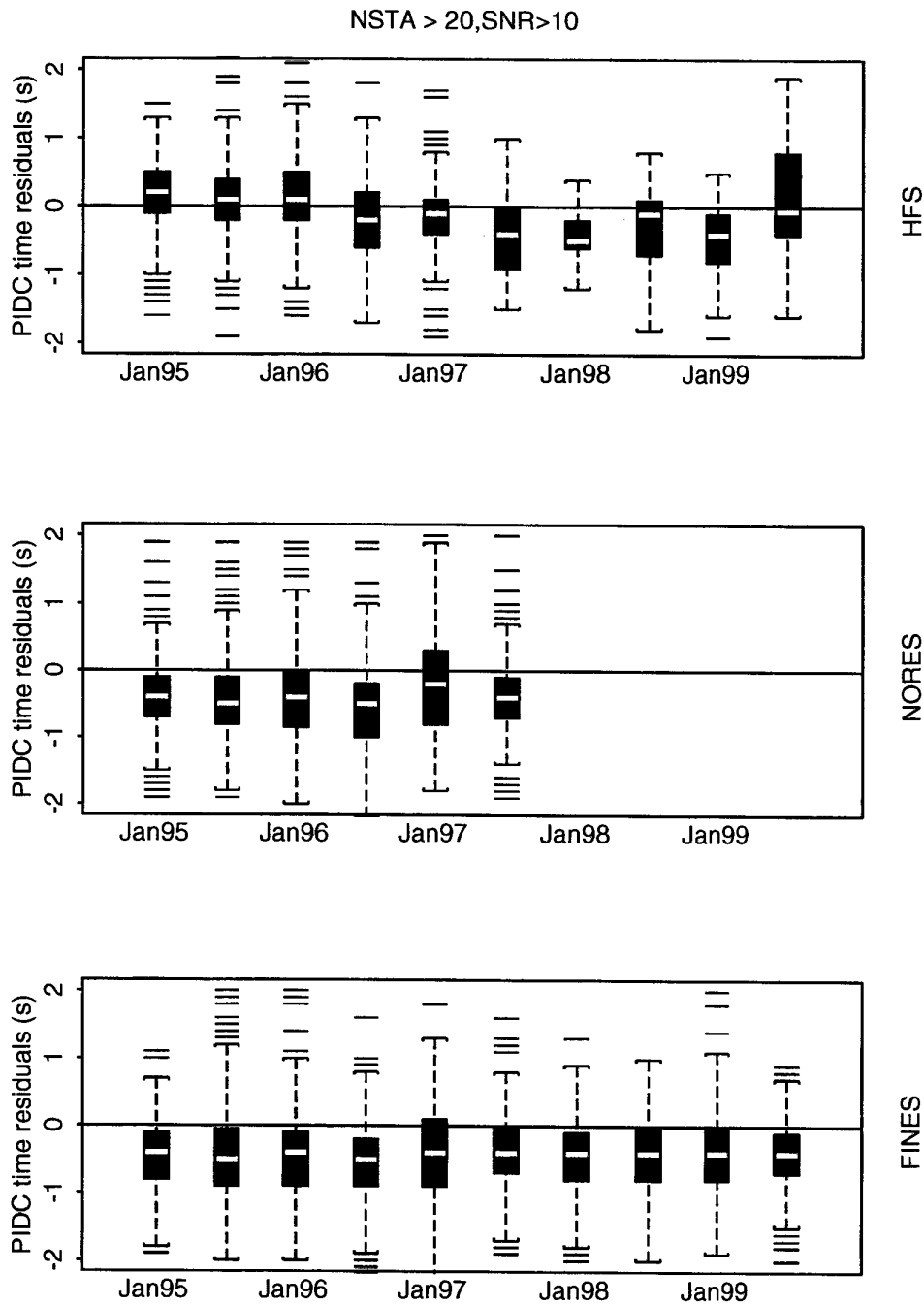
Fig. 6.3.4. *Time residuals of P-phases reported in the pIDC REBs for events located with more than 20 stations having signals with an SNR at the investigated station greater than 10. The white line in the center of the bars represent the semiannual median value, and the size of the bars and whiskers represent the scatter in the observations.*
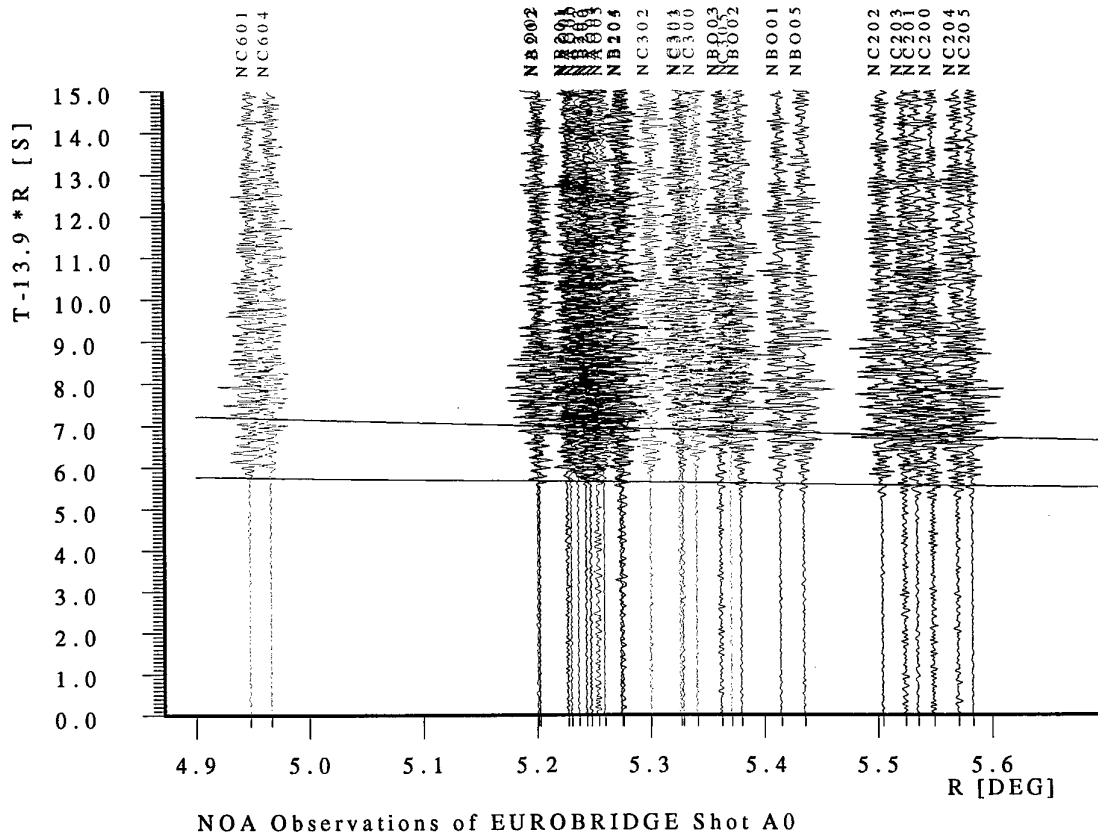
Fig. 6.3.5. *Section of Eurobridge shot A0 recorded at each individual sensor of the large-aperture NORSAR array (NOA) with travel-time curves of the Fennoscandian model superimposed. The site names of the array are given above each trace, and the sensors belonging to the same sub-arrays are displayed using the same color.*
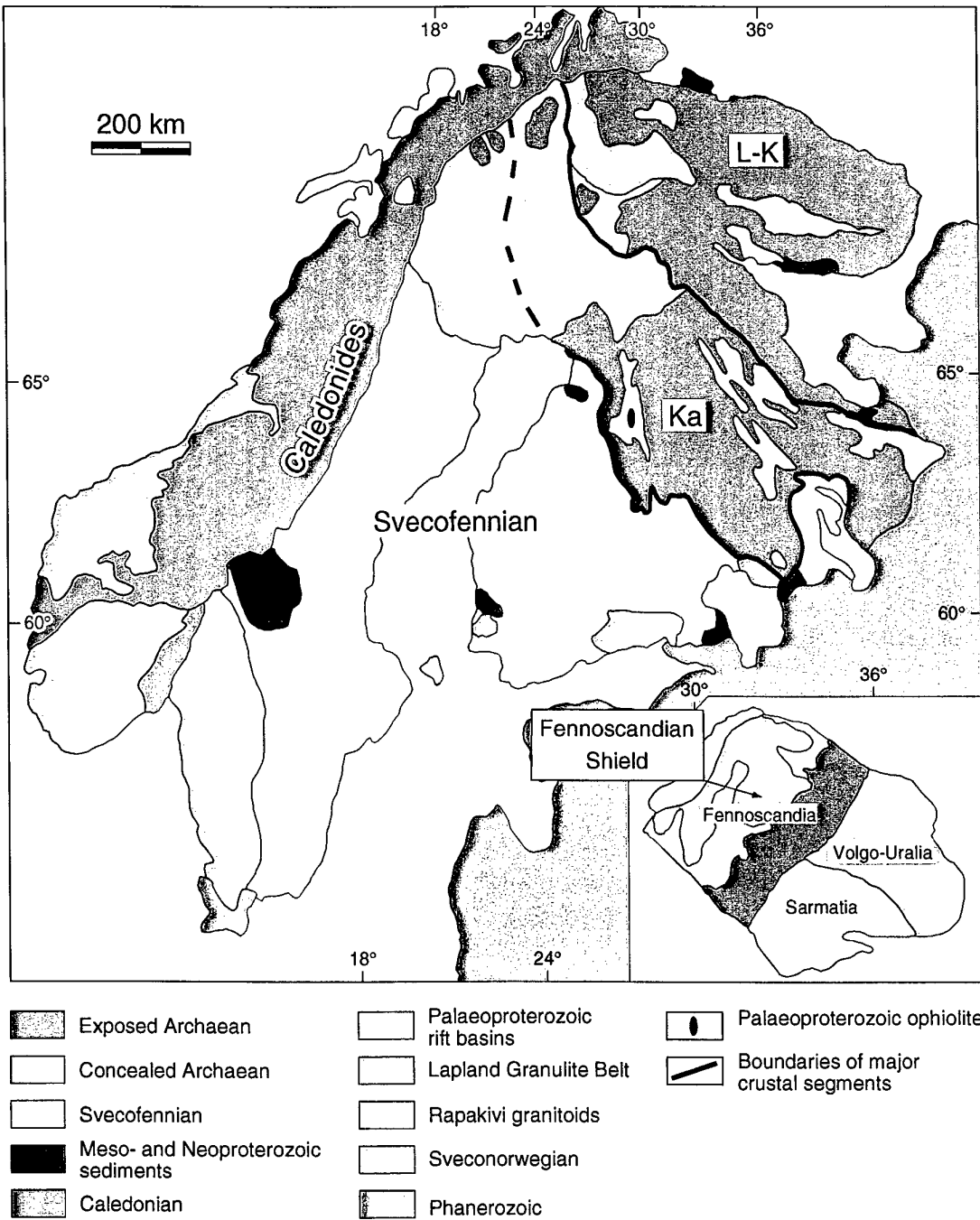
Fig. 6.3.6. *Simplified geological map of the Baltic Shield and surroundings (modified from Boyd et al., 1985 and Öhlander et al., In Gorbatshev, 1993). The figure was copied from the Euro-probe home page on http://www.geofys.uu.se/eprobe/Projects/svekal/Svekalap.htm*
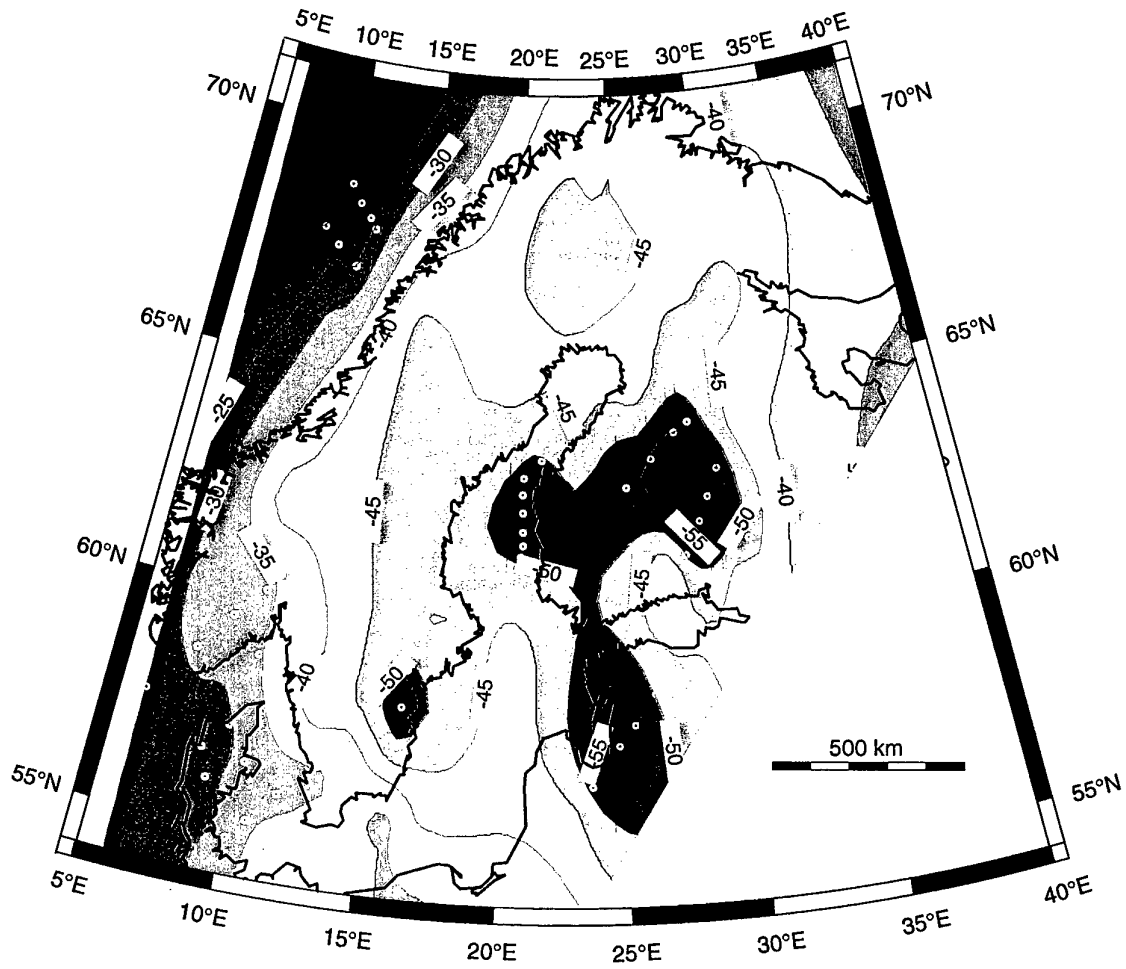
Fig. 6.3.7. *Moho depth in Fennoscandia (modified after Luosto, 1991). Dots mark points where the crustal thickness has been determined. The figure was copied from the Europrobe home page on http://www.geofys.uu.se/eprobe/Projects/svekal/Svekalap.htm*

Fig. 6.3.8. *Section of Eurobridge shots recorded at FINES with travel-time curves of the Fennos-candian model superimposed. The manually picked arrival times are shown by bold bars.*
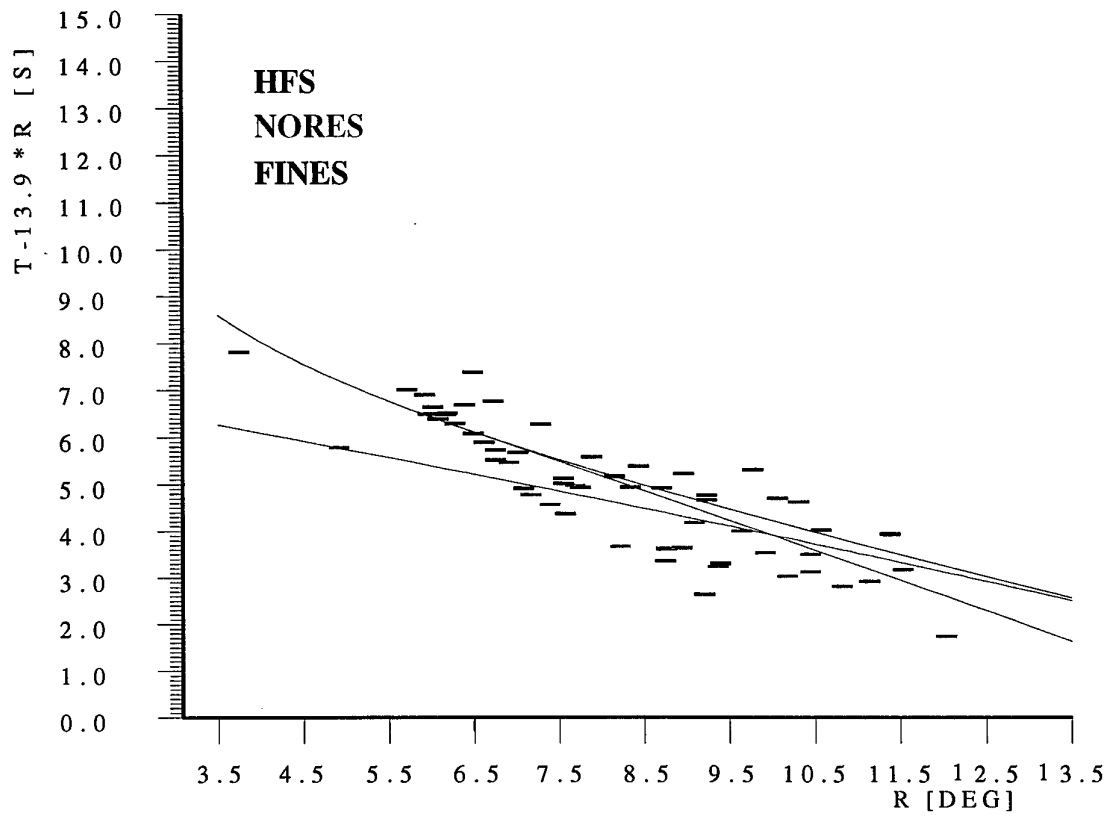
Fig. 6.3.9. *P-phase arrival time picks of the Eurobridge shots at HFS, NORES, and FINES with travel-time curves of the Fennoscandian model superimposed.*

ARCESS Observations of the EUROBRIDGE Experiment
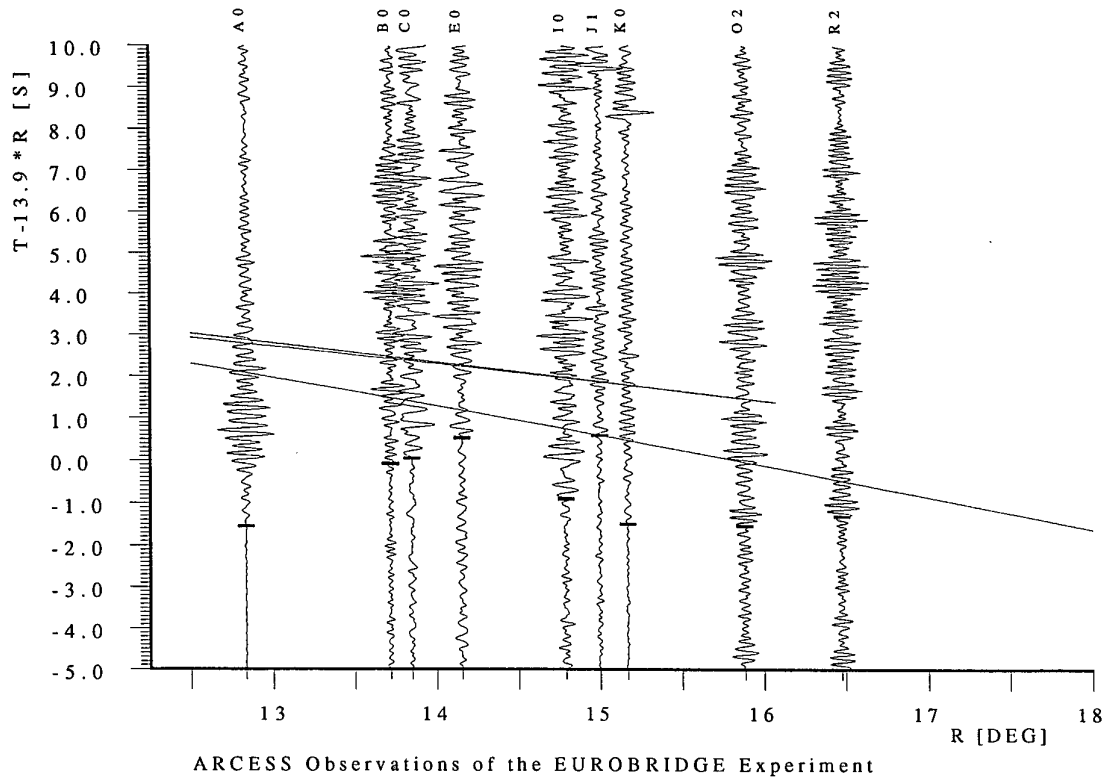
Fig. 6.3.10. *Section of Eurobridge shots recorded at ARCES with travel-time curves of the Fennoscandian model superimposed. The manually picked arrival times are shown by bold bars.*

Running median of 5, NSTA>20, SNR>10
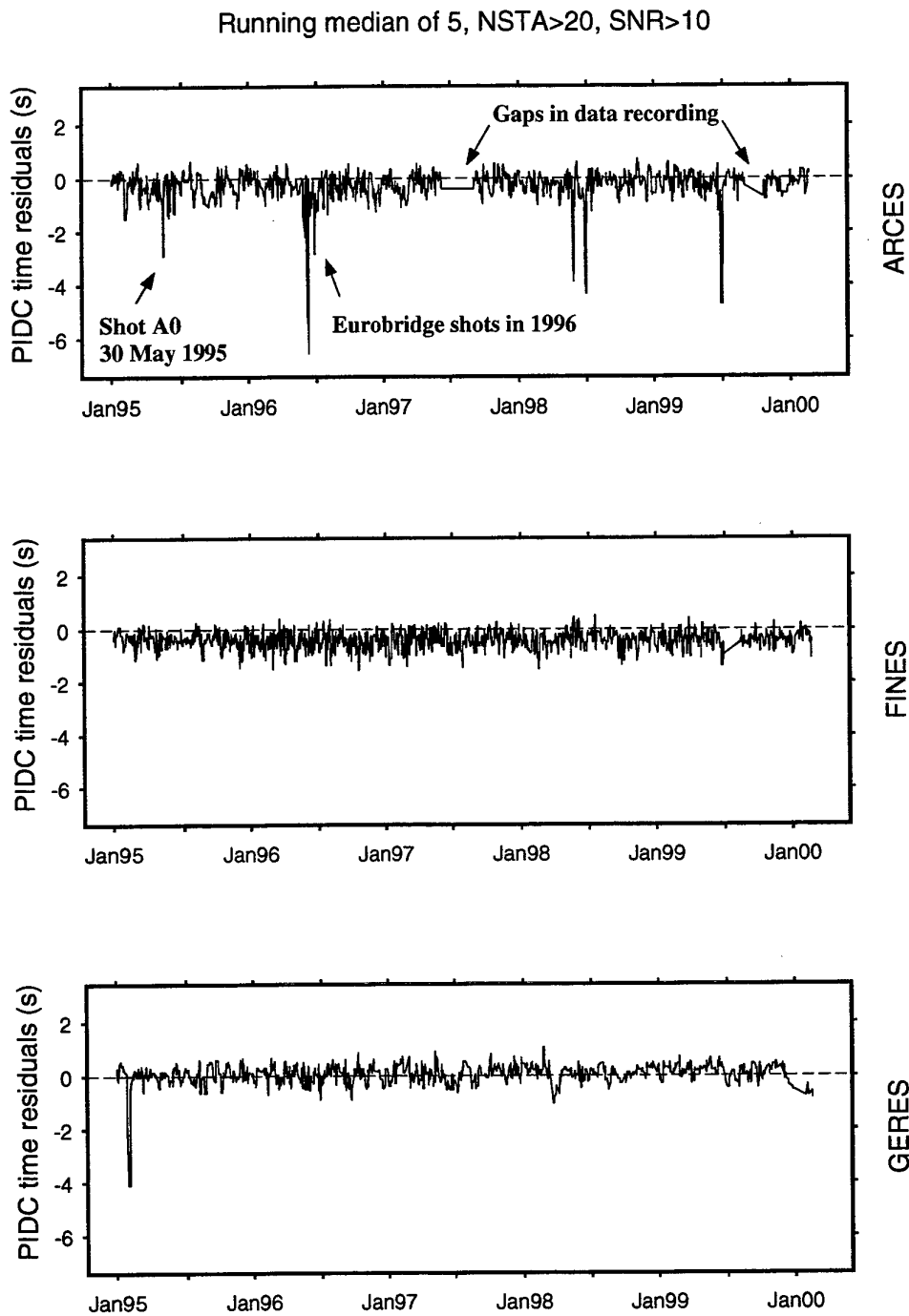
Fig. 6.3.11. *Time residuals in the pIDC REBs for the period 1995-2000 for ARCES, FINES, and GERES. Events located with phases at more than 20 stations, and having signals with an SNR > 10 at the investigated station were considered. For visualization, running medians of 5 subsequent events are plotted.*

Running median of 5, NSTA>20, SNR>10
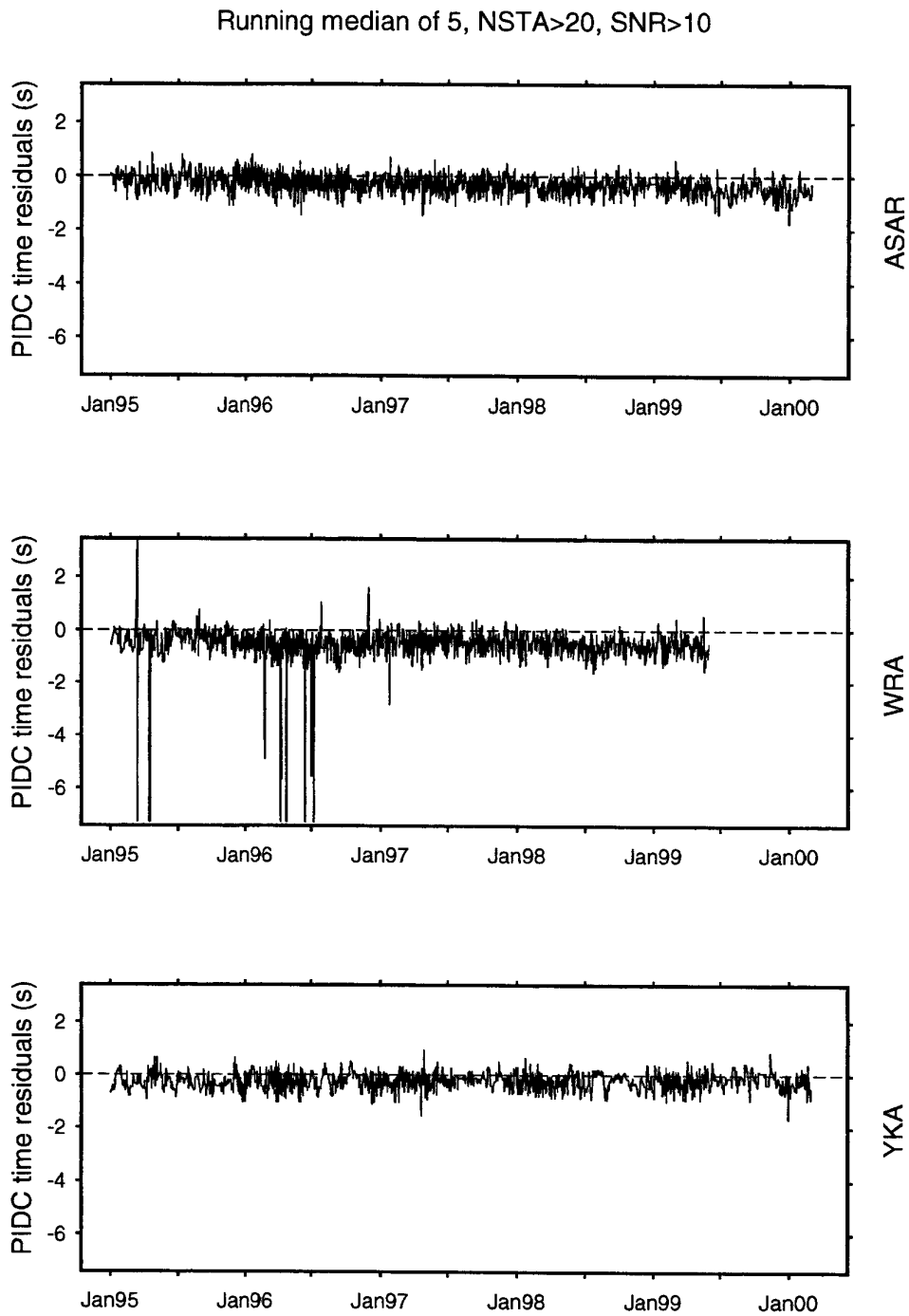
Fig. 6.3.12. *Time residuals in the pIDC REBs for the period 1995-2000 for the IMS arrays ASAR, WRA, and YKA. Events located with phases at more than 20 stations, and having signals with an SNR > 10 at the investigated station were considered. For visualization, running medians of 5 subsequent events are plotted.*

6.4   Recent profiling experiments in the Spitsbergen area - calibration data for the SPITS array

Introduction

In 1992, the seismic array SPITS was installed on Spitsbergen, the main island of the Svalbard Archipelago. Today, this array is part of the International Monitoring System (IMS) network as one of its auxiliary seismic stations. The Svalbard Archipelago is located at one edge of the Eurasian plate, with the continental shelf and the boundary with the North American plate 100 to 500 km to the west and the north. This plate boundary is part of the mid-Atlantic ridge system (MARS) and is characterized by its high natural seismicity. To the east and to the south of Svalbard is the large continental shelf which forms the Barents Sea. The last Soviet nuclear test took place on Novaya Zemlya, an island group also located in the Barents Sea and only about 1100 km apart from the SPITS array.

The seismic travel times for local and regional events around the SPITS array are influenced by the large variations in the crustal structure around Svalbard. During the last years several scientific and commercial reflection and refraction experiments have been undertaken in the sea around the Svalbard Archipelago. Airgun shots and small explosions conducted for these experiments were observed with the SPITS array.

Høgden (1999) interpreted SPITS data from a commercial reflection survey in the Barents Sea east of the Svalbard Archipelago. This survey was carried out by the Norwegian Petroleum Directorate (NPD) from August 24 to October 4, 1994 using airgun sources along 14 profiles. He analyzed two of these profiles in more detail and interpreted the first P onsets from sources at distances between 170 and 350 km from SPITS. The cross-over distance of Pn could be observed at about 210 km which corresponds to a depth of the Mohorovicic discontinuity of about 37 km. However, one disadvantage of these data was the short time difference between the single airgun shots of 10 seconds only, so that the coda of the first onset and later arrivals interfered with the signal of the next shot.

Scientific reflection and/or refraction surveys usually do not have this problem because in such experiments the reflections/refractions from structures in deeper parts of the crust and the uppermost mantle are also of interest. Therefore larger time differences are used between the consecutive shots.

Recently, exact source parameters from such experiments became available and resulted in a unique set of ground-truth information that can be used to calibrate local and regional travel-time curves around SPITS. The topic of this contribution is to document the data of four seismic surveys conducted in 1997 and 1999, as a first step towards a systematic investigation of all available seismic survey informations around the Svalbard Archipelago.

Data from seismic profiling west and north-west of Spitsbergen

During the arctic summers of 1997 and 1999 the German Institute for Polar and Oceanic Sciences (Alfred-Wegener-Institute) carried out in cooperation with the Polish Academy of Sciences four reflection/refraction experiments to investigate the structure of the continental shelf, the slope of the shelf, the deep-see area, and the corresponding part of the mid-atlantic ridge system west and north-west of Spitsbergen. Along these four profiles airgun shots were carried

out every one minute during which the vessel moved about 180 meters. In addition, on three of the profiles, small explosions were also fired using 25 or 50 kg of conventional explosives. The not yet published source information (for more details see Table 6.4.1) for these experiments was kindly supplied to us by Oliver Ritzmann of the Alfred-Wegener-Institute (pers. communication). Shots along all profiles were observed at SPITS with reasonably high SNR. The airgun shot profiles and the positions of the 50 explosions on the three profiles of 1999 are plotted on maps in Fig. 6.4.1.

Because all exact airgun positions are available, the data could be analyzed using the double-beam technique (Krüger *et al.*, 1993) to improve the signal-to-noise ratio (SNR). The single airgun shots were generally detectable at the single sites of the SPITS array. Using the classical beamforming, we can theoretically improve the SNR by a factor of 3 because SPITS consists of 9 vertical sensors (receiver beam). The horizontal distance between the single airgun shots was about 180 meters and about 5 airgun shots cover a distance which is about the aperture of the SPITS array (1 km). So, without larger loss of coherence of the signals, we can also sum up the energy of several airgun shots to one seismogram (source beam). Combining both beam types, we get the so called double beam with a theoretically SNR increase of up to a factor of 6.7 with respect to a single station observation, if we can add 9 sites and 5 airgun shots. In Fig. 6.4.2 the advantage of this procedure is shown for a short part of a seismogram section with data from Profile 1. At the bottom, the single seismograms as observed at a single site of the SPITS array (SPB4) are shown, in the middle we see the corresponding receiver beams of the SPITS array, using the theoretical backazimuth and a common apparent velocity of 9 km/s in the beamforming. At the top, the result of the double beam technique is shown: we stacked up to 5 single-airgun-shot beams to one double beam. The stepwise improvement of the SNR is obvious.

In Fig. 6.4.3 the entire seismogram section of the double beams for Profile 1 is shown. For distances below about 0.9 deg from the array, a lower crust phase is clearly seen as the first onset. The second onset is the Moho reflection PmP. Around the cross-over distance of Pn the picture becomes very complicated: the onsets are delayed and the travel-time curve of the first onsets is complex. This is the region where the seismic waves bottom below the west coast of Spitsbergen, a region with crustal thickening and a known north-south striking tectonic boundary (see *e.g.* Eiken, 1994). At distances larger than about 1.8 deg the observed amplitudes decrease drastically, which could be a damping effect due to the vicinity of the MARS.

Fig. 6.4.4 shows the double beams calculated for the observations of Profile 2. As seen on the map (Fig. 6.4.1, upper part) the ship was moving for a large part of the profile at approximately the same distance from SPITS (1.8 to 2 deg). This explains the higher density of observations in this distance range in the seismogram section. The quality of the Pn onsets differ along the profile and for larger distances close to the MARS (>~ 3 deg) onsets from the airgun shots are hardly identifiable. At distances between 1.8 and 2.3 deg, secondary P onsets with larger amplitudes than the first onstes are visible. This feature can also be seen on the seismogram section for the explosion sources along the same profile (Fig. 6.4.1, bottom). The distance between the single explosion was too large to apply the double-beam technique, therefore Fig. 6.4.5 contains only the corresponding receiver beams. The theoretical travel-times calculated for a surface focus with the spherical standard Earth model AK135 (Kennett *et al.*, 1995) are shown. The P velocities of this model are shown in Fig. 6.4.9, and the travel-time curves for the distance range covered by the profiles investigated here can be seen in Fig. 6.4.10.

Profile 3 (Fig. 6.4.6) approximately covers the same distance range as Profile 2. But on this profile the secondary P onsets are much more pronounced. The corresponding seismogram section of the explosion sources (Fig. 6.4.7) shows clear variations in the first P onset times indicated by black bars. The array beams and the onset times picked (bars) were also added to the seismogram section in Fig. 6.4.6. Note that the observations of the explosion sources with their higher SNR help to identify onsets of the airgun shots. Fig. 6.4.7 also contains travel-time curves calculated for a regional velocity model of the Barents Sea (Kremenetskaya and Asming, 1999) which cannot be used to explain these observations. The velocities of this model were also plotted in Fig. 6.4.9, and Fig. 6.4.10 also contains the travel-time curves for the Barents Sea model for the distance range covered by the profiles investigated here.

Finally, Fig. 6.4.8 shows the double beams of the Profile 4 observations. This profile was located between Profiles 1 and 2. Again, we can identify different P onsets at distances up to 1.8 deg. For larger distances (> ~ 2.6 deg) the airgun shots were carried out on the other side of the MARS (see also Fig. 6.4.1, top) and no seismic energy of these distant airgun shots can be identified in the seismogram section.

Conclusions

- The structure of the crust and the uppermost mantle around the IMS station SPITS is very heterogeneous.

- Observed travel times from GT0 events show strong deviations from predictions by standard models.

- Airgun shots of deep seismic profiling experiments (DSS) can be observed with small aperture arrays up to several hundred kilometers away. Therefore, source parameters of commercial and scientific DSS experiments represent useful ground-truth information.

- Numerous DSS experiments in the sea around Spitsbergen enabled us to derive azimuth-dependent travel-time curves for local and regional distances.

- The ground-truth data base will be used to reanalyze in more detail the previously reported large slowness deviations observed at SPITS (*e.g.* Kværna *et al.*).

- Exact travel times for distances up to of about 350 km are now available for different azimuth directions from the SPITS array. This travel time information will be used for a more precise location of local and regional events observed at SPITS.

J. Schweitzer

References

Eiken, O., editor (1994): Seismic atlas of western Svalbard - a selection of regional seismic transects. Norsk Polarinstitutt Oslo, *Meddelelser 130*, 73 pp. and 14 enclosures.

Høgden, S. (1999): Seismotectonics and crustal structure of the Svalbard region. Cand. Scient. thesis, Department of Geology, University of Oslo, 142 pp.

Kennett, B.L.N., Engdahl, E.R., and Buland, R. (1995): Constraints on seismic velocities in the Earth from traveltimes, *Geophys. J. Int. 122*, 108-124.

Kremenetskaya, E. and V. Asming (1999): Location calibration of the Barents region. In: Workshop on IMS location calibration, IDC technical experts group on seismic event location, Oslo, 12 - 14 January 1999, Technical Documentation.

Krüger, F., M. Weber, F. Scherbaum and J. Schlittenhardt (1993): Double beam analysis in the core-mantle boundary region. *Geophys. Res. Lett. 20*, 8089-8115.

Kværna, T., J. Schweitzer, L. Taylor, and F. Ringdal (1999): Monitoring the European Arctic using regional generalized beamforming. *Semiannual Technical Report 1 October 1998 - 31 March 1999. NORSAR Sci. Report 2-98/99*, Keller, Norway, 78-94.

Table 6.4.1. **Parameters of the profiles investigated. Date gives the days on which this profile was carried out, Lat-1 (Lat-2) and Lon-1 (Lon-2) are the start (end) points of the profiles, and Source indicates the source type (A for airguns, E for conventional explosions) and the number of sources on this profile.**

| Profile	Date	Lat-1 [deg]	Lon-1 [deg]	Lat-2 [deg]	Lon-2 [deg]	Source
1	06 September 1997 - 07 September 1997	77.82908	16.66815	76.77796	6.83346	A (1597)
2	21 August 1999 - 23 August 1999	78.82621	0.24860	80.18131	17.20085	A (2476)
2	21 August 1999 - 22 August 1999	79.74350	10.0110	79.21780	4.13780	E (25)
3	26 August 1999 - 27 August 1999	80.96566	7.09669	78.82445	11.27687	A (1455)
3	26 August 1999	79.80120	10.25390	80.70650	8.56010	E (20)
4	01 September 1999 - 02 September 1999	78.94233	12.01583	78.50227	0.03603	A (1628)
4	03 September 1999	78.91730	9.56190	78.87150	8.54527	E (5)
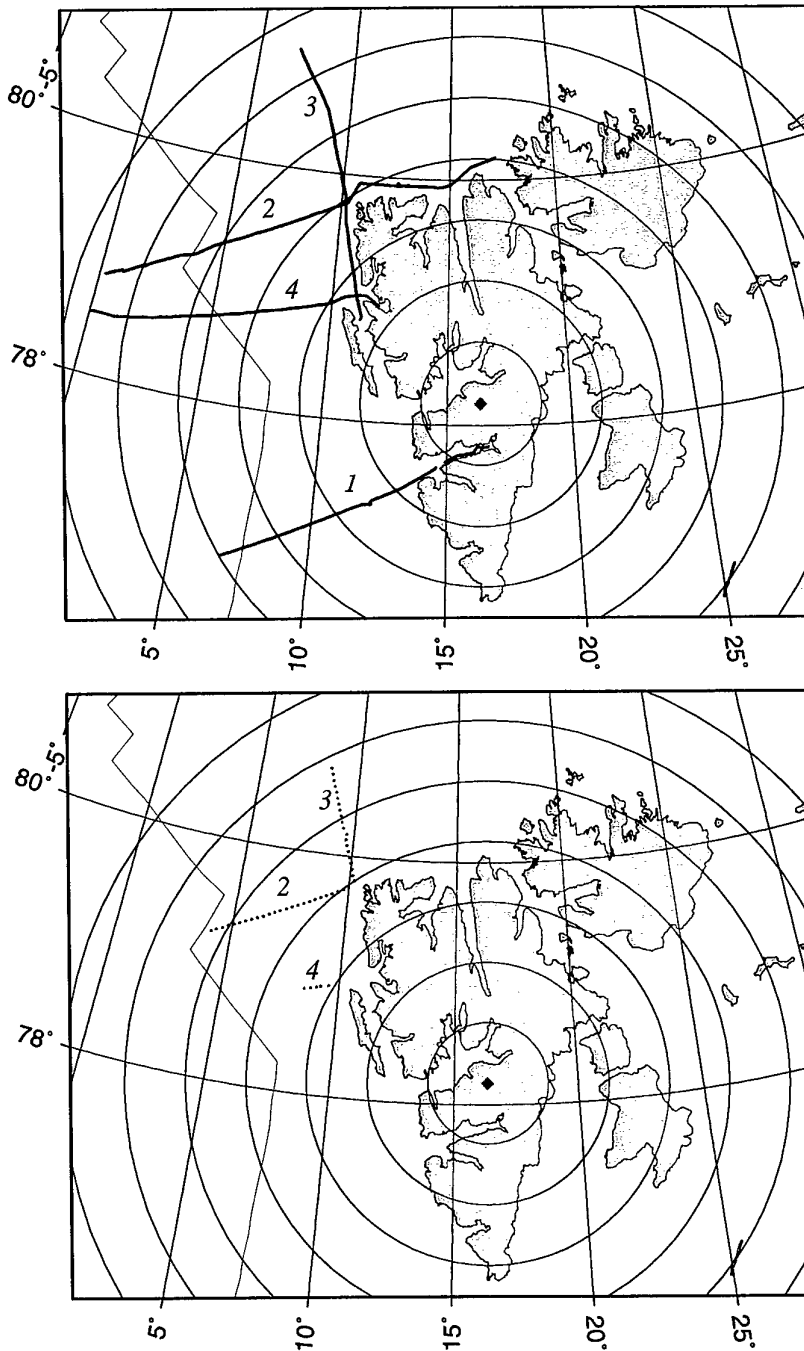
Fig. 6.4.1. *Maps of the Spitsbergen area showing the location of the SPITS array, equidistant circles around the array in steps of 0.5 deg, and the plate boundary (MARS) between the Eurasian and the North American plate. The upper map shows the positions of the four airgun profiles and the lower map the positions of the three profiles shot with conventional explosives (for more details see Table 6.4.1).*
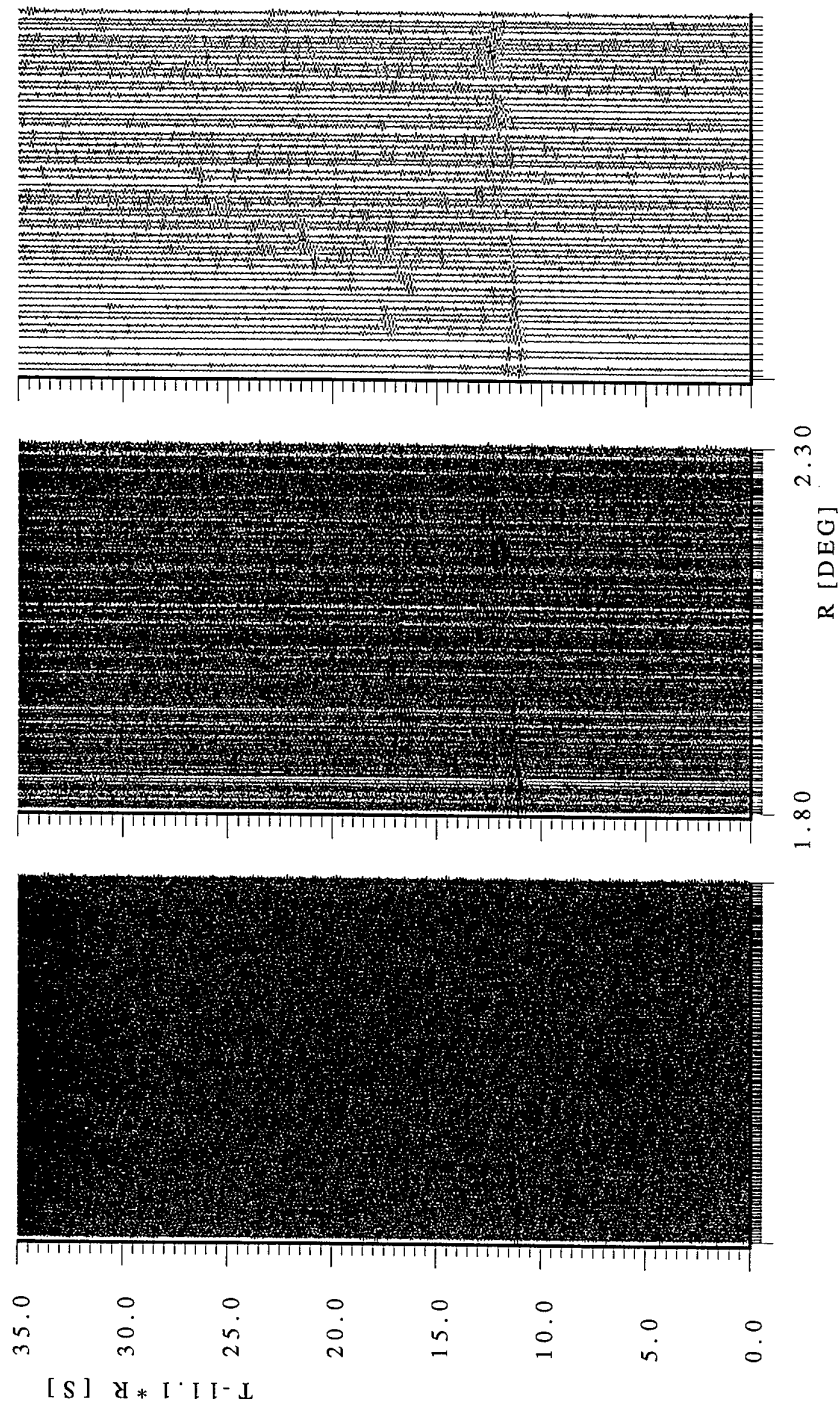
Fig. 6.4.2. *This figure shows the improvement of the SNR due to the double-beam technique (Krüger et al., 1993). At the bottom, single seismograms of station SPB4 from airgun shots of Profile 1 are shown. The epicentral distance is between 1.8 and 2.3 deg, the seismograms are filtered with a Butterworth bandpass filter between 5 and 10 Hz, and the traces were individually normalized. In the middle part of the figure the corresponding beams of the SPITS array are shown, and at the top the double beams after summing up to 5 single-airgun-shot beams to a common beam.*
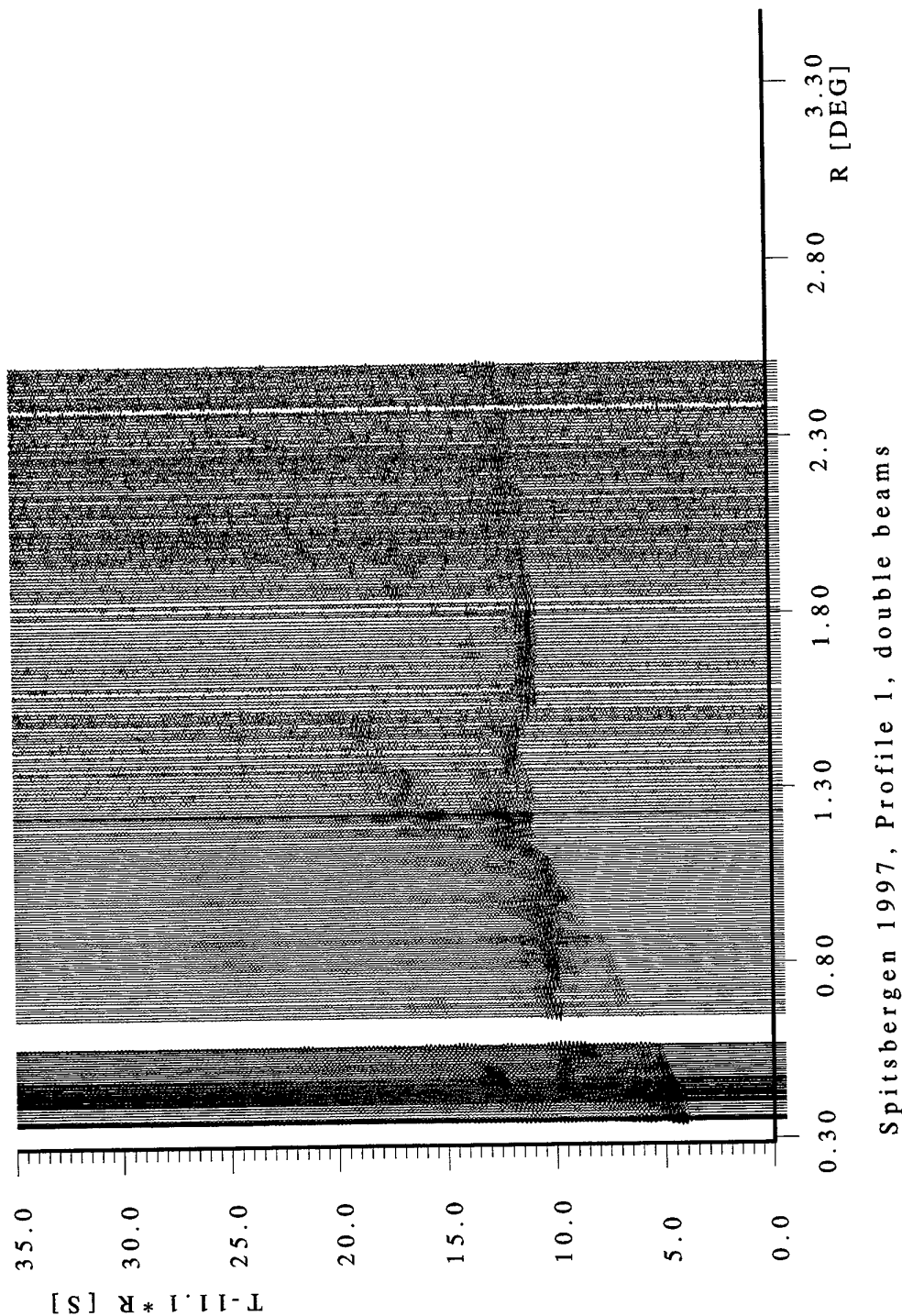
Fig. 6.4.3. *Seismogram section of double beams calculated from Profile 1 shots observed at SPITS. As in Fig. 6.4.2, all seismograms are filtered between 5 and 10 Hz and all traces were individually normalized. The seismogram section was reduced with 11.1 s/deg which corresponds to an apparent velocity of 10 km/s. The larger gap in the seismogram section is due to an island which the ship had to circumnavigate (gap in the blue line for Profile 1 in Fig. 6.4.1).*
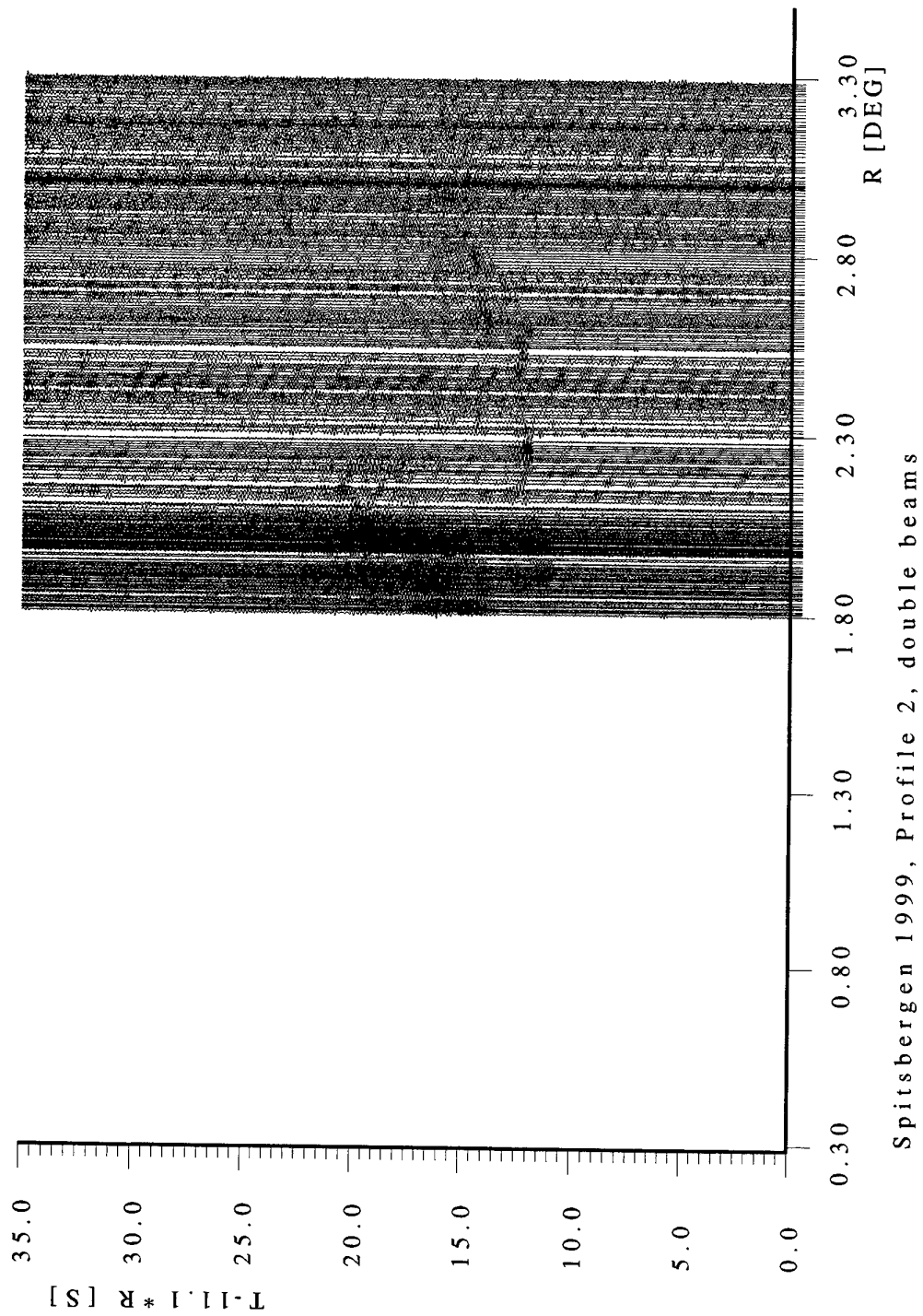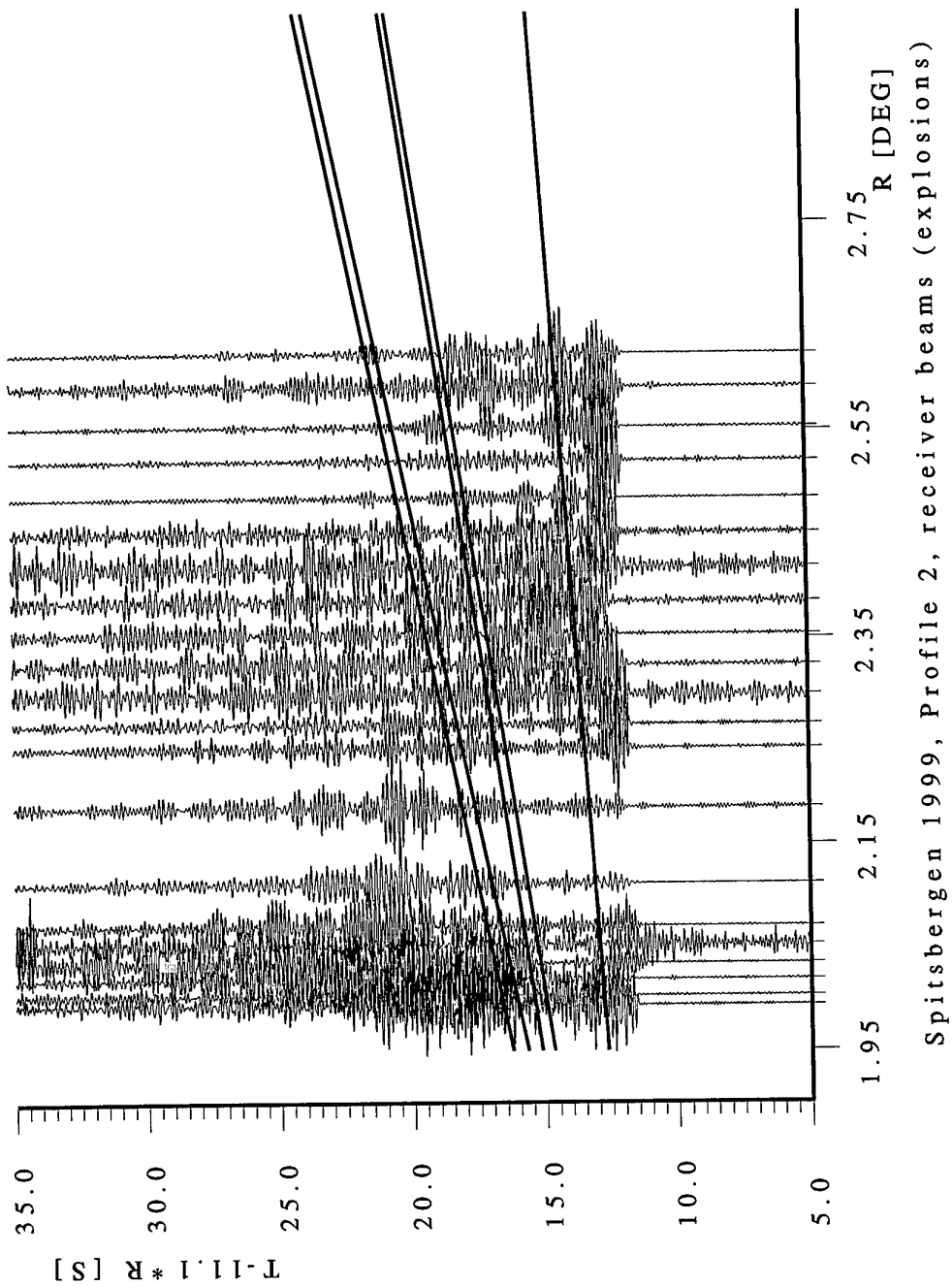
Fig. 6.4.4. *Seismogram section of double beams calculated from Profile 2 airgun shots observed at SPITS. Filters and reduction velocity are as used for Fig. 6.4.3.*

Fig. 6.4.5. *Seismogram section as in Fig. 6.4.4, but now for receiver beams for the observed conventional explosions along Profile 2 (see Fig. 6.4.1, bottom). In addition, theoretical travel-time curves for a surface source calculated using the spherical Earth model AK135 (Kennett et al., 1995) are plotted.*
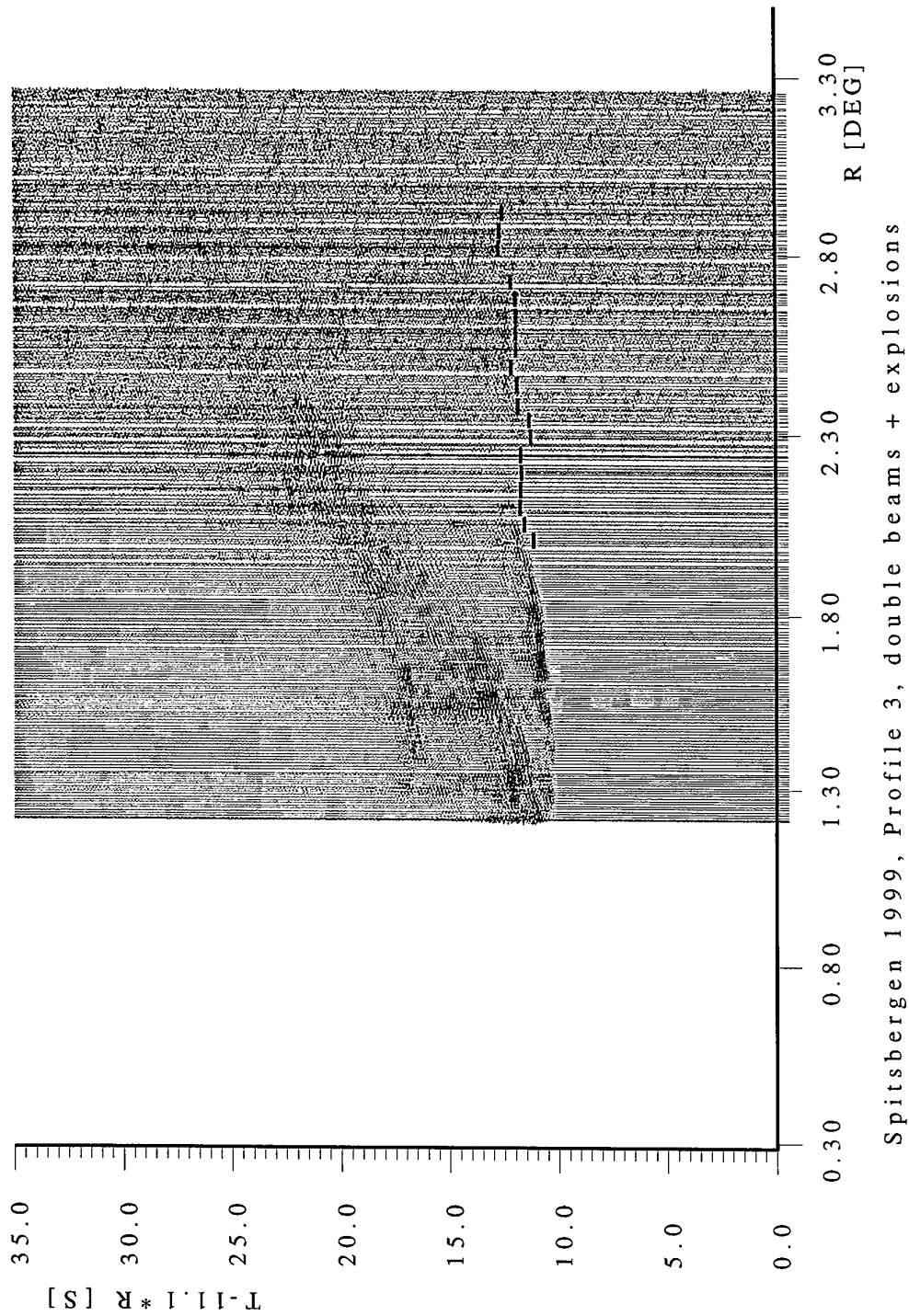
Fig. 6.4.6. *Seismogram section of double beams as in Fig. 6.4.3, but for the Profile 3 observations. In addition, the receiver beams of the observed explosions along this profile as shown in the expanded plot of Fig. 6.4.7 are included in this plot. The vertical bars indicate the first onset times from Fig. 6.4.7.*
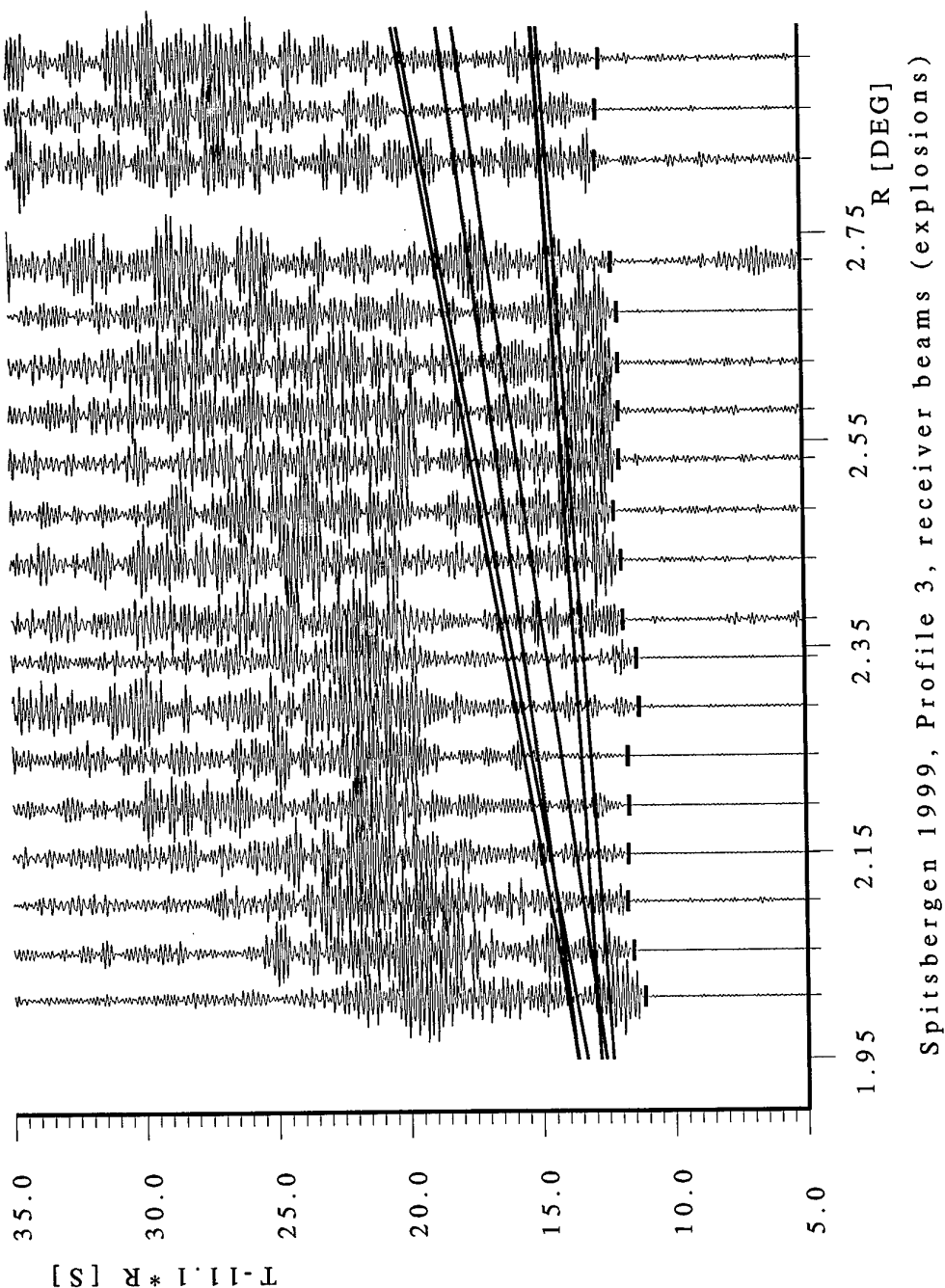
Fig. 6.4.7. *Seismogram section for the receiver beams for the observed conventional explosions conducted along Profile 3 (see also Fig. 6.4.1, bottom). In addition, theoretical travel-time curves for a surface source calculated using a regional model for the Barents region (Kremenetskaya and Asming, 1999) are plotted. The vertical bars are the first onset times as picked in this study.*
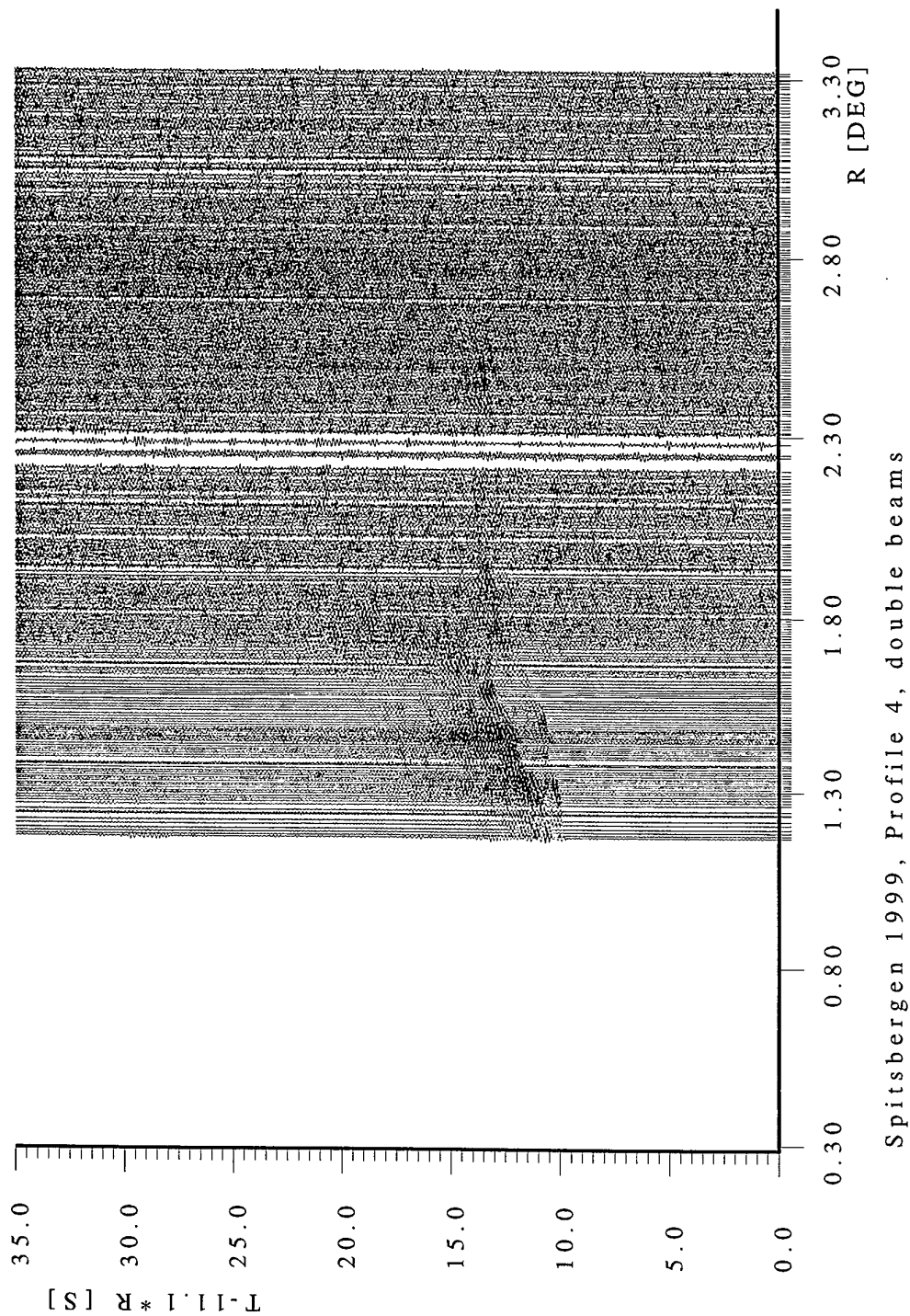
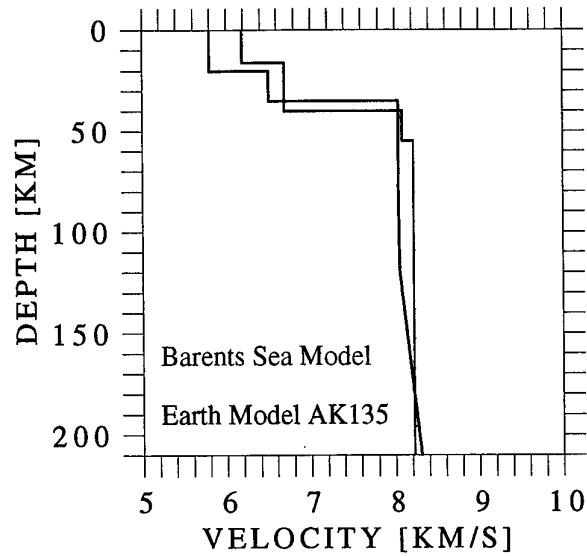**Fig. 6.4.8.** *Seismogram section of double beams as in Fig. 6.4.3, but for the Profile 4 observations.*

Fig. 6.4.9. *The two P-velocity models used as reference in this study. The model AK135 is a global Earth model (Kennett et al., 1995) and the Barents Sea model is a regional velocity model (Kremenetskaya and Asming, 1999).*
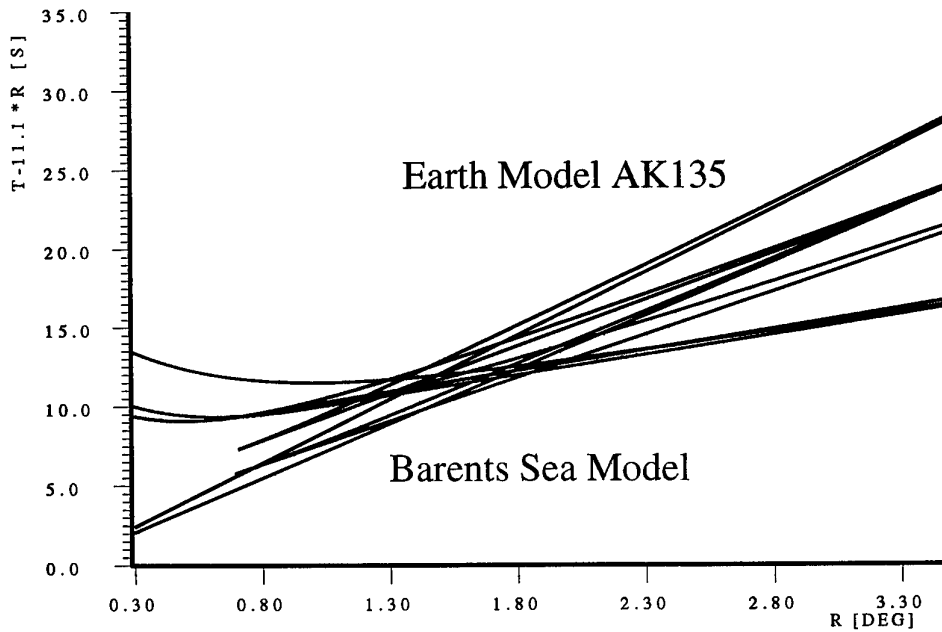

Fig. 6.4.10. *P phase travel-time curves for the two models used as reference in this study (see Fig. 6.4.9).*

6.5   Waveform quality analysis and data conditioning for the SPITS array

Introduction

We have for a long time noticed spikes in the data stream from the SPITS array (e.g., Schweitzer, 1998). In particular, the channel *SPB5_sz* has a severe problem. As shown in the lower trace of Fig. 6.5.1, the largest spikes are seen on the raw data trace, but after filtering more spikes become visible. This is illustrated in the middle trace of Fig. 6.5.1 where the data are differentiated twice.

We will in this contribution describe a new spike detector algorithm that identifies such one-sample spikes, without being sensitive to common seismic signals. The spike detector output is shown in the top trace of Fig. 6.5.1, where we observe high detector values for the spikes, but no effect of the strong signal occurring around 02.37. The data gaps at 02.40 are also handled well by the algorithm.
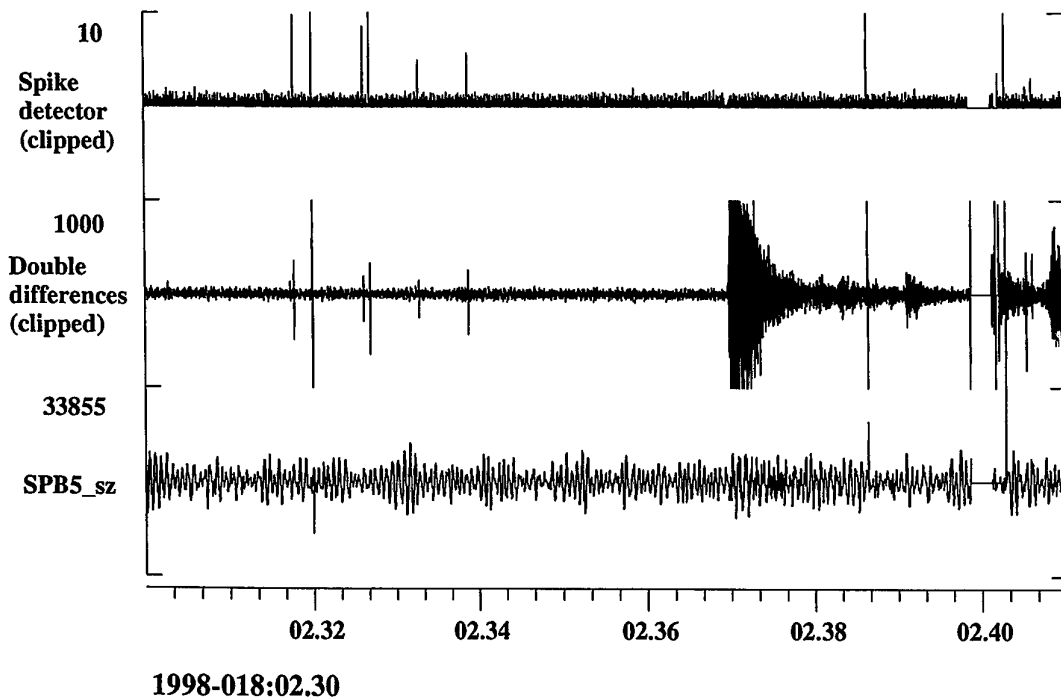

Fig. 6.5.1. *Illustration of data spikes at the SPITS array channel SPB5_sz (lower trace). In the middle trace the data are differentiated twice to accentuate the spikes, and the top trace shows the corresponding spike detector output.*

Intervals where the spike detector output exceeds a predefined threshold (typically 4) are declared as spikes, and the raw data are corrected using an interpolation scheme. The corrected data channel is shown in lower trace of Fig. 6.5.2, and the corresponding double differences and spike detector output are shown in the traces above. After correction there are no one-sam-

ple data spikes left. The spikes seen on the double differences of Fig. 6.5.2 are associated with the data gaps, for which the spike detector has little sensitivity.
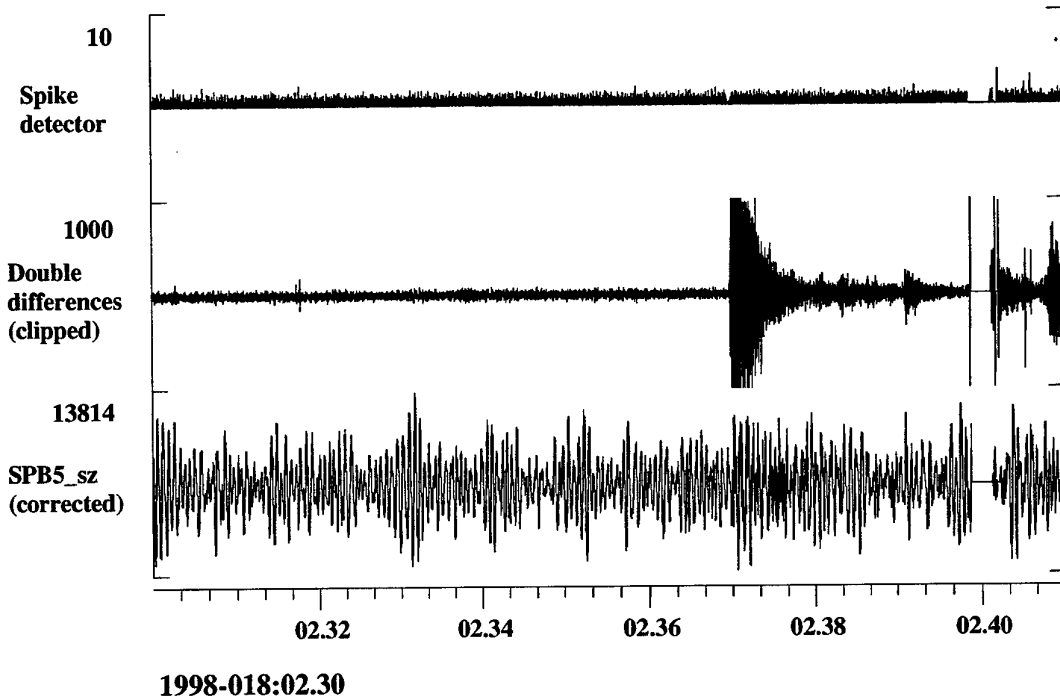

Fig. 6.5.2. *The lower trace shows the spike corrected version of channel SPB5_sz, with the original seen in the lower part of Fig. 6.5.1. The middle and upper traces are the corresponding high-pass filtered data and the spike detector output.*

The spike detector algorithm

In order to find a detector algorithm that is sensitive to spikes but insensitive to strong seismic signals, we have to utilize the features that separate these populations. Our assumption is that the energy associated with a spike is usually restricted to one (or a very few) samples, whereas seismic signals in almost all cases have energy with a duration of several samples. The developed spike detector procedure utilizing this difference is illustrated in Fig. 6.5.3, and we will in the following describe the different steps:

Step 1: *High-pass filter the data using double differences*

In order to increase the signal-to-noise ratio (SNR) of the spikes, a differential filter is applied twice to the data. This acts as a high-pass filter, and we see from trace no. 2 at the bottom of Fig. 6.5.3 that the SNR is increased and that the original one-sample spike is now transformed into three samples.

Step 2: *Calculate an LTA-like reference level for the spike detector*

The spike detector developed is a running procedure where we test each data sample against a reference level. From experiments we have found the maximum amplitude $max(abs(ddiff<t_w>))$ within a time window following each test sample to be very useful. The trace $ddiffmax(t) = max(abs(ddiff<t_w>))$ is number 3 from the bottom of Fig. 6.5.3.

Step 3: *Calculate the spike detector output*

As illustrated in trace nos. 2 and 3 from top of Fig. 6.5.3, the spike detector output for a given time t is calculated as $abs(ddiff(t)) / ddiffmax(t+\tau)$, where τ corresponds to the time shift of the reference level. To ensure that two- or three-sample spikes also fall outside the reference time window, the window start time is shifted about 0.2 seconds relative to t.

Step 4: *Define spike detections*

From testing of several data intervals we have found that a trigger threshold of 4 is a good initial value for defining spikes. For each spike detection interval, the time of the spike is taken to be the maximum.

Step 5: *Correct spikes using spline interpolation*

The spike in the raw data is replaced by a spline interpolated value of the data surrounding the initial spike, as shown in the top trace of Fig. 6.5.3.

Step 6: *Iterate the procedure*

The procedure can be applied iteratively to the spike corrected data. If spikes are still detected, we assume that the data contain other types of data problems, and we have the option to replace a longer time interval with spline interpolated data.
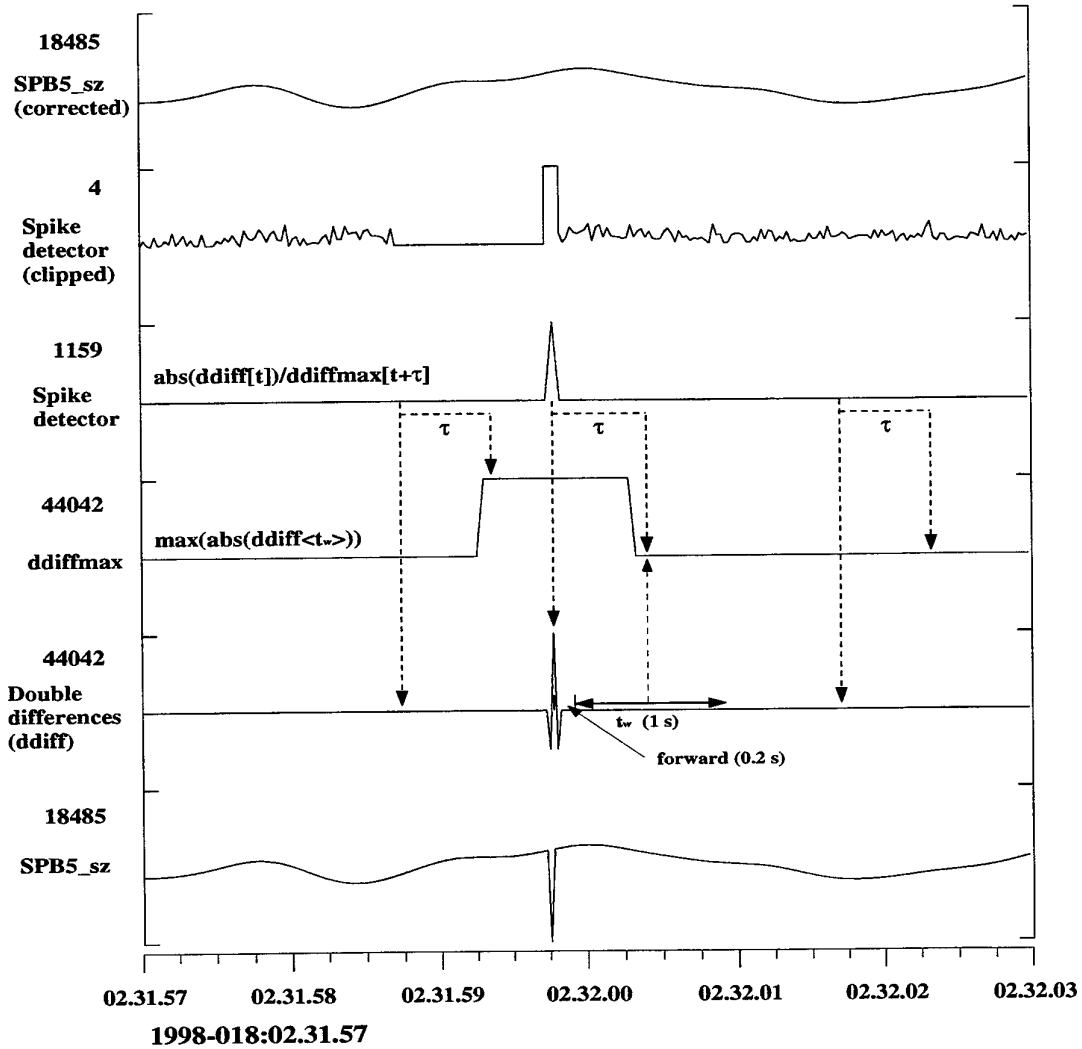
Fig. 6.5.3. *Figure illustrating the spike detector algorithm. See text for details. The numbers to the left of each trace give the amplitude maximum.*
The lower trace shows the raw data for SPITS channel SPB5_sz, including a clear spike.
Trace no. 2 from the bottom shows the data after applying a differential filter twice.
The reference level for the spike detector is shown in trace no. 3 from the bottom. This is calculated as $\underline{max(abs(ddiff \leq t_w))}$ *where the maximum is taken within a window* $<t_w>$ *of typically 1 second.*
Trace no. 3 from the top shows the spike detector output calculated as
$\underline{spidet(t) = abs(ddiff(t)) \, / \, ddiffmax(t+\tau)}$. *The arrows indicate the time shifts used in the numerator and denominator of the equation. In trace no. 2 from the top the spike detector output is plotted with a maximum amplitude of 4, which is the detection threshold currently used.*
The top trace shows the channel SPB5_sz after correction, using a spline interpolated value of the data surrounding the initial spike

The example shown in Fig. 6.5.3 illustrates that the method works well for simple spikes. In Fig. 6.5.4 the method is applied to a high SNR P_n phase from an event located at a distance of approximately 250 km, and we can see that the spike detector has little sensitivity to such signals.
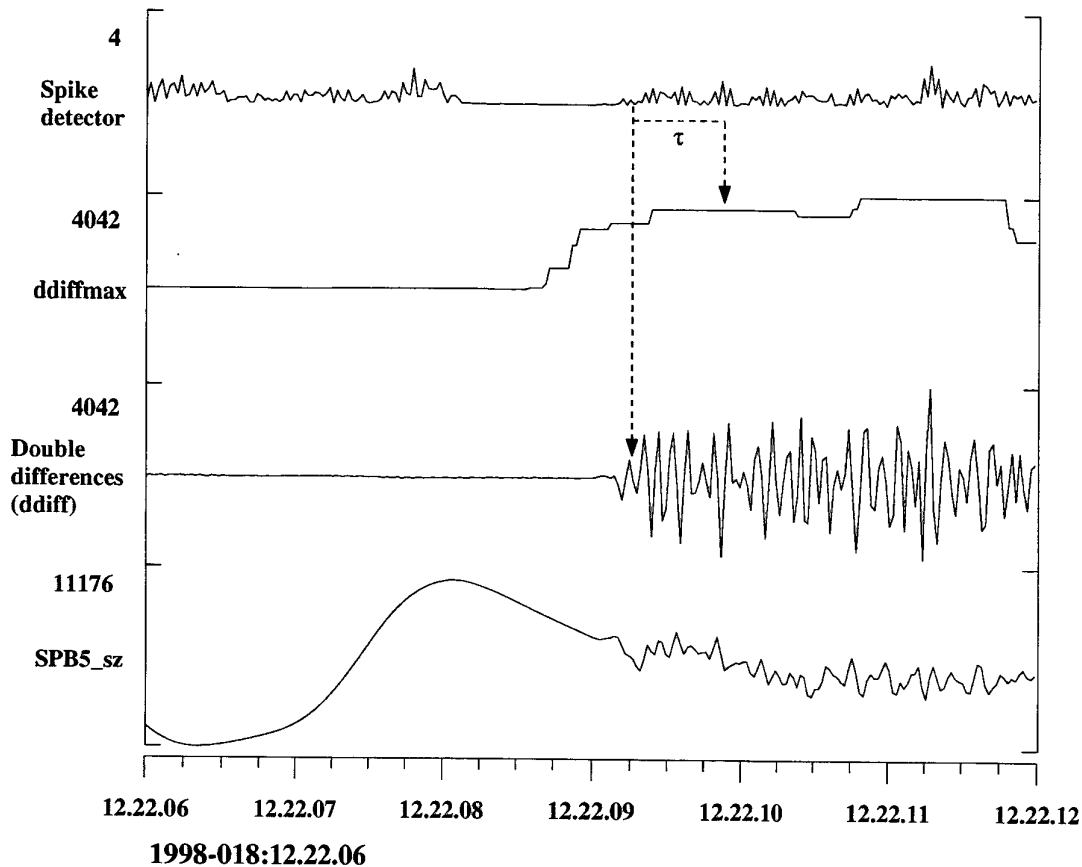

Fig. 6.5.4. *Figure illustrating the spike detector algorithm applied to a P_n phase from an event located approximately 250 km from the SPITS array. See caption of Fig. 6.5.3 for an explanation of the figure.*

For signals from very local events, having impulsive characteristics and of short duration, the spike detector has some sensitivity as illustrated in Fig. 6.5.5. However, a detection threshold of 4 in almost all cases prevents such signals being declared as spikes. In addition, we have introduced a test where amplitudes on both sides of the declared spike are compared. A large difference between these amplitudes strongly indicates that we have a signal, and the spike detection is consequently rejected. With this additional test, the spike detector has a very low false alarm rate.
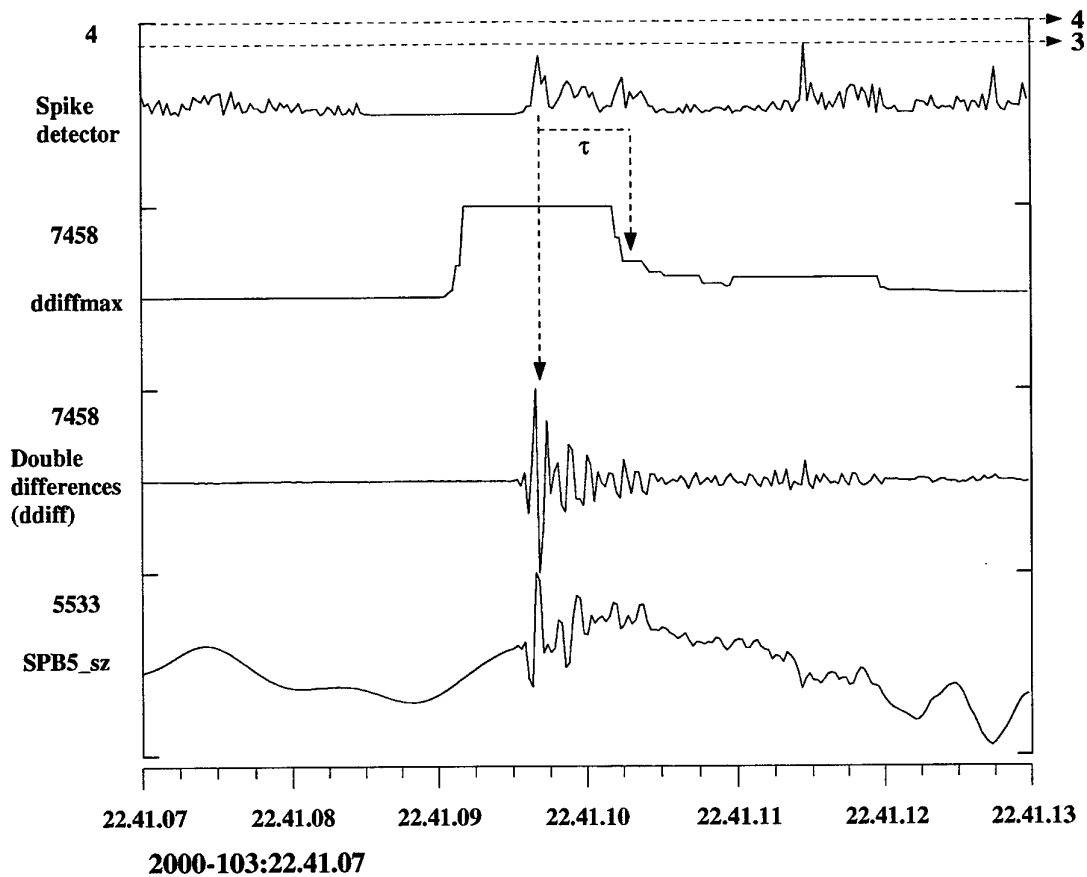
Fig. 6.5.5. *Figure illustrating the spike detector algorithm applied to an event located a few kilometers from the SPITS array. See caption of Fig. 6.5.3 for an explanation of the figure.*

Discussion

The spike detector and the corresponding data correction procedure provides an efficient method to remove well separated one-sample spikes from seismic data. In cases with more complicated data errors, like very frequent spikes possibly in combination with data gaps, the procedures also have some merit, in particular when applied iteratively. Even for such complicated cases, exemplified in the right most part of Figs. 6.5.1 and 6.5 2, the data quality is significantly improved.

Concerning the cause of the spikes in the SPITS data channel *SPB5_sz*, we are investigating a problem within the data acquisition system. However, our experience is that such data problems frequently occur on other types of systems, and that the developed procedure is of general use.

The procedure has been operationally tested at NORSAR, and has shown to significantly improve the processing quality of the SPITS array. However, a systematic study quantifying the

performance of the method remains to be done. This is important for determining the optimum trigger threshold and the corresponding false alarm rate.

The algorithm is available in NORSARs processing system EP through the following two commands:

corrspike <n>

> Run the spike detector on n data channels and correct the spikes. In addition the processing parameters can be adjusted using additional arguments to the command.

detspike

> Run the spike detector on the top data channel on the data stack and correct the spikes. In addition, the high-pass filtered data (double differences), the detector reference levels, and spike detector output are put on top of the data stack, as shown in Fig. 6.5.5.

References

Schweitzer, J. (1998). Tuning the automatic data processing for the Spitsbergen array (SPITS). In: NORSAR Semiannual Tech. Summ. 1 April - 30 September 1998, NORSAR Sci. Rep. 1-98/99, Kjeller, Norway, 110-125.

T. Kværna

6.6   Third Level Seismo-geographical Regionalization of Fennoscandia

Background

Gutenberg and Richter (1949, 1954) divided the earth into 50 seismic regions. These regions were subdivided in 1965 into a total of 728 regions (Flinn and Engdahl, 1965). The boundaries were drawn along latitudes and longitudes in order to automatically assign an epicenter to a named region. In 1985, the IASPEI Commission on Practice established a working group with the mandate to correct and modernize the Flinn-Engdahl regionalization (Young et al., 1996). The revised regionalization was still a rough subdivision providing only coarse information. Fig. 6.6.1 shows one example of this regionalization, where region 642, (Norwegian Sea) covers an area from 61°N to 75°N.

At the meeting in Istanbul, 1989, the third level regionalization presented for Germany was accepted as a primary example, and other countries were requested to submit level 3 regionalization for regions of their responsibility. The expectation is that this effort will eventually lead to a global level 3 regionalization.

On behalf of the IASPEI Commission on Practice, Fennoscandia has been subdivided into small seismotectonic and geographical units. Taking geological history and the tectonic conditions into consideration, even areas with a very low seismicity could be subdivided. This subdivision has been implemented in the bulletins presented by NORSAR. Now the coordinates of an epicenter can be automatically assigned to a named region, which is often more easily conceived by the casual reader.

The regions along the national borders (to Germany and Britain) have been defined in cooperation with these countries where the 3 level regionalization already existed. The regionalization is now on the way to be extended, and will hopefully soon comprise all of Europe.

Earlier versions of the regionalization of Fennoscandia had been presented and discussed at the 1997 IASPEI meeting in Thessaloniki and the 1998 ESC meeting in Tel Aviv. The here presented regionalization was approved at the 1999 Commission on Practice meeting at IUGG, Birmingham.

Principles

The level 3 regions are seismo-geographical because they are defined with respect to political boundaries, seismic activity, geological development and tectonic features.

Meaningful and useful regionalization for the purpose of earthquake location requires a balance between familiar geopolitical boarders, geological structures and seismicity patterns, and in many instances these three criteria are independent and define overlapping areas. In some cases, however, the scientist must make the best mixture out of all three. To avoid confusion, we have tried to use non-geological terms such as "region" or "area" when describing primarily geopolitically defined areas, and geologic terms such as "basin" or "ridge" for primarily seismically or geologically defined regions. E. g. Area 58 is called "Knipovitch region" instead of "Knipovitch ridge" due to the size of this region (Fig. 6.6.2 and Table 6.6.1).

Some seismotectonic units cross coast lines and national borders. In such cases we have tried to maintain these borders also in the regionalization.

Nomenclature

The final zonation for Fennoscandia is shown in Fig. 6.6.2. with numbers and names as shown in Table 6.6.1.

The Scandinavian languages have specific vowels which have been translated to combination of English vowels:

æ ä (Æ) --> ae
ø ö (Ø) --> oe
å (Å) --> aa

Table 6.6.1: Numbers and names assigned to the regiona in the 3rd level zonation of Fennoscandia.

No.	Geographical area
1	NORTHWESTERN GERMANY
2	CENTRAL NORTH SEA (CENTRAL GRABEN)
3	Eastern North Sea
4	Horda Platform
5	Oeygarden Fault Zone
6	Fyn Denmark
7	Sjaelland Denmark
8	Jylland Denmark
9	Kattegat
10	Bornholm and Nearby Sea
11	Central Norbotten Sweden
12	Swedish-Finish Border Zone
13	Bothnian Region Sweden
14	Vaesterbotten Sweden
15	Malmoehus Sweden
16	South-Western Goetaland Sweden
17	South-Eastern Goetaland Sweden
18	Gotland Region Sweden
19	Vaestmanland Region Sweden
20	Vaermland Region Sweden
21	Eastern Goetaland Sweden
22	Moere Shelf
23	Viking Graben
24	Sogn-Moere Region Norway
25	Oppland-Hedmark Norway

Table 6.6.1: Numbers and names assigned to the regiona in the 3rd level zonation of Fennoscandia.

No.	Geographical area
26	Gaevleborg Region Sweden
27	Vaesternorrland Sweden
28	Kopparberg Region Sweden
29	Jaemtland Sweden
30	Southern Gulf of Bothnia
31	Southwestern Finland Finland
32	Lake Saimaa Area Finland
33	Lake Paijanne Area Finland
34	Southern Bothnia Finland
35	Lake Ladoga-Bothnian Bay Finland
36	Northern Karelia Finland
37	Kainuu Area Finland
38	Kuusamo Area Finland
39	Southern Lapland Finland
40	Central Lapland Finland
41	Eastern Lapland Finland
42	Northern Lapland Finland
43	Nordland Region Norway
44	Mid-Norway Norway
45	Moere Basin
46	Northern North Sea
47	Voering Basin
48	Voering Plateau
49	Norway Basin
50	Troendelag Platform
51	Lofoten Margin
52	Mohns Ridge
53	Jan Mayen Region
54	Eastern Lofoten Basin
55	Western Barents Sea
56	Senja Fracture Zone
57	Western Lofoten Basin
58	Knipovich Region
59	West Spitsbergen Svalbard
60	Storfjorden-Heer Land Svalbard

Table 6.6.1: Numbers and names assigned to the regiona in the 3rd level zonation of Fennoscandia.

No.	Geographical area
61	New Friesland Svalbard
62	Nordaustlandet Svalbard
63	Barentsoeya-Edgeoeya Svalbard
64	Hinlopen-Olga Strait Svalbard
65	South-Western Norrbotten Sweden
66	Northern Finnmark Norway
67	Central Finnmark Norway
68	Troms Norway
69	Oslo Region Norway
70	Skagerrak
71	Hardanger Norway
72	Rogaland Norway
73	Agder Norway
74	Telemark-Buskerud Norway

C. D. Lindholm, NORSAR, Norway

J. Schweitzer, NORSAR, Norway

E. Wolf, NORSAR, Norway

H. Bungum, NORSAR, Norway

K. Atakan, Institute of Solid Earth Physics, University of Bergen, Norway

S. Gregersen, Kort og Matrikkelstyrelsen, Copenhagen, Denmark

K. Arhe, Institute of Seismology, University of Helsinki, Finland

J. Malaska, Institute of Seismology, University of Helsinki, Finland

References

Flinn, E.A. and Engdahl, E.R. (1965): A proposed basis for geographic and seismic regionalization. *Rev. Geophys.*, **3**, p123.

Gutenberg, B. and C. F. Richter (1949): Seismicity of the earth and associated phenomena. Princeton Univ. Press. 273 pp.

Gutenberg, B. and C. F. Richter (1954): Seismicity of the earth and associated phenomena. Princeton Univ. Press. 2nd edition, 310 pp.

Young J. B., B. W. Presgrave, H. Aichele, D. A. Wiens and E. A. Flinn (1996): The Flinn-Engdahl regionalization scheme: The 1995 revision. *Phys. Earth and Plan. Int.*, **96**, pp. 223-297
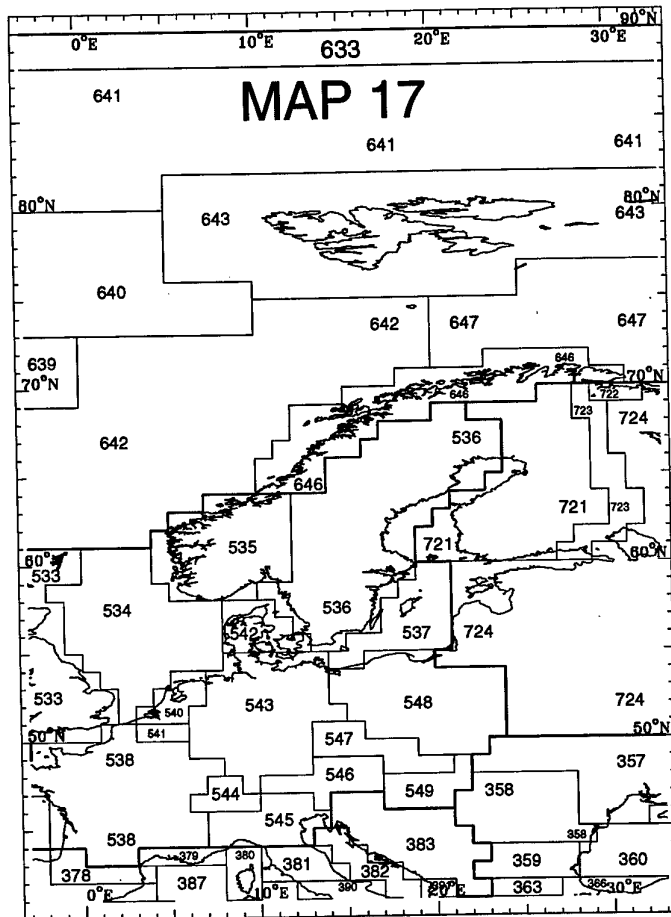
Fig. 6.6.1. *Flinn-Engdahl zonation for northwestern Europe. (Flinn and Engdahl, 1965; Young et al., 1996).*
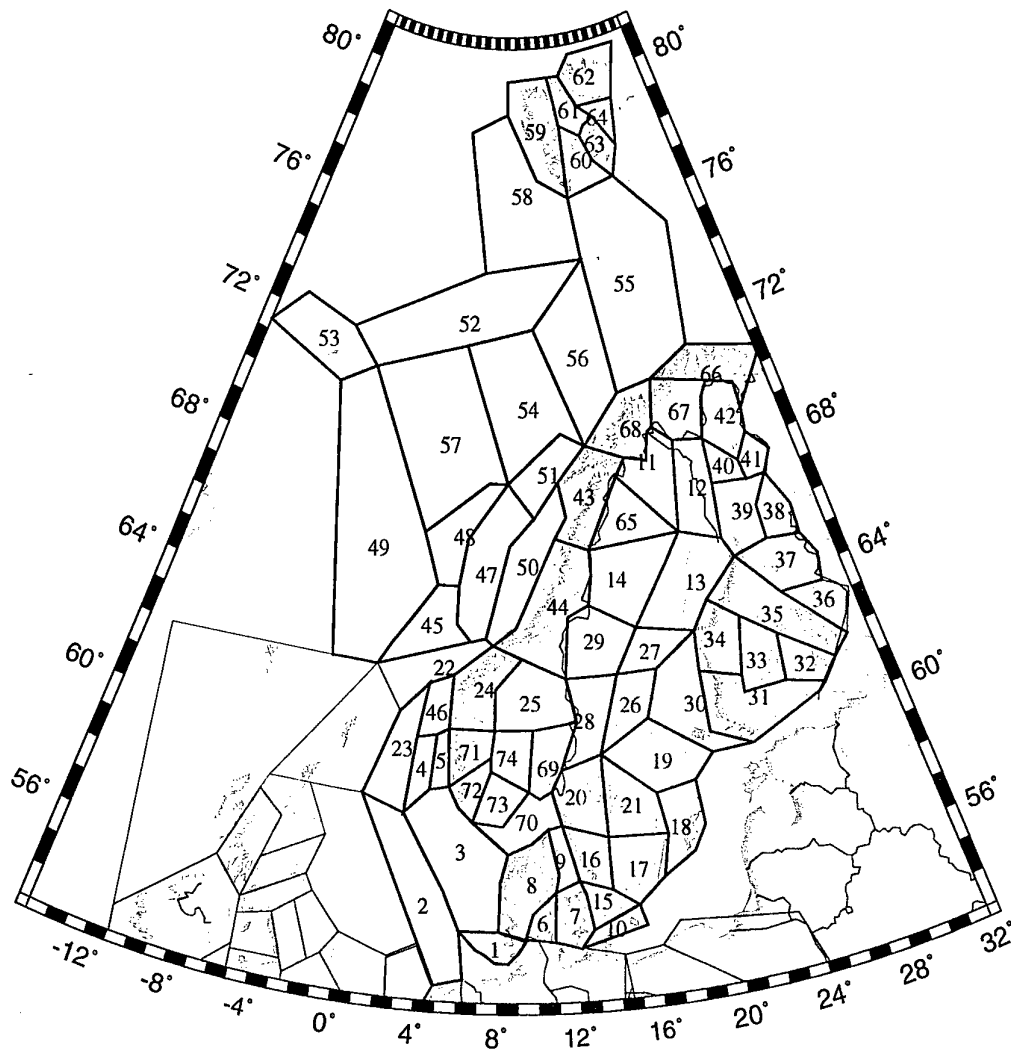
Fig. 6.6.2. *Detailed zonation of Fennoscandia from the present zonation with names as given in Table 6.6.1.*

6.7   Crustal structure of the Barents Sea – important constraints for regional seismic velocity and travel-time models

Introduction

The Barents Sea covers the continental shelf of northwestern Eurasia (Fig. 6.7.1). It is bounded by young passive margins to the west and north that developed in response to the Cenozoic opening of the Norwegian-Greenland Sea and the Eurasia Basin, respectively. The Barents Sea contains some of the deepest sedimentary basins known and it preserves a relatively complete succession of sedimentary strata ranging in age from Late Paleozoic to Quaternary, locally exceeding 15 km in thickness (Faleide et al. 1993, Gudlaugsson et al. 1998).

Deep seismic reflection and refraction data have greatly improved our understanding of the deep basins and the underlying crystalline crust in the Barents Sea and of the crustal transition across the western continental margin (Faleide et al. 1991).

In this report, we review the Barents Sea crustal structure and discuss how the crustal configuration and composition affects regional models for seismic velocities and travel-times.

Geological framework

The western Barents Sea comprises three distinct regions (Faleide et al. 1993, Gudlaugsson et al. 1998):

- The western Barents Sea-Svalbard continental margin consists of three regional segments: a southern sheared margin along the Senja Fracture Zone; a central rifted complex southwest of Bjørnøya associated with volcanism; and a northern sheared and rifted margin along the Hornsund Fault Zone. The continent-ocean transition occurs over a narrow zone along the line of early Tertiary break-up and is covered by a thick Upper Cenozoic sedimentary wedge.

- The Svalbard Platform covered by flat-lying Upper Paleozoic and Mesozoic, mainly Triassic, strata.

- A province between the Svalbard Platform and the Norwegian coast characterised by sub-basins and highs with increasingly accentuated structural relief to the west. Jurassic, Cretaceous, and locally Paleocene-Eocene strata are preserved in the basins.

The eastern Barents Sea comprises two wide and deep north-northeast trending basins of Late Paleozoic-Triassic age separated by a shallow saddle (Johansen et al. 1993).

Direct information on the nature of the crystalline crust beneath the Barents Sea sedimentary basins is scarce, but available, mostly indirect, evidence indicates that the basement underlying much of its central and western parts was consolidated during the Caledonian Orogeny. An older, Baikalian, basement underlies the southeastern Barents Sea (Gudlaugsson et al. 1998).

Upper Paleozoic (Devonian-Permian) rocks in the western Barents Sea are expected to be similar to those of Svalbard and Bjørnøya (Devonian-Carboniferous clastics and Upper Carboniferous-Lower Permian carbonates and evaporites). The eastern Barents Sea had marine conditions earlier with deposition of Devonian and Carboniferous limestones.

The Mesozoic succession comprises mostly clastic rocks. Thick Triassic rocks occur throughout the Barents Sea and comprise coarsening upwards sequences. The Lower-Middle Jurassic interval is dominated by sandstone while shales dominate the Upper Jurassic and Cretaceous interval. Early Tertiary, mostly fine-grained clastics, are only preserved in the southwestern Barents Sea and on Spitsbergen.

In somewhat simplified terms, the post-Caledonian geological history of the Barents Sea has involved (Faleide et al. 1993, Johansen et al. 1993, Gudlaugsson et al. 1998):

- A Devonian tectonic regime in the west comprising both extensional and compressional events, so far known on Svalbard only. Devonian rifting affected the eastern Barents Sea.

- Widespread rifting in the Carboniferous and Permian.

- Gradual development towards non-fault-related regional subsidence in Permian and Triassic times.

- M iddle-Late Jurassic and Early Cretaceous rifting in the southwestern Barents Sea, associated with regional magmatism and uplift in the northern Barents Sea.

- Late Cretaceous uplift of most of the Barents Sea, but continued faulting and subsidence in the southwesternmost Barents Sea.

- Early Tertiary continental breakup and margin formation related to the opening of the Norwegian-Greenland Sea and Eurasia Basin.

- Late Cenozoic uplift and glacial erosion.

Data

A comprehensive deep seismic database covers the Barents Sea, including deep seismic reflection profiles recorded to 14-16 s two-way time and deep seismic refraction/wide-angle reflection profiles using both two-ship (ESP) and OBS techniques. We have used the deep seismic data to constrain the first-order crustal structure and deep seismic velocity distribution.

In addition, we have used a regional grid of conventional seismic reflection profiles recorded to 6-10 s twt and a large number of sonobuoy refraction profiles to elucidate the shallow structure.

Gravity and magnetic data have also been useful constraining the deep basin configuration and crustal structure.

Important geological information is also obtained from exploration wells and outcrops onshore (Svalbard, Franz Josef Land, Novaya Zemlya, Finnmark-Kola).

Velocity structure

The large number of velocity-depth profiles plotted in Fig. 6.7.2 show the wide range of velocities measured at various depths in the Barents Sea compared to the regional velocity model of Kremenetskaya and Asming (1999). To reveal the large lateral and vertical velocity variations in the Barents Sea region we need a regional 3D velocity model.

Fig. 6.7.3 summarises a generalised velocity structure for the Barents Sea including depth ranges to some of the key interfaces in the Barents Sea subsurface:

- The geology at the top of the bedrock (beneath a thin cover of Quaternary sediments) varies laterally because of varying Late Cenozoic uplift and erosion. The surface (top of bedrock) velocity varies typically between 2 and 4 km/s depending on the amount of missing overburden due to erosion. The highest velocities and erosion estimates are found in the northwestern Barents Sea including Svalbard.

- Mesozoic strata (mainly sandstones and shales) reveal a velocity gradient reaching velocities of typically 4-4.5 km/s at the base of the Triassic.

- Upper Carboniferous-Lower Permian carbonates (mainly limestones and dolomites) and Upper Permian silicified clastics are characterised by high velocities (~6 km/s). Detailed measurements (sonic logs) in wells reveal considerable variations within this unit but parts of it have velocities in the order of 6 km/s irrespective of burial depth. Depths to the top of this high-velocity layer ranges between 0-10 km.

- A velocity inversion occurs below the carbonate platform. Carboniferous and Devonian clastic rocks have velocities of 5+ km/s. The velocity inversion is difficult to detect by standard interpretation techniques applied to the seismic refraction data. This may cause errors in the depth estimates for underlying interfaces such as top of the crystalline basement and moho at the base of the crust.

- The crystalline basement has velocities of 6+ km/s. Depths to top basement ranges between 0-20 km.

- Magmatic underplating characterised by 7+ km/s velocities are probably present east of Svalbard (Høgden 1999).

- 8+ km/s are measured in the upper mantle. Moho-depths typically range between 20-40 km).

Crustal transects

Differences in crustal structure are illustrated by a series of regional transects which are based on an integrated interpretation of the deep seismic data supplemented with conventional seismic reflection and refraction profiles. In order to bring out the primary crustal features, only the main structural elements and sedimentary units of the upper crust are shown.

The moho relief and structure of the lower crust are mainly constrained by the deep seismic reflection and refraction data. In the interpolation between the deep crustal reflectors and/or refractors we have used results from gravity modelling along some of the transects.

Two regional crustal transects across the Barents Sea have been constructed between the Novaya Zemlya test site and the seismic arrays SPITS and ARCES respectively (Figs. 1 and 4). The most prominent features in both transects are the wide and deep East Barents Sea basins. The deeper fault-controlled part of these basins, interpreted as being either Devonian (Johansen et al. 1993) or Carboniferous-Permian (Verba et al. 1992) in age, is associated with crustal thinning and high seismic velocities in the crust (Verba et al. 1992) indicating an extensional tectonic setting. The total sedimentary thickness reaches 17 km and the average depth to moho is about 35 km. The velocities in the upper crystalline crust are 5.8-6.4 km/s and in the lower crust they are 6.8-7.0 km/s and higher (Davydova et al. 1985).

The areal configuration of the East Barents Sea basins and their Late Permian-Early Triassic subsidence, contemporaneously with inversion and folding on Novaya Zemlya (Ulmishek 1982), suggests that the primary driving forces of the regional subsidence may be related in some way to active-margin and continental-collision processes culminating in the Uralian Orogeny at the eastern Barents Sea margin (Vågnes et al. 1994, Gudlaugsson et al. 1998).

The geology of the western Barents Sea exhibits distinct regional differences (see N-S transect in Fig. 6.7.4). South of 74°N, the southern Barents Sea sedimentary basin province is characterised by a number of sub-basins and highs. This region is dominated by Late Paleozoic to early Tertiary extensional events. The structural relief becomes increasingly accentuated towards the margin, reflecting westward retreat of the areas affected by rifting with time. North of about 74°N, a relatively flat-lying succession of Upper Paleozoic and Mesozoic strata reflects a general platform setting in a region largely unaffected by the late Mesozoic extension.

A series of crustal transects across the western continental margin is shown Fig. 6.7.5. The change in crustal type, from continental to oceanic, occurs over a narrow zone and is closely related to the primary shear and rift structures along the margin.

In a regional sense, continental breakup took place within two distinctly different provinces, the Mesozoic sedimentary basin region in the southwestern Barents Sea, and the platform further north comprising Svalbard and the Svalbard Platform. In the platform province Mesozoic and Upper Paleozoic strata cover a thick crystalline crust. The base of the crust is well defined in the deep seismic reflection profiles and corresponds to an 8+ km/s velocity at a depth of 30-35 km in the deep seismic refraction data. In contrast, the basinal region exhibits an accentuated basement relief with thick local sediment accumulations. Moho depths range from 20 to 30 km. Within the basins, continuous reflectors interpreted as sedimentary sequence boundaries are observed down to a maximum depth of 9.5 s twt, or approximately 20 km. An extended crystalline crust of only a few kilometres in thickness exists beneath the basin axis, suggesting that the Cretaceous rifting almost reached breakup (Faleide et al. 1993, Breivik et al. 1998).

The oceanic crust has a normal thickness (5-8 km) but higher velocities associated with top basement (6-7 km/s) than normal oceanic crust. Depths to moho in the oceanic domain typically ranges between 10-15 km (Jackson et al. 1990, Faleide et al. 1991). Oceanic basement is overlain by a 5-7 km thick sequence of Cenozoic sediments (Faleide et al. 1996).

The continent-ocean transition is less clear at the rifted margin segment (Fig. 6.7.5, transect 2) because volcanic extrusives mask most of the underlying structures. Two deep reflectors may bound an underplated magmatic body but we do not have velocity control to support this interpretation.

The northern transects (3-5) which represent breakup within a platform region reveal significant differences in crustal thickness, structural style and sediment accumulation with respect to the southern transects. Both the deep seismic reflection and refraction data define the moho at depths of 30-32 km beneath the western Svalbard Platform.

On Svalbard, moho is well defined as a fairly horizontal and continuous reflector at the base of the reflective crust at a depth of 32 km (Fig. 6.7.5, transect 4). It deepens to 35 km under the foldbelt in western Isfjorden. Further west, rapid crustal thinning towards the continent-ocean transition is observed. The large variations in crustal structure around Svalbard will affect seismic travel times for local and regional events recorded at the SPITS array. For example,

between the plate boundary (Knipovich Ridge) in the Greenland Sea and SPITS the moho depth varies between 10-35 km over a distance of 200-250 km.

Gravity modelling, constrained by the deep seismic data, indicate lateral density (and velocity?) variations in the upper mantle (Breivik et al. 1999).

Further work

Further work may include:

- Calculation of synthetic travel-times along 2D transects and comparing these to travel-time predictions from the Barents Sea regional velocity model.

- Analysis of wide-angle profiles recorded at SPITS and ARCES using commercial and academic seismic surveying (mainly with airguns but also explosives) as source. Such data sets have proven useful focusing on the velocity structure of the lower crust and uppermost mantle (Høgden 1999, Schweitzer 2000).

- Construction of a regional 3D crustal velocity model.

Summary

The crustal and seismic velocity structure of the Barents Sea varies significantly:

- Thickness of sedimentary cover varies between 0 – 20 km

- Depth to moho varies between 20 – 45 km

- Thickness of crystalline crust varies between 10 – 45 km

The crustal heterogeneity of the Barents Sea region should be revealed by regional velocity models.

Jan Inge Faleide

References

Breivik, A.J., Faleide, J.I. & Gudlaugsson, S.T. (1998) Southwestern Barents Sea margin: late Mesozoic sedimentary basins and crustal extension. Tectonophysics 293, 21-44.

Breivik A.J., Verhoef J. & Faleide J.I. (1999) Effect of thermal contrasts on gravity modeling at passive margins: Results from the western Barents Sea. J. Geophys. Res. 104, 15293-15311.

Davydova, N.I., Pavlenkova, N.I., Tulina, Yu.V. & Zverev, S.M. (1985) Crustal structure of the Barents Sea from seismic data. Tectonophysics 114, 213-231.

Faleide, J.I., Gudlaugsson, S.T., Eldholm, O., Myhre, A.M. & Jackson, H.R. (1991) Deep seismic transects across the sheared western Barents Sea-Svalbard continental margin. Tectonophysics 189, 73-89.

Faleide J.I., Vågnes E. & Gudlaugsson S.T. (1993) Late Mesozoic-Cenozoic evolution of the southwestern Barents Sea. In: Parker, J.R. (ed.) Petroleum geology of Northwest Europe: Proceedings of the 4th Conference. Geological Society, London, 933-950.

Faleide J.I., Solheim A., Fiedler A., Hjelstuen B.O., Andersen E.S. & Vanneste K. (1996) Late Cenozoic evolution of the western Barents Sea-Svalbard continental margin. Global and Planetary Change 318, 53- 74.

Gudlaugsson S.T., Faleide J.I., Johansen S.E. & Breivik A.J. (1998) Late Palaeozoic structural development of the south-westeren Barents Sea. Mar. Petrol. Geology 15, 73-102.

Høgden, S. (1999) Seismotectonics and crustal structure of the Svalbard region. Cand. scient. thesis, Department of Geology, University of Oslo, 142 pp.

Jackson H.R., Faleide J.I. & Eldholm O. (1990) Crustal Structure of the Sheared Southwestern Barents Sea Continental Margin. Mar. Geol. 93, 119-146.

Johansen S.E, Ostisky B.K., Birkeland Ø., Fedorovsky Y.F., Martirosjan V.N., Bruun Christensen O., Cheredeev S.I., Ignatenko E.A. & Margulis L.S. (1993) Hydrocarbon potential in the Barents Sea region: play distribution and potential. Norw. Petrol. Soc. Spec. Publ. 2, 273-320.

Kremenetskaya, E. & Asming, V. (1999) Location calibration of the Barents region. In: Workshop on IMS location calibration, IDC technical experts group on seismic event location, Oslo, 12-14 January 1999, Technical Documentation.

Schweitzer, J. (2000) Recent profiling experiments in the Spitsbergen area - calibration data for the SPITS array. NORSAR Sci. Rep. 2-1999/2000 (this volume).

Ulmishek, G. (1982) Petroleum geology and resource assessment of the Timan-Pechora Basin, USSR, and the adjacent Barents-Northern Kara Shelf. Argonne National Laboratory, Rep. ANL/EES-TM-199, 197 pp.

Verba, M.L., Daragan-Sushchova, L.A. & Pavlenkin, A.D. (1992) Riftogenic structures of the western Arctic Shelf investigated by refraction surveys. Int. Geol. Rev. 34, 753-764.

Vågnes, E., Amundsen, H.E.F., Johansen, S.E. & Stensen, L.R. (1994) Late Permian-Early Triassic subsidence in the Barents Sea: reflecting a reorganisation of mantle convection patterns? In: Johansen, S.E. Geological Evolution of the Barents Sea, with special emphasis on the Late Palaeozoic Development, dr. scient. thesis, Department of Geology, University of Oslo.
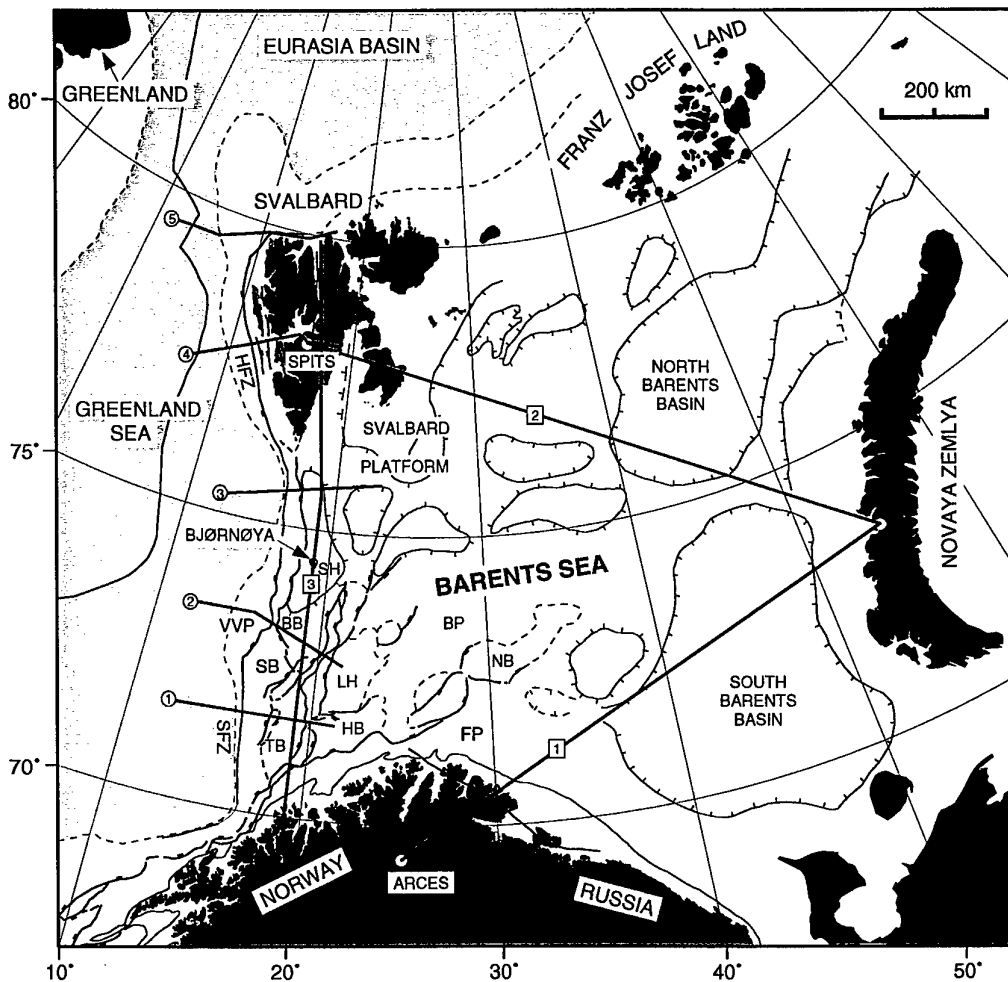
Fig. 6.7.1. *Regional setting – main geological provinces and structural elements in the Barents Sea and surrounding areas. Location of crustal transects in Figs. 4 and 5 and the seismic arrays SPITS and ARCES also shown. BB = Bjørnøya Basin, BP = Bjarmeland Platform, FP = Finnmark Platform, HB = Hammerfest Basin, HFZ = Hornsund Fault Zone, LH = Loppa High, NB = Nordkapp Basin, SFZ = Senja Fracture Zone, SB = Sørvestsnaget Basin, SH = Stappen High, TB = Tromsø Basin, VVP = Vestbakken Volcanic Province.*
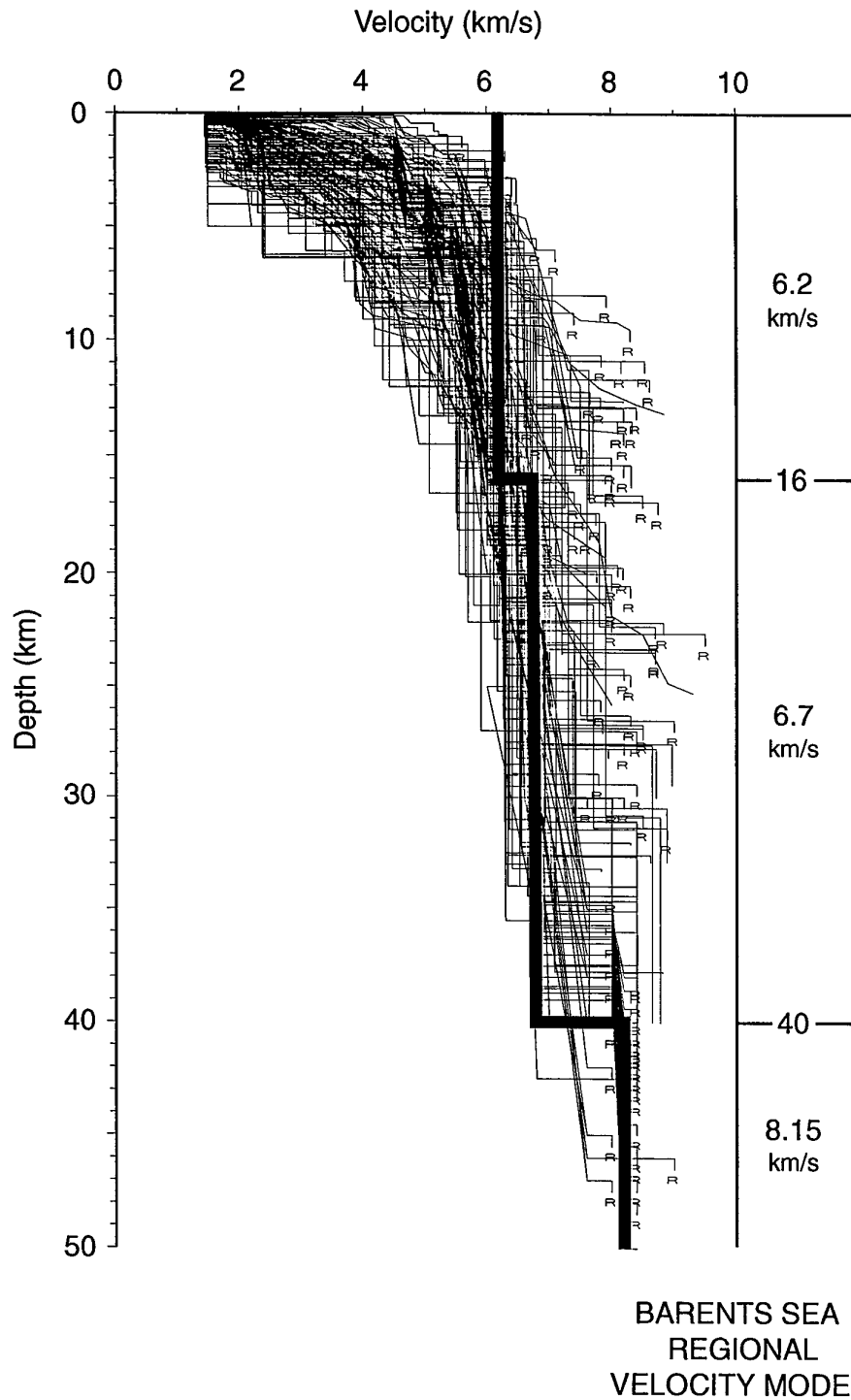
Fig. 6.7.2. *Velocity-depth profiles from most of the Barents Sea (stored in the VELO database compiled by the University of Oslo) compared to the Barents Sea regional velocity model of Kremenetskaya and Asming (1999).*
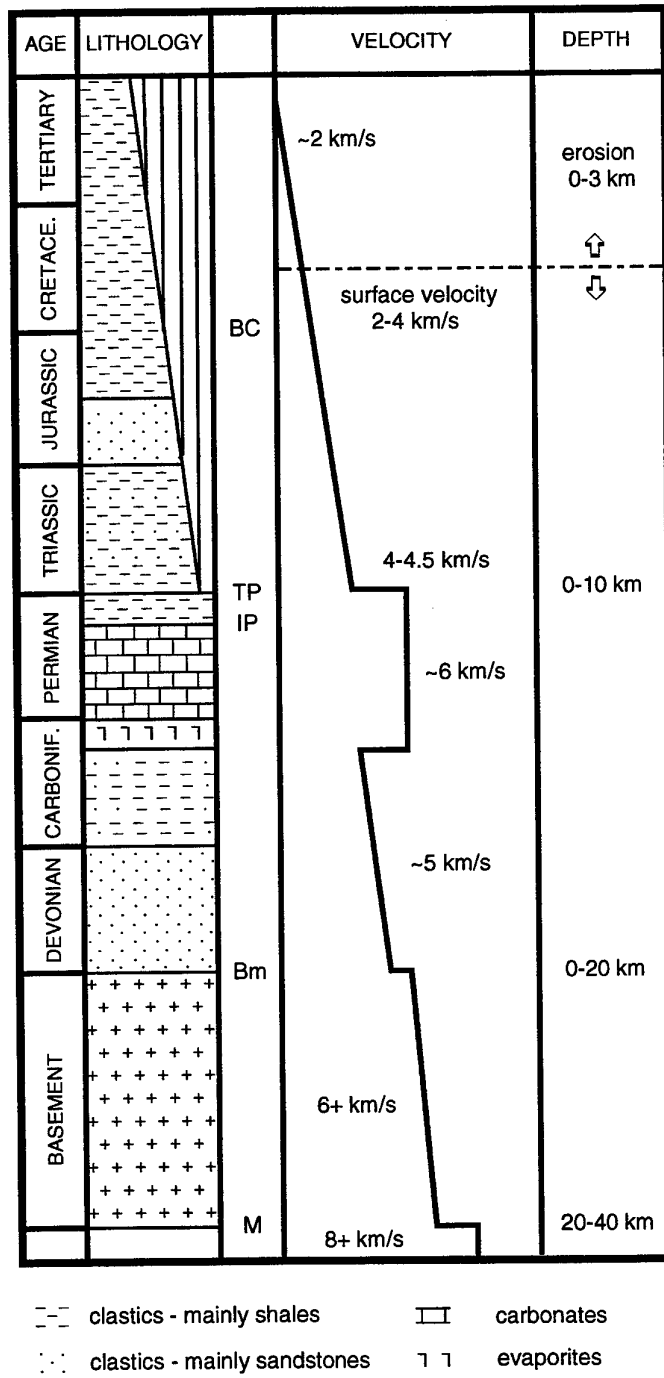
Fig. 6.7.3. *Generalised velocity-depth structure in the Barents Sea showing typical velocities and depth ranges of the main sedimentary and crustal units.*
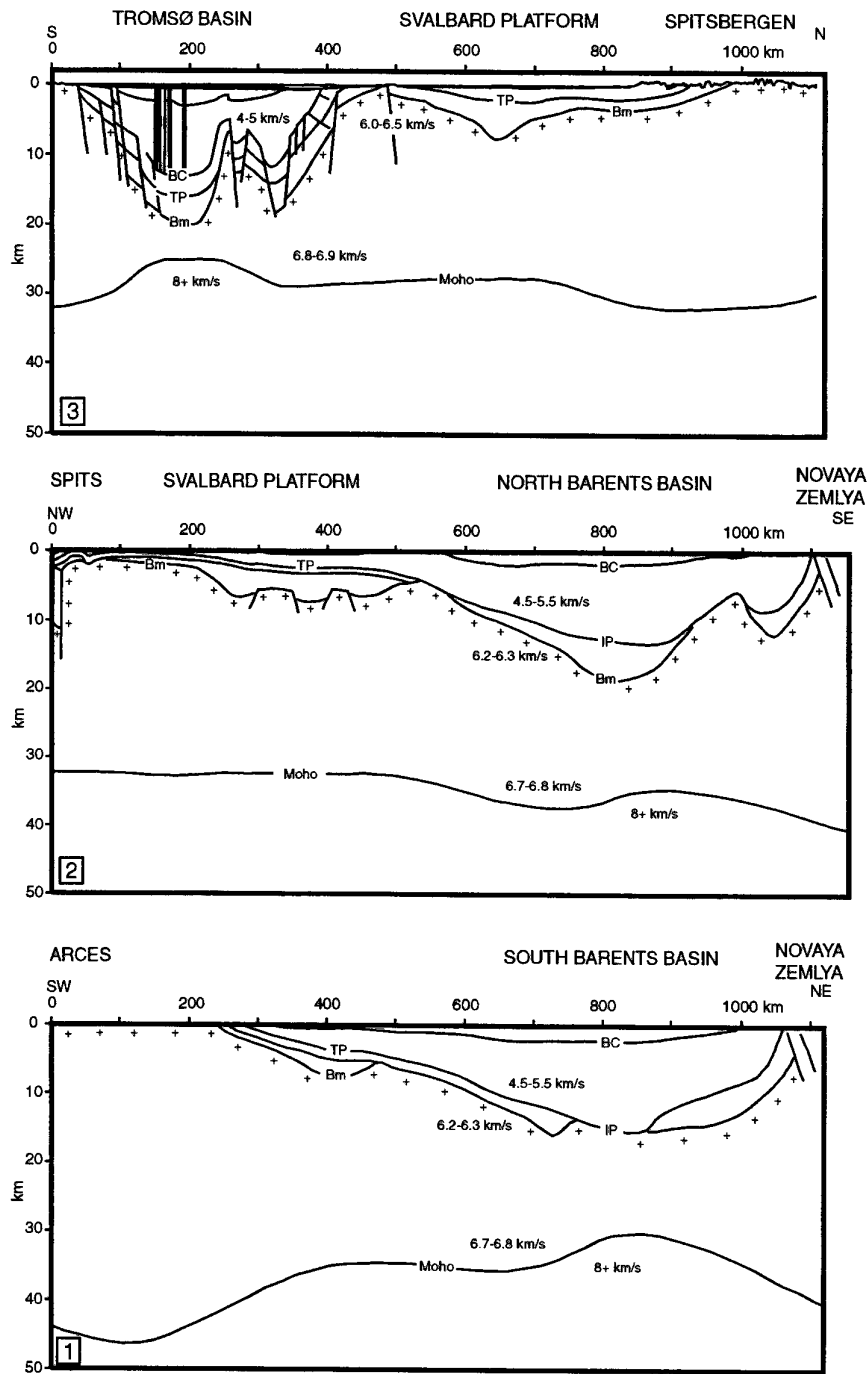
Fig. 6.7.4. *Regional crustal transects across the Barents Sea. (1) ARCES to the Novaya Zemlya test site, (2) SPITS to the Novaya Zemlya test site, and (3) N-S profile in the western Barents Sea from the coast of Norway, across Bjørnøya, to the northern coast of Svalbard. See Fig. 6.7.1 for location and Fig. 6.7.3 for identification of the main interfaces in the Barents Sea subsurface.*
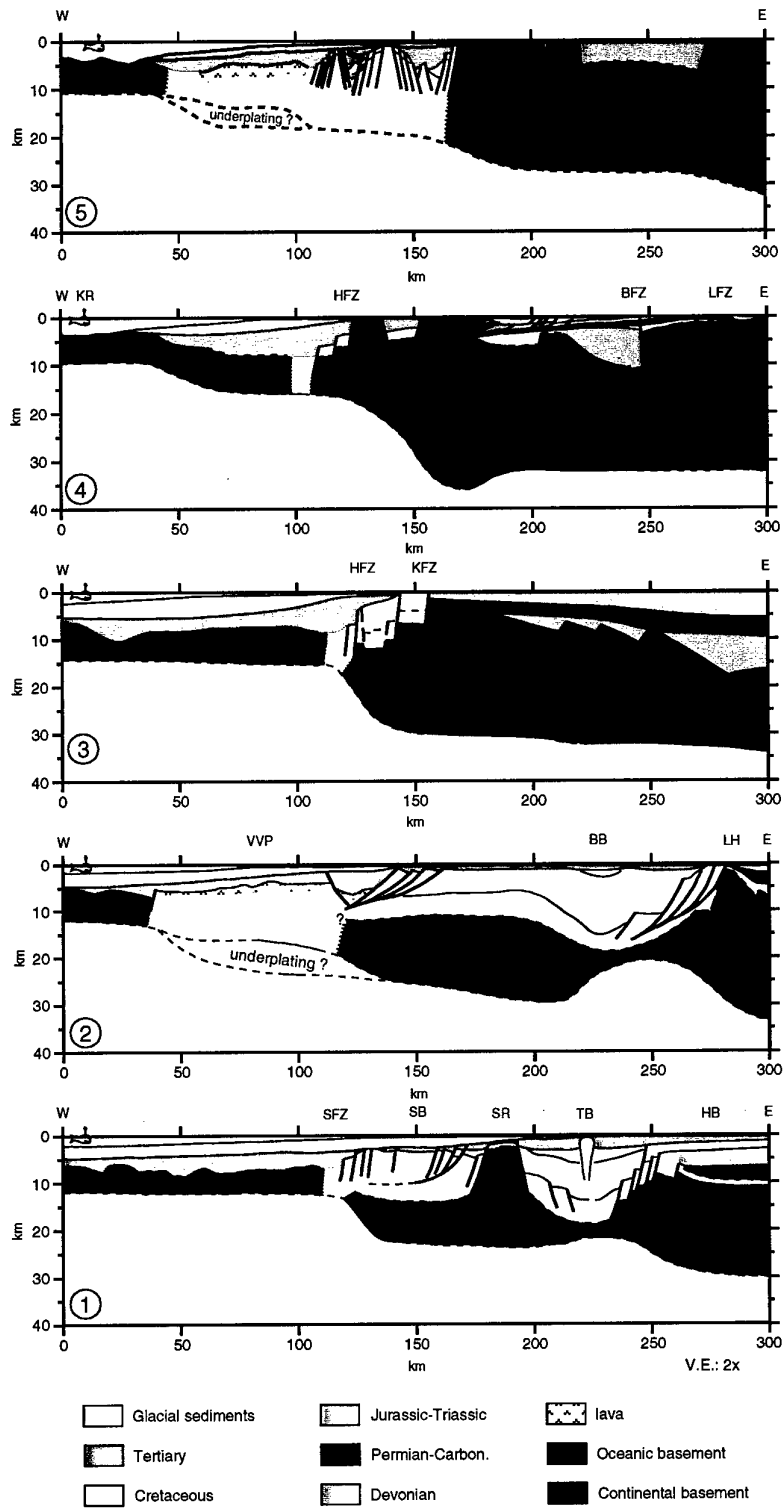
Fig. 6.7.5. *Regional crustal transects across the western Barents Sea-Svalbard margin. See Fig.6.7.1 for location.*